

FAKULTÄT MASCHINENBAU

Master of Science in Manufacturing Technology

Institut für Umformtechnik und Leichtbau

Prof. Dr.-Ing. Dr. h.c. Matthias Kleiner

Prof. Dr.-Ing. Dr.-Ing. E.h. A. Erman Tekkaya

Master Thesis

Numerical Investigation of the Effect of Process Parameters to Optimize a Superplastic Forming Process

by

Elif Sedes

Matriculation no: 162951

Supervisors:

Prof. Dr.-Ing. Dr.-Ing. E.h. A. Erman Tekkaya (IUL)

Assist. Prof. Dr. Mehmet Ipekoglu (TAU)

M.S.c. Kerim Isik (IUL)

Issued on: 16.11.2016

Submitted on: 26.07.2017

**TURKISH-GERMAN UNIVERSITY
INSTITUTE FOR GRADUATE STUDIES IN SCIENCE AND ENGINEERING
MASTER'S PROGRAM IN MECHANICAL ENGINEERING
(MANUFACTURING TECHNOLOGY)
THESIS PRESENTATION PROTOCOL**

26.07.2017

The result of the thesis presentation of Elif SEDES, who is registered in the joint graduate program Manufacturing Technology between Turkish-German University and Technical University Dortmund with the registration number 1261011101, titled "Numerical Investigation of the Effect of Process Parameters to Optimize a Superplastic Forming Process" held on 26.07.2017 at 10.00 is presented below.

Successful

Extension (3 months)

Unsuccessful

Thesis Presentation Committee:

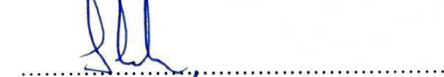
Prof. Dr.-Ing. Dr.-Ing. E.h. A. Erman TEKKAYA
(Co-advisor)



Assist. Prof. Dr. Mehmet İPEKOĞLU
(Co-advisor)



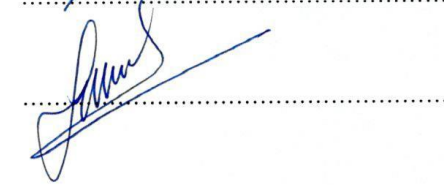
Assist. Prof. Dr. Selim COŞKUN
(Member)



Assist. Prof. Dr. Alpay ORAL
(Member)



Assist. Prof. Dr. Sibel ÖZENLER
(Member)



Acknowledgements

This Master thesis project is carried out by the collaboration between Technical University Dortmund and Turkish-German University. The problem and topic for this thesis are defined by TUSAS Engine Industries (TEI). This thesis has been completed under guidance and constant supervision of Prof. Dr.-Ing. Dr.-Ing. E.h. A. Erman Tekkaya (Institut für Umformtechnik und Leichtbau, TU Dortmund), Assist. Prof. Dr. Mehmet Ipekoglu (Department of Mechatronic Systems Engineering, Turkish-German University) and M.Sc. Kerim Isik (Institut für Umformtechnik und Leichtbau, TU Dortmund).

First and foremost, I would like to express my thankfulness to my supervisor Prof. Dr.-Ing. Dr.-Ing. E.h. A. Erman Tekkaya, for motivating and helping me to get knowledge about metal forming technology.

I would like to deeply thank Assist. Prof. Dr. Mehmet Ipekoglu for being my supervisor and his guidance, suggestions and help in each step of my thesis, not only for technical issues but also for encouraging me to succeed my master degree.

I also would like to appreciate M.Sc. Kerim Isik for his suggestions, guidance and help. His insights, supportive criticisms, encouragements and leadings in each step of my study made me always confident.

I also would like to thank my manager Mustafa Tuksal, my colleagues Nitel Muhtaroglu and Nuri Cizioglu for their help, enthusiasm and supportive criticisms.

Finally, yet importantly, I would like to express my appreciation and thanks to my husband Caner Sedes and my parents for their help, understanding and their best wishes for my success. I am grateful for their understanding for the time that I took from them for studying my master thesis. It would be impossible for me to complete my study if I had not felt their support behind me.

Abstract

Superplastic forming (SPF) is an alternative manufacturing method to produce complex shapes in one step without assembling operations which are not possible with other methods. SPF process enables to get near net shape products without surface finish operation necessities. SPF process can produce parts with nearly 1000% elongations with good mechanical properties. SPF process also reduces the weights of the products because it eliminates assembly processes. Furthermore, SPF process increases cycles of components before failure. Mentioned assets of SPF make it a very important process choice in aviation industry, in which good mechanical properties, low weights and long service lives are required.

The main purpose of this thesis is to investigate process parameters of SPF process for Ti6Al4V material using finite element method (FEM) in order to obtain an optimum process which results in both good product quality and reasonable cost. For this purpose, first analysis results were compared to an experimental study to test accuracy of the used method, next the process parameters were investigated for rectangular and conical parts. Then, a tool was developed to be used in the factory for estimating process time of SPF process with given process parameters. Finally, application of SPF process is conducted for an aircraft blowout door in order to choose an optimum process for production.

Keywords: Superplastic Forming, Superplasticity, Finite Element Method, Machine Learning, Data Mining, Aviation, Aerospace

Table of Contents

List of Figures	3
List of Tables	7
Formula Symbols and Abbreviations	9
1 Introduction	12
1.1 Motivation and Objective of the Thesis	13
1.2 Outline of the Thesis	14
2 State of the Art	16
2.1 Metal Forming.....	16
2.1.1 Bulk Metal Forming	17
2.1.2 Sheet Metal Forming	18
2.2 Superplastic Forming	19
2.2.1 Theory of Superplasticity	22
2.2.2 Superplastic Blow Forming	27
2.2.3 Superplastic Forming Process Parameters	28
2.2.4 Technological and Economical Aspects of SPF Process	31
2.3 Information about Superplastic Titanium Alloys.....	33
2.4 Finite Element Formulation of SPF Process	34
2.4.1 Implicit and Explicit Approaches.....	35
2.4.2 Finite Element Analysis of SPF Process in ABAQUS Software	36
2.4.3 Modelling of SPF Process in ABAQUS Software	37
2.5 Machine Learning and Data Mining	40
2.5.1 Regression Technique for Machine Learning	42
3 Aim and Scope of the Thesis Work	45
4 Investigation of Effect of Process Parameters to SPF Process	47
4.1 Comparison of Finite Element Analysis Study with Experimental Results ..	47
4.2 Investigation of Process Parameters for SPF Process for a Rectangular Part	55

4.2.1	Investigation of the Effect of Loading Profile.....	57
4.2.2	Investigation of Effect of Process Temperature	61
4.2.3	Investigation of Effect of Strain Rate	64
4.2.4	Investigation of Effect of Sheet Thickness.....	68
4.2.5	Investigation of Friction Coefficient	70
4.2.6	Investigation of Effect of Die Entry Radius	74
4.2.7	Investigation of Forming Behaviour for Different Time Steps.....	75
4.3	Investigation of Process Parameters to the SPF Process for a Conical Part ..	81
4.3.1	Investigation of Effect of Entry Radius of the Die.....	82
4.3.2	Investigation of Effect of Die Aspect Ratio	86
4.3.3	Investigation of Effect of Friction Coefficient	89
4.4	Comparison of Forming Behaviour of Rectangular and Conical Box Forming.....	93
5	Development of an Equation for Estimation of Process Time for SPF Process by Machine Learning for a Rectangular Box	96
6	Application of SPF Process for an Aircraft Blowout Door	99
7	Cost Analysis of SPF Process for the Factory	106
8	Conclusion	108
	Bibliography	111
	Appendix	115

List of Figures

Figure 2.1: Classification of forming processes (Nptel, 2016).....	16
Figure 2.2: Basic bulk deformation processes: a) rolling, b) forging, c) extrusion, and d) drawing (Groover, 2012).....	17
Figure 2.3: Basic sheet metal working operations: a) bending, b) drawing, c) shearing: 1) as punch first contacts sheet, and 2) after cutting (Groover, 2012).....	18
Figure 2.4: Bi-Sn alloy (1950% elongation) (Marinho et al., 2012).....	19
Figure 2.5: Development of SPF maximum elongation through years (Marinho et al., 2012).....	20
Figure 2.6: Simple female forming example for large one-piece truck cab roof in SP5083 alloy (Barnes, 2007).....	21
Figure 2.7: GBS while superplastic deformation (Sieniawski and Motyka, 2007).....	23
Figure 2.8: A typical stress strain rate diagram with change of strain rate sensitivity (Deshmukh, 2003).....	25
Figure 2.9: Relation between flow stress, elongation at fracture and m with strain rate (Marinho et al., 2012).....	26
Figure 2.10: Steps of superplastic blow forming process (N.N., 2008).....	27
Figure 2.11: Effect of grain size to strain rate (Sieniawski and Motyka, 2007).....	30
Figure 2.12: Effect of grain size to working temperature (Sieniawski and Motyka, 2007).....	30
Figure 2.13: Fatigue curve comparison for fan blades for SPF (1) and conventional (2) methods (Afrikantov, 1992).....	32
Figure 2.14: Strain rate sensivity diagram of superplastic materials (Ghosh and Hamilton, 1986).....	34
Figure 2.15: Positive normals for general membranes (Deshmukh, 2003).....	38
Figure 2.16: Coulomb friction in ABAQUS (Deshmukh, 2003).....	39
Figure 2.17: Illustration of data mining process cycle (N.N., 2016).....	41
Figure 2.18: Representation of simple linear regression (Analyticsvidhya, 2016).....	43

Figure 2.19: Robustness comparison of LS and LMS regression methods (Dallal,1992)	44
Figure 3.1: Process chart for the thesis.....	46
Figure 4.1: Finite element model for SPF process	49
Figure 4.2: Formed rectangular box in ABAQUS for 1.4 MPa constant pressure application.....	51
Figure 4.3: Pressure-time cycles applied in experiment for different constant target strain rates (Vasin et al., 2003).....	53
Figure 4.4: Pressure scheme applied to the workpiece for FE simulations.....	54
Figure 4.5: Rigid surface for the rectangular die.....	56
Figure 4.6: Assembly of sheet metal and die.....	56
Figure 4.7: Deformed shape of sheet metal after 1000 second for constant pressure application for element size 0.8 mm.....	59
Figure 4.8: Sheet thickness distribution at blank for constant pressure application.....	59
Figure 4.9: Sheet thickness distribution at blank for constant strain rate application.....	60
Figure 4.10: Pressure schedule for automatic pressure application for strain rate 10^{-2} 1/sec.....	61
Figure 4.11: Sheet thicknesses comparison a) for 840° and b) for 900° process temperatures.....	62
Figure 4.12: Comparison of applied pressure for 840 and 900 degrees.....	62
Figure 4.13: Pressure time profiles at different target strain rates.....	64
Figure 4.14: Minimum sheet thickness-time profiles at different target strain rates.....	65
Figure 4.15: Sheet thickness distribution at the end of the forming process for a) 10^{-4} 1/sec., b) 5×10^{-4} 1/sec., c) 10^{-3} 1/sec., d) 10^{-2} 1/sec. strain rates.....	67
Figure 4.16: Sheet thickness distribution for a) 0.8 mm, b) 1 mm and c) 1.2 mm sheet thicknesses.....	69

Figure 4.17: Coulomb frictional behaviour (Hibbit and Hibbit, 2001).....	71
Figure 4.18: Pressure profile for different friction coefficients for a constant target strain rate of 10^{-3}	73
Figure 4.19: Comparison of sheet thickness distribution for different friction coefficients.....	74
Figure 4.20: Dividing formed part to four different zones according to equivalent creep strain.....	76
Figure 4.21: Creep strain for different forming zones with respect to forming time.....	77
Figure 4.22: Dividing formed part to four different zones according to sheet thickness distribution.....	78
Figure 4.23: Equivalent creep strain change according to distance from sheet initial position.....	79
Figure 4.24: Dividing formed part to four different zones according to sheet thickness distribution.....	80
Figure 4.25: Investigation of thinning for different zones.....	80
Figure 4.26: Geometrical schematic of conical die.....	82
Figure 4.27: Mesh view for conical die and sheet.....	83
Figure 4.28: Formed configuration of sheet metal	84
Figure 4.29: Sheet thickness distribution for a) 10 mm and b) 12 mm die entry radii...	85
Figure 4.30: Schematic view of contact relations between die and sheet while SPF of a conical part (Hwang et al., 1997)	86
Figure 4.31: Thickness distribution for die entry diameters a) 108 mm and b) 128 mm.....	88
Figure 4.32: Pressure profile for different friction coefficients for 10^{-3} 1/sec. constant target strain rate.....	90
Figure 4.33: Comparison of sheet thickness distribution for different friction coefficients.....	91

Figure 4.34: Comparison of pressure changes for conical and box forming for different friction coefficients.....	92
Figure 4.35: Comparison of applied pressure and minimum sheet thicknesses for conical and rectangular box forming.....	93
Figure 4.36: Dividing formed part to four different zones according to sheet thickness distribution.....	94
Figure 4.37: Comparison of thinning percent for a) rectangular box and b) conical box	95
Figure 5.1: Process time calculator tool for SPF process of a rectangular box.....	98
Figure 6.1: Representation of half die-sheet geometry to simulate SPF process for aircraft blowout door.....	100
Figure 6.2: Representation of die-sheet meshes to simulate SPF process for aircraft blowout door.....	101
Figure 6.3: Deformed shape of sheet for test number 5.....	104
Figure 6.4: Equivalent stress plot of sheet for test number 5.....	104
Figure 6.5: Thickness distribution plot of sheet for test number 5.....	105

List of Tables

Table 2.1: Summary of change in microstructure in the three regions (Marinho et al., 2012).....	26
Table 4.1: Experiment results for application of constant gas pressure to the sheet.....	48
Table 4.2: Material properties for Ti6Al4V (Vasin et al., 2003).....	49
Table 4.3: Analysis results for different element sizes.....	50
Table 4.4: Comparison of analysis time with experiments.....	51
Table 4.5: Comparison of analysis results with experiments.....	51
Table 4.6: Comparison of analysis results with experimental data for different target strain rates.....	54
Table 4.7: Experimentally determined power law creep properties (Warren and Wadley, n.d.).....	57
Table 4.8: Analysis results for different element sizes.....	58
Table 4.9: Summary of results obtained for process temperatures of 840 and 900 degree	63
Table 4.10: Summary of the results obtained for different target strain rates.....	66
Table 4.11: Summary of the results obtained for different sheet thicknesses.....	68
Table 4.12: Comparison of results obtained of different friction coefficients at different target strain rates.....	72
Table 4.13: Comparison of final thicknesses for different die entry radii	75
Table 4.14: Geometric properties of conical die for different analyses.....	83
Table 4.15: Geometrical properties of test specimen.....	84
Table 4.16: Results for different die entry radii.....	84
Table 4.17: Geometric properties of conical die for different AR values.....	87
Table 4.18: Results summary for different aspect ratio of the die.....	87
Table 4.19: Comparison of results obtained of different friction coefficients at 10^{-3} target strain rates.....	89

Table 6.1: Process parameter alternatives for production of blowout door.....	102
Table 6.2: Summary of obtained results for different process parameters.....	103
Table 7.1: Total cost calculation for FEA study (TEI, 2017).....	106
Table 7.2: Estimated cost calculation for experiments and comparison with FEA study (TEI, 2017).....	107

Formula Symbols and Abbreviations

Formula Symbols

Symbol	Unit	Description
$\dot{\varepsilon}$	-	Strain rate
ε	-	Strain
D	-	Diffusion coefficient
C_m	-	Dimensionless constant
G	MPa	Shear modulus
b	μm	Burgers vector
K	J/K	Boltzmann constant
T	K	Absolute temperature
d	μm	Average grain size
σ	MPa	Applied stress
q	-	Dimensionless exponent
m	-	Strain rate exponent
D_0	m^2/s	Independent coefficient of diffusion
Q	kJ/mol	Activation energy of creep process
R	$\text{J}/\text{mol} \times \text{K}$	Gas constant
n	-	Strain hardening coefficient
T_{def}	K	Deformation temperature
T_m	K	Melting temperature
L	mm	Element length
E	MPa	Young Modulus
ρ	kg/m^3	Density
Δt	s	Time step
$\dot{\varepsilon}_{opt}$	-	Target strain rate
γ	-	Ratio of equivalent strain rate to target strain rate
$r+1$	-	Iteration number
P_{r+1}	MPa	Applied pressure at iteration number $r+1$
c	-	Power law multiplier

Symbol	Unit	Description
Y	-	Dependent variable
X	-	Independent variable
a	-	Intercept
b	-	Slope of line
e	-	Error terms
β	-	Regression coefficients
ν	-	Poisson's ratio
μ	-	Friction coefficient
p	MPa	Critical frictional shear stress
h	mm	Height of the die
$d1$	mm	Outer diameter of the die
$d2$	mm	Inner diameter of the die
r_e	mm	Entry radius of the die
r_f	mm	Root radius of the die
α	-	Inclined angle of the die
AR	-	Aspect ratio of conical die
T	second	Predicted process time
t	mm	Sheet thickness
P_i	MPa	Initial Pressure
L	mm	Sheet length
w	mm	Sheet width
h_f	mm	Final dome height

Indices

Indice	Description
<i>def.</i>	Deformation
<i>sec.</i>	Second
<i>Max.</i>	Maximum
<i>Min.</i>	Minimum
<i>Eqv.</i>	Equivalent
<i>thick.</i>	Thickness

<i>coeff.</i>	Coefficient
\$	United States Dolar
<i>Lub.</i>	Lubrication

Abbreviations

Abbreviation	Description
SPF	Superplastic Forming
TEI	Tusas Engine Industries
TAI	Turkish Aerospace Industry
GE	General Electric
FE	Finite Element
Al	Aluminium
Ti	Titanium
Cu	Copper
Mg	Magnesium
DB	Diffusion Bonding
FSP	Fine Structure Plasticity
ISP	Internal Stress Plasticity
GBS	Grain Boundary Sliding
DC	Dislocation Creep
FLD	Forming Limit Diagram
FEM	Finite Element Method
FEA	Finite Element Analysis
MIT	Massachusetts Institute of Technology
CPU	Central Processing Unit
LS	Least Square
LMS	Least Median of Squares
WEKA	Waikato Environment for Knowledge Analysis

1 Introduction

High fuel cost builds the need for application of lightweight materials in automotive and aerospace industry. SPF is an alternative manufacturing method of light weight alloys for manufacturing complex shapes at high temperatures. (Shojaeefard et al., 2014)

SPF process is a near-net shape process which is used to shape superplastic materials that can withstand to large tensile deformations. This process can generally be applied to Aluminium (Al) and Titanium (Ti) alloys at high temperatures and special conditions. SPF has ability to form complex shapes which are impossible with other conventional methods. Cold forming and hot forming processes used to be preferred in industrial applications for producing complex shaped geometries before SPF process is developed. In SPF process, the workpiece is clamped to the die and heated to SPF temperature, then inert gas pressure is applied to workpiece with a predetermined rate to get the shape of the die. This process enables parts to be elongated nearly 1000% and mechanical properties obtained are good with low flow stresses, furthermore, net shape geometries are achieved with SPF process. Surface finish obtained after SPF process is also sufficient and this emits surface finish operations after forming process as in the conventional methods. SPF process also permits to produce large parts and this can also eliminate assemblies and can also enable to reduce part weights. (Sieniawski and Motyka, 2007)

Compared to conventional methods for instance fabricating, SPF improves fatigue strength properties, so it increases cycles to the failure. Furthermore, SPF reduces metal consumption significantly, labour and machining costs are decreased with this process. Because lower pressures are applied to the specimen, lower power equipment are required, so manufacturing costs could also be decreased. (Ermachenko et al., 2011)

Mentioned assets of SPF process make it very important in many industrial applications, especially in Aviation industry, since product quality and light weight is a very important criterion. SPF process plays an important role in Aviation industry since 30 years for its numerous advantages.

Besides than advantages of SPF process, it has disadvantages, too. SPF process is an expensive process according to conventional processes, since it requires very high process temperatures. Furthermore, it requires very small grain sizes which require expensive treatments to the material and low strain rates which make process to continue for a very long time. This makes this process incapable for mass production. (Marinho et al., 2012)

In selecting a process as a method to produce a part in industry, both technological and economic factors need to be considered. Although, mentioned advantages make the process very important in Aviation industry, since quality and lightweight are most important criteria, cost and time aspects also need to be considered.

Most important process parameters affecting SPF process are process temperature, pressure cycle, die radius, thickness of the sheet material, lubrication, material type and grain size of the material. The effect of various parameters to the SPF process could be investigated by finite element analysis in order to obtain an optimum process for economical and quality aspects.

1.1 Motivation and Objective of the Thesis

TEI is a joint venture company of Turkish Aerospace Industry (TAI), General Electric Aviation (GE) company, Turkish Armed Forces Foundation and Turkish Aeronautical Association and produces components for different Aerospace companies. The problem and topic for this thesis are defined by TEI.

TEI desires to add SPF process to its manufacturing capabilities, because it could succeed elongations until 1000%, also TEI aims to decrease weight of components by removing joints that are used in conventional processes such as cold, hot forming for assembly purpose, because SPF enables to produce complex parts in one step. Furthermore, increasing service lives and saving cost are another reasons for preferring this method as an alternative approach. In order to compete with other suppliers for aviation industry, TEI needs to include SPF to its current capabilities. Before adding SPF to current manufacturing capabilities, TEI desires to learn the process deeply.

The motivation for this thesis is to investigate effect of process parameters of SPF process for Ti6Al4V material with aid of finite element analysis (FEA) program. Since the experiments have high costs especially for Aviation industry materials, TEI desires to save cost by investigating process parameters with FEA instead of doing experiments for considerably expensive aviation materials.

The motivation could be succeeded by analysing of SPF process with the aid of a FE software ABAQUS for different process parameters. Process parameters are investigated for rectangular and conical parts for simplification, and ABAQUS creep module is used to simulate forming process, since the experiment capability is absent, current analysis approach is compared with experiment results obtained from literature. Process parameters are investigated by running several analyses with creating scripts in order to have an automated process. Furthermore, this study includes development of a tool for predicting forming time of SPF process for a rectangular box without doing several analyses by using machine learning and data mining techniques. Later, SPF of an aircraft blowout door for different process choices are investigated in order to find an optimum process to manufacture. Finally, a cost analysis study is conducted for this project in order to estimate the profit gain by conducting FEA study instead of realizing experiments.

1.2 Outline of the Thesis

There are eight chapters in this thesis work. The thesis structure is organized as explained below:

Chapter 1. Introduction

This chapter gives a general introduction and outline for the motivation and objective of the thesis.

Chapter 2. State of the Art

This chapter gives an overview about the theory of subjects such as metal forming, SPF, information about superplastic Ti alloys, FE formulation of SPF process and machine learning and data mining. The metal forming processes are divided in two groups as bulk and sheet metal forming, and they are briefly described whereas SPF process is explained in detail. Theory of SPF process and superplasticity are given, technological

and economical aspects of SPF process are explained and superplastic behaviour of Ti alloys are described. This chapter also contains information about FEA of SPF process in detail. Furthermore, machine learning and data mining techniques are briefly explained in this chapter.

Chapter 3. Aim and Scope of the Thesis Work

This chapter explains the aim and scope of the thesis work.

Chapter 4. Investigation of Process Parameters to SPF Process

This chapter includes comparison of FEA results of SPF process of a rectangular part with experimental results obtained from literature. Forming behaviour of SPF process is also investigated in detail in this chapter. Furthermore, this chapter contains investigation of process parameters for rectangular and conical parts for SPF process.

Chapter 5. Development of an Equation for Estimation of Process Time for SPF Process by Machine Learning for a Rectangular Box

This chapter is dedicated to development of an equation to estimate process time of SPF process for a rectangular box.

Chapter 6. Application of SPF Process for an Aircraft Blowout Door

In this chapter, SPF process application is presented for an aircraft blowout door, an optimum process is aimed to obtain from various process choices.

Chapter 7. Cost Analysis of SPF Process for the Factory

In this chapter, a cost analysis study is conducted in order to compare numerical analysis study cost with a possible experimental effort cost.

Chapter 8. Conclusion

This chapter includes final conclusions of the thesis work and recommendations for further studies.

2 State of the Art

2.1 Metal Forming

Forming is a process to obtain the desired shape and size from a raw material by exposure of the workpiece to plastic deformation by applying tensile, compressive, bending or shear force or combination of these forces. (Nptel, 2016)

Metal forming processes are defined as deformation processes, that metal billet or blanks are shaped by tools or dies. Processes of metal forming are controlled based on certain parameters such as material of workpiece, tool/work piece conditions, mechanics of plastic deformation named as metal flow, used equipment and requirements that expected from a finished product. These parameters affect selection of processing conditions such as operation temperature, lubrication between workpiece and tool, also choosing workpiece, tool geometry and materials. (ASM, 2016).

Metal forming processes are divided into two main groups; bulk and sheet metal forming as shown in **Figure 2.1**.

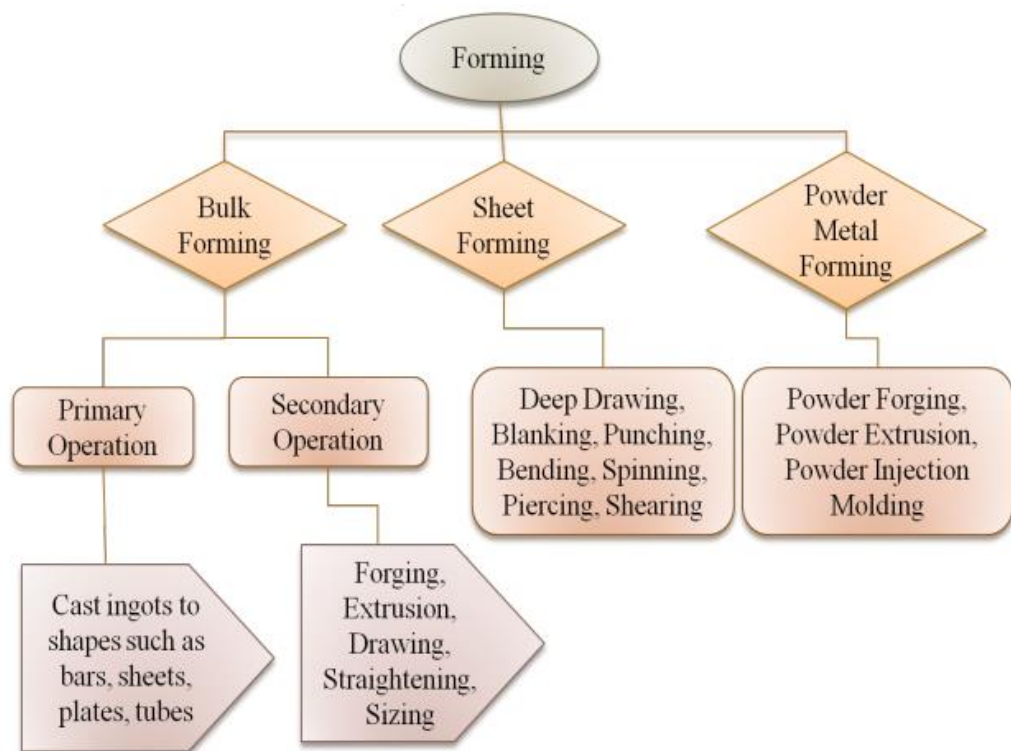


Figure 2.1: Classification of forming processes (Nptel, 2016)

2.1.1 Bulk Metal Forming

Bulk metal forming starting material form is generally billet, rod or slab. Formed part surface to volume ratio increases, since part is applied to a large compressive loads. Processes which are categorized under bulk forming have following features;

- Workpiece encounters very large and permanent plastic deformations,
- Workpiece has in the end significant change in shape or cross section
- Plastic deformed portion of workpiece is mostly larger than elastic deformed region, so elastic recovery is not possible.

The portion of the workpiece undergoing plastic deformation is generally much larger than the portion undergoing elastic deformation; therefore, elastic recovery after deformation is negligible. Extrusion, forging, rolling and drawing are most common forming processes which can be categorized under bulk metal forming. (Altan et al., 1983, Altan et al., 2004) Main bulk forming processes are shown in **Figure 2.2**.

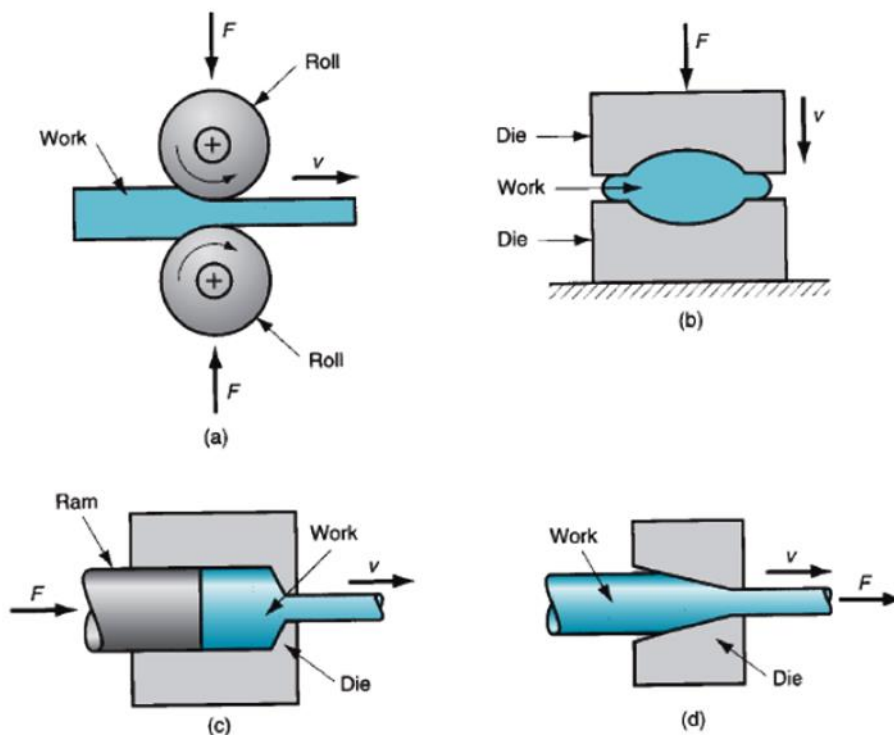


Figure 2.2: Basic bulk deformation processes: a) rolling, b) forging, c) extrusion, and d) drawing (Groover, 2012)

In bulk metal forming, deformation is three dimensional, this is the main feature which distinguishes bulk metal forming from sheet metal forming, because in sheet metal forming processes deformations are mostly in plane of sheet metal. (Forging, 2016)

2.1.2 Sheet Metal Forming

Sheet metal forming procedures consist of cutting and forming of relatively thin sheet metals. Sheet metal thicknesses are typically between 0.4-6 mm. Forming of sheet metals are generally carried out at room temperature. In sheet metal forming, only workpiece form changes, but workpiece cross section does not change. Forming is accomplished with a punch and die. Sheet metal forming is mostly divided to two main categories, one of them is cold forming in which forming is carried at room temperature, second one is named as hot forming, in which material is heated to a temperature higher than melting temperature of the workpiece. Sheet metal forming has a very significant commercial role, since number of consumer and industrial products of sheet metal formed parts consist of automobiles, airplanes, railway cars, office, furniture, home appliances. Sheet metal parts have generally good dimensional accuracy, good surface finish, high strength and low cost relatively. Basic sheet metal forming processes are shown **Figure 2.3**.

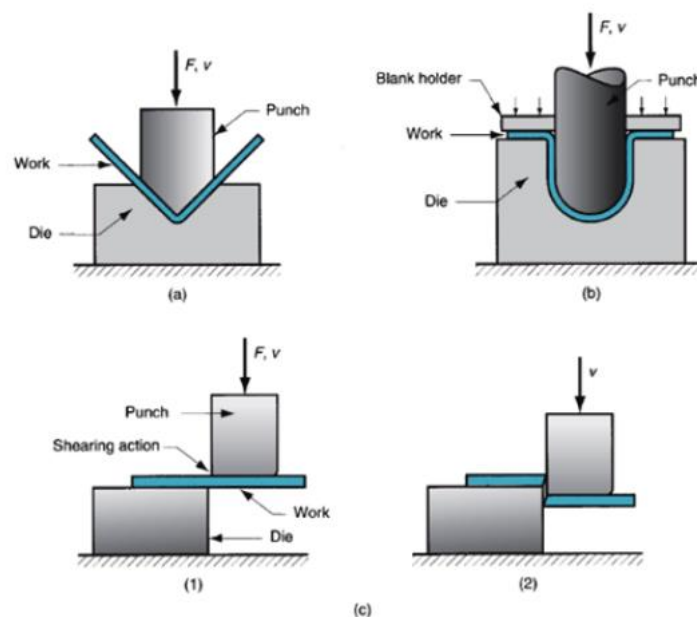


Figure 2.3: Basic sheet metal working operations: a) bending, b) drawing, c) shearing: 1) as punch first contacts sheet, and 2) after cutting (Groover, 2012)

2.2 Superplastic Forming

SPF process is a sheet metal forming process which is capable of withstanding large uniform elongation before necking. High fuel cost is driving the need for using lightweight materials in automotive and aerospace industry, this can be realized by replacing steel with light weight alloys. SPF is an alternative manufacturing method of light weight alloys for forming complex shapes at high temperatures by usage of gas pressure. Superplastic materials have ability to withstand to elongations nearly 1000% at elevated temperatures and low strain rates. (Shojaeefard et al., 2014)

Since today, many researches have been conducted for superplasticity and SPF, they were crucial to establish the limits to the utilize of SPF process. In 1934, Pearson succeed 1950% elongation in Bi-Sn alloy. (Marinho et al., 2012)

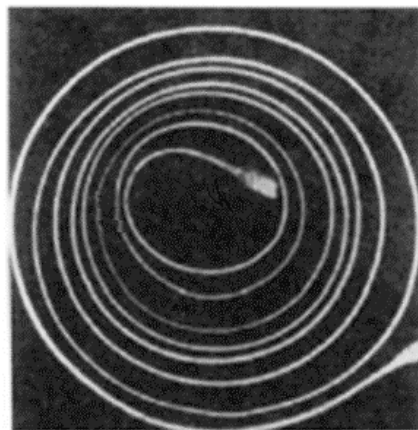


Figure 2.4: Bi-Sn alloy (1950% elongation) (Marinho et al., 2012)

Since 1964, main research focus was to find out maximum stretching by hot uniaxial tests, technological researches started after study of Backofen, they begun to investigate strain rate sensitivity exponent in more details. Backofen, Turner & Avery, in 1964, from the Massachusetts Institute of Technology (MIT), they published their well-known paper which is sheet of Superplastic AlZn eutectoid alloy was pneumatically formed as a bubble. Their research put the necessity of new technology, SPF.

Prof. Backofen and his research group authorized importance of strain rate sensitivity index as the neck-free tensile elongation characteristic of superplastic materials at MIT. Furthermore, they also researched Ti, Copper (Cu) and Magnesium (Mg) alloys.

While Backofen established his study in 1964, Dr. Field found out that extraordinary formability is possible with superplastic materials by working Backofen's study. Later in 1965, Dr. Field did first SPF patent application with usage of sheet-tube forming for thermoforming plastics.

The first laboratory for investigation of SPF is 'Electricity Council Research Center, Capenhurst', and first conference about SPF was done here in 1969.

In 1971, the first commercial SPF company in the world was founded as ISC Alloys Ltd., Avonmouth Bristol, United Kingdom, the aim of this company was to produce complex-shaped components using ZnAl eutectoid alloy with low-cost tooling and forming times.

After 1969, much progress was achieved to scale up special process requirements to achieve feasible production. Then, largest uniform elongation which is nearly 8000% is obtained with commercial bronze. (Marinho et al., 2012) This is clearly illustrated in

Figure 2.5.

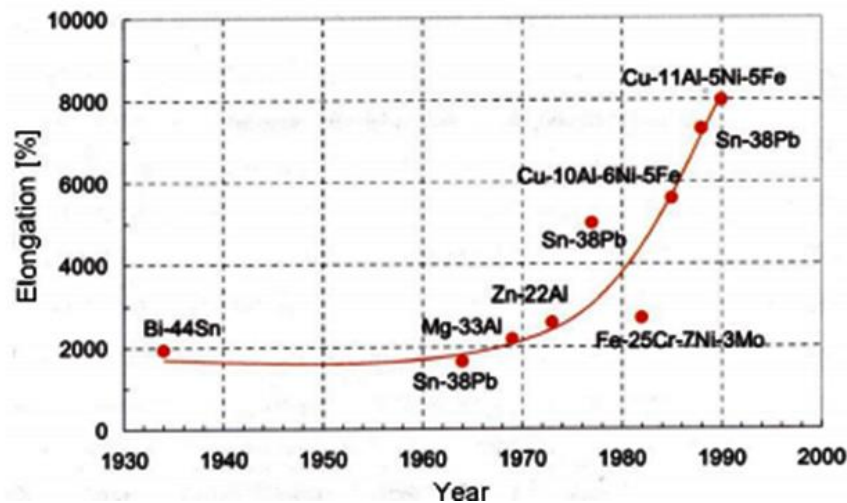


Figure 2.5: Development of SPF maximum elongation through years (Marinho et al., 2012)

At the beginning of 1970s, developments initiated also in Aerospace industry, first one was the SPF of Ti alloy and combination of SPF and diffusion bonding (DB), this attempts are done with help of government funding. First commercial application of SPF was a jack housing with SPF of a Ti alloy by British Aerospace Filton for A310 Airbus aircrafts.

In 1980s, SPF of Ti alloys broadened, and 10 years later, an aerospace contractor company Rohr Industries had produced more than 400 different parts with SPF process. In these days, there have been many innovations with superplasticity to achieve controlled process which means all of the variables (temperature, strain rate, position...) of SPF process need to be controlled to have an optimum forming process. (Marinho et al., 2012)

SPF technology has been developed in recent years, in the past, sheet was heated, clamped to the die and stretched to the tool surface, a formed part for large one-piece truck cab roof in SP5083 alloy can be seen in **Figure 2.6**, but nowadays non-planar clamp line tooling arrangement is utilized. Press is closed after loading and heating, then it is bent drawn to conform with shaped clamp line. With this method, more unstrained material enters the tool and less strain is generated into the preformed sheet since it is formed pneumatically. This technique permits to obtain parts more quickly with less strain and more uniform thickness distribution. (Barnes, 2007)



Figure 2.6: Simple female forming example for large one-piece truck cab roof in SP5083 alloy (Barnes, 2007)

Superplastic materials have high flow stress sensitivity to strain rate, so this process is achieved at very low strain rates. SPF process has very advantageous features comparing to conventional forming processes, SPF has ability of near net shaping, producing multiple parts in one stage, just a little spring back and less tooling cost prices are main

advantages of SPF processes, but SPF process can be achieved in a more time, because high forming ability is realized at low strain rates, this handicap of SPF is main topic of many scientists to develop an optimum process for SPF. SPF is a valuable process to fabricate complex parts used in the aircraft and automobile industries and some of materials showing superplastic behaviour are listed below;

- Titanium (Ti6Al-V)
- Aluminum (2004, 2419, 7475)
- Zinc-Aluminum
- Bismuth-Tin
- Aluminum-Lithium alloys (2090, 2091, 8090) (Shojaeefard et al., 2014)

2.2.1 Theory of Superplasticity

Superplasticity is capability of polycrystalline materials to perform high strains at a high temperature under low stresses which is dependent on strain rate. Tensile elongation of superplastic materials can be more than 2000%. There are two types of superplasticity; fine structure plasticity (FSP) and internal stress superplasticity (ISP). FSP can be defined as internal structural aspect of materials, while ISS is occurred by external conditions such as thermal or pressure cycling, and they cause internal structural deformations which concludes high internal stress independent from external stresses. (Sieniawski and Motyka, 2007)

Under low strain ranges and temperatures above $0.4T_m$, in fine-grained isotropic metallic materials FSP occurs. High strain rate sensitivity parameter ($m > 0.3$), conversion of texture while deformation, low lattice dislocation activity in grains, severe grain boundary sliding (GBS), lack of strain hardening are crucial aspects of superplastic deformation. (Grabski, 1973, Mukherjee 2002)

Experiments on microstructural processes prove that there exists cooperative grain-boundary sliding related to sliding of groups of grains. **Figure 2.7** shows GBS during a superplastic deformation on metallic materials.

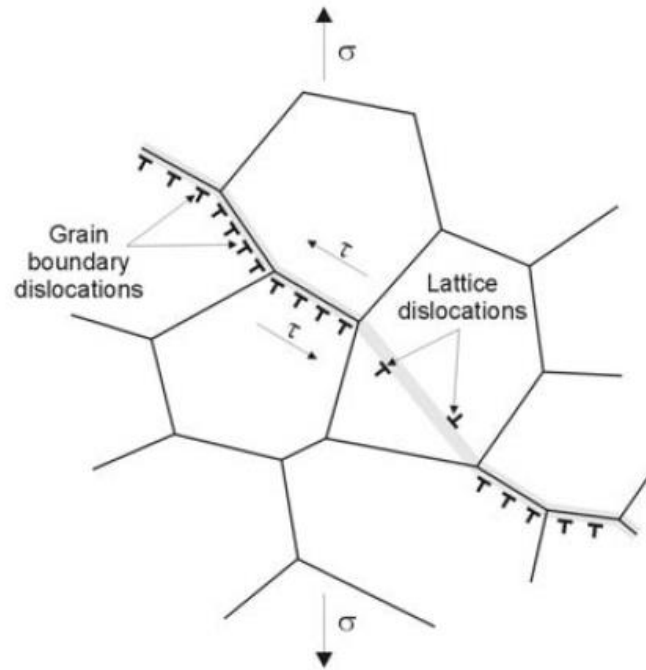


Figure 2.7: GBS while superplastic deformation (Sieniawski and Motyka, 2007)

Most effective group of superplastic materials are two-phase alloys which are Al6Cu0.4Zr, Ti6Al4V, Ni9Si3.1V2Mo, since one of the phases provides grain size stability and at a deformation temperature material is undoubtedly less sensitive to grain growth. (Sieniawski and Motyka, 2007)

The mechanism controlling behaviour of high temperature plastic deformation in polycrystalline materials is expressed with **Equation (2.1)**.

$$\dot{\varepsilon} = \frac{C_m D G b}{K T} \left(\frac{b}{d}\right)^q \left(\frac{\sigma}{G}\right)^m \quad (2.1)$$

Here;

$\dot{\varepsilon}$: strain rate;

D : diffusion coefficient;

C_m : Dimensionless constant [-], incorporating all structural parameters except grain size;

G : Shear modulus [N/mm²], [MPa];

b : Burgers vector [μm];

K : Boltzmann constant [1,381 x 10⁻²³ J/K];

T : Absolute temperature [K];

d : Average grain size [μm];

σ : Applied stress [N/mm^2], [MPa];

q : Dimensionless exponent [-];

m : Strain rate exponent [-].

This equation is developed by Mukherjee-Bird-Dorn, and it is being used more than 30 years and shows good results for metal alloys which have been used for over three decades, showing good results with materials such as metal alloys. The diffusion exponent of equation is also calculated as below;

$$d = D_0 \varepsilon^{\frac{Q}{RT}} \quad (2.2)$$

D_0 : Independent coefficient of diffusion [m^2/s];

Q : Activation energy of creep process [kJ/ mol];

R : Gas constant, 8.314 [J/ mol x K];

ε : Strain.

If Equation 2.1 is substituted to 2.2 **Equation (2.3)** is obtained;

$$\varepsilon^{\circ} = \frac{C_m D_0 \varepsilon^{\frac{Q_c}{RT}} G b}{KT} \left(\frac{b}{d}\right)^q \left(\frac{\sigma}{G}\right)^{\frac{1}{m}} \quad (2.3)$$

Equation (2.3) is rewritten to relate the flow stress (σ_e), the strain rate (ε°) and strain (ε); in its new form, it is called a Norton-Hoff power law equation and expressed as below;

$$\sigma_e = K \cdot \varepsilon^n \cdot \varepsilon^{\circ m} \quad (2.4)$$

K : Material constant (Boltzman constant);

m : Strain rate exponent;

n : Strain hardening coefficient. (Marinho et al., 2012)

In high temperature plastic region, effect of n is known very small and m has dominant effect to the equation, so **Equation (2.4)** can be simplified to equation below;

$$\sigma_e = K \cdot \varepsilon^{\circ m} \quad (2.5)$$

where σ is named as the flow stress. (Marinho et al., 2012)

Figure 2.8 shows how stress/strain diagram is affected with strain rate sensitivity index.

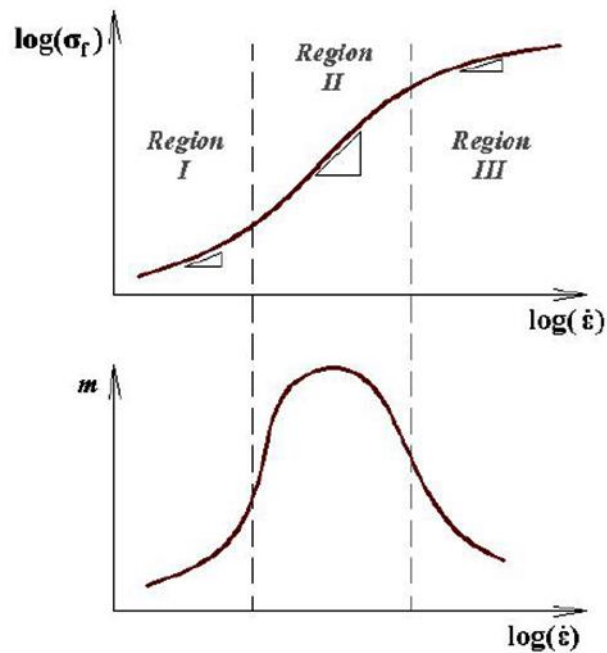


Figure 2.8: A typical stress strain rate diagram with change of strain rate sensitivity (Deshmukh, 2003)

Superplastic behaviour of materials can only happen in region II, because strain rate sensitivity has highest values at that region. For most of the superplastic materials m lies in region of 0.4 to 0.8. If there exists necking in a material as a result of tensile straining, it causes locally high strain rates and if there are high values of m , there will be sudden increase in flow stress in necked region. As a result, necking experiences strain rate hardening which obstructs its development further, hence high strain rate sensitivity causes resistance to development of necking and brings about high tensile elongations behaviour of superplastic materials.

There is not only one mechanism to define deformation in region II, and this region is not still explained well, but GBS is accepted to be the main mechanism accompanied by diffusion, dislocation climb and glide. Region III is controlled by dislocation creep (DC) (power-law creep). In this region, deformation caused slip lines and high dislocation densities are observed, furthermore high grain elongations and crystallographic texture occur. (Deshmukh, 2003)

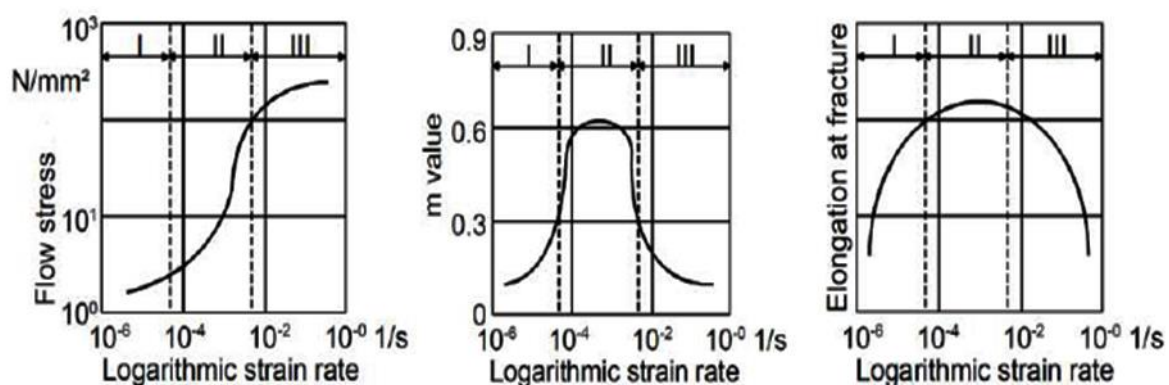


Figure 2.9: Relation between flow stress, elongation at fracture and m with strain rate (Marinho et al., 2012)

Figure 2.9 illustrates relations between m values, logarithmic strain rate and rupture elongation. Logarithmic strain rate is very important in region II, in this zone elongation at rupture and value of m has their maximum in that region. Region I is insensitive, because both m and rupture elongations are minimum here, same behaviour could be seen in region III, also. As a result, SPF happens only in region II. **Table 2.1** summarizes microstructure changes in three regions.

Table 2.1: Summary of change in microstructure in the three regions (Marinho et al., 2012)

Region I	Region II	Region III
Flow stress does not depend on strain rate, low m values are seen, small deformations only	High m values occur, strain rate has important effect on flow stress, large deformations can occur	Flow stress does not dependent on strain rate, low m values are seen, small deformations only
Limited elongation of individual grains	Nearly no elongations of individual grains occur, grains move together, only small changes of neighbour grains	Limited elongation of individual grains

It should be considered that there is not only one model to express mechanical and metallurgical features in SPF. Sometimes, it is not possible to obtain same results from mechanical tests as in the SPF process. (Marinho et al., 2012)

2.2.2 Superplastic Blow Forming

SPF is a pressurized forming method that has ability to manufacture complex shapes from superplastic alloys and is also named as superplastic blow forming. **Figure 2.10** shows steps of superplastic blow forming processes, as seen in the figure, to form the sheet, a die cavity and gas pressure is required, sheet is clamped to the die and pressure of the gas is applied to it.

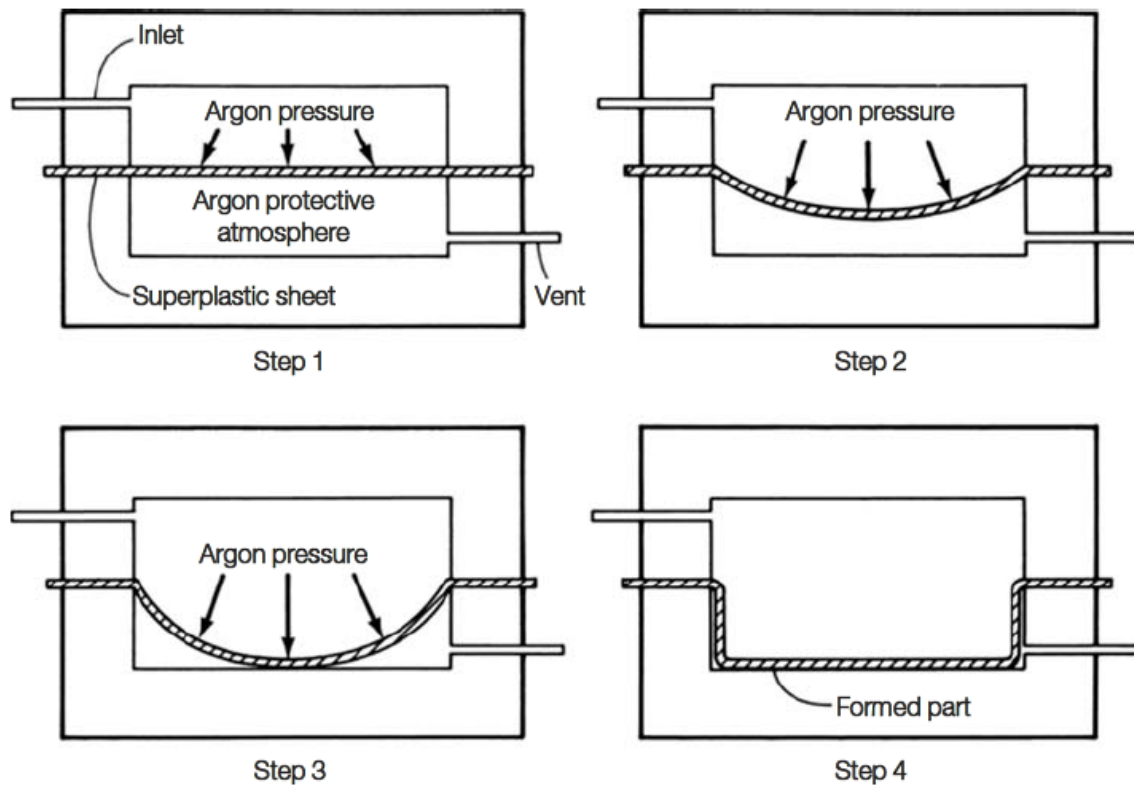


Figure 2.10: Steps of superplastic blow forming process (N.N., 2008)

In order to realize forming process, an inert atmosphere is required, argon gas is generally used for pressurization, and argon gas also saves inert atmosphere to maintain forming process. Profile of pressure versus time needs to be determined prior to process, because controlled rate of deformation is required. At the beginning of process, workpiece is not in contact with the die, deformation happens at the pole of the sheet. As a result of that, high deformation strains occur at that region during initial stages, later specimen has contact with the die, and corners are filled at the end of the forming process. Corners have greatest strains, so these regions can fail easier compared to other regions of the sheet metal. (Deshmukh, 2003)

2.2.3 Superplastic Forming Process Parameters

Although SPF process has many advantages which are mentioned in Chapter 2.2, forming process is expensive with this method, because temperatures of forming are very high (process temperature has to be nearly %60 of melting temperature), furthermore strain rate should be less than 10^{-2} s^{-1} and grain size of the specimen needs to be less than $10 \text{ }\mu\text{m}$. Small grain size materials are not unfortunately cost effective, since they require expensive processes to be obtained. Low strain rates make the process long and not suitable for mass production. It is important to consider both economic and technological aspects of SPF technology before deciding to produce a part with SPF method. (Cappetti et al., 2010)

Many investigations have been done by researchers since now to optimize process of SPF, for instance the effects of temperature and forming speed on the forming limit diagram by Naka and others. (Naka et al., 2001)

Furthermore, Luckey and others achieved simulation of improvement of SPF process with thickness profile. (Luckey et al., 2009)

2.2.3.1 Temperature

Deformation temperature T_{def} should be greater than the half of the absolute melting temperature T_m , for the occurrence of superplasticity.

$$T_{def} > \frac{1}{2}T_m \quad (2.6)$$

Depending on the used material, temperature value activating and balancing GBS and DC changes. High working temperature increases contribution of GBS to final elongation and reduces strain hardening. Although high temperature improves mechanical characteristics of product, it causes molecular phenomenon like rising grain size. Moreover, high forming temperature decreases life time of die and presses because of higher stresses. Therefore, better mechanical presses with improved mechanical properties but with high costs are required. (Cappetti et al., 2010)

2.2.3.2 Pressure Cycle

During SPF, contact areas between sheet and die increase and strain rate reduces. To have constant strain rate, pressure during process must increase with time. Control of strain rate is very significant since it affects three flow phenomenon and Backofen sensitivity coefficient m . With increasing strain rate, strain hardening rises and it causes worse mechanical properties of product. With fixed temperature, m value increases at first up to a maximum strain rate value then it decreases. (Cappetti et al., 2010)

2.2.3.3 Die

One of the most important parameter is the radius of the die since it affects the thinning and breaks. For instance, small radius at the top of the die prevents material flow towards the center of blank and increases global thinning. Furthermore, complex and very deep dies also obstruct material flow. (Cappetti et al., 2010)

2.2.3.4 Lubrication

Lubrication helps sliding between blank and die and it influences thinning of blank. It has a direct influence on friction force level during process. High friction coefficient causes high friction forces which results non-homogeneous thickness distribution. Therefore, in SPF processes it is important to reduce friction coefficient by utilizing lubrication. (Cappetti et al., 2010)

2.2.3.5 Grain Size

Superplastic materials ought to have equiaxial and fine grained structure, it is known that grain refined materials have higher strain rates and they require less forming temperature. **Figure 2.11** shows how strain rate is increasing for small grain sizes, and **Figure 2.12** illustrates forming temperature decreases for small grain sizes. (Sieniawski and Motyka, 2007)

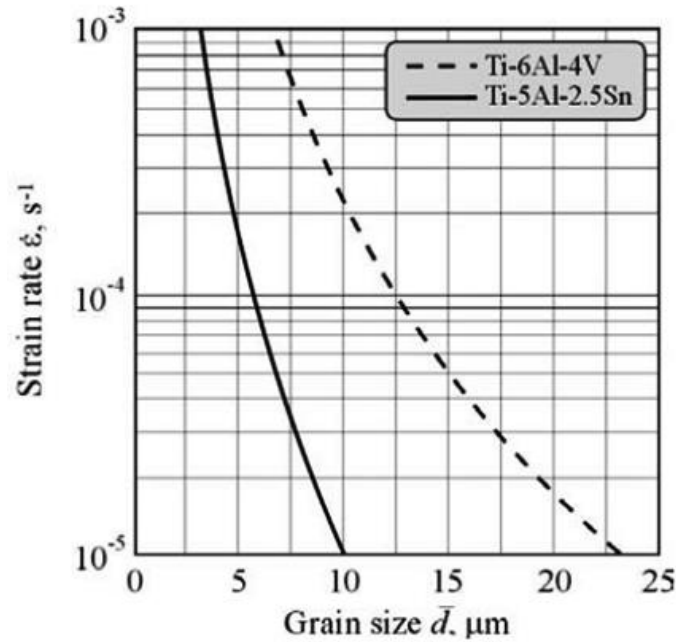


Figure 2.11: Effect of grain size to strain rate (Sieniawski and Motyka, 2007)

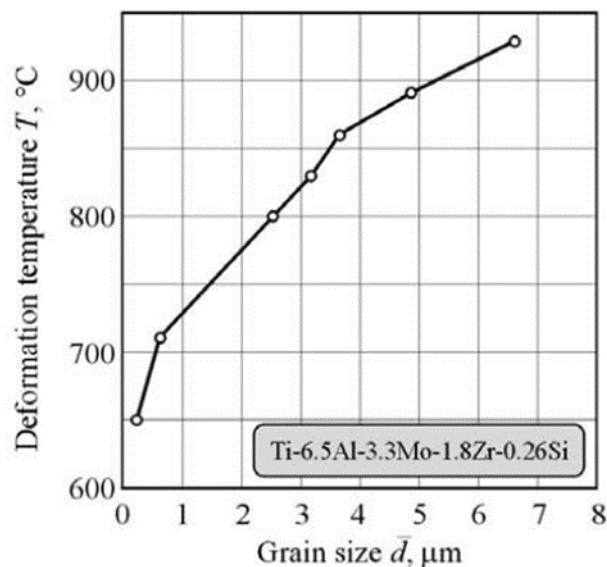


Figure 2.12: Effect of grain size to working temperature (Sieniawski and Motyka, 2007)

When evaluating aspects of SPF process, some features need to be considered such as distribution of thickness, maximum thinning, forming time, required pressure, occurring stresses and cost of manufacturing. Maximum thinning and distribution of thickness are related to mechanical features of product which are stiffness, strength, they also determine quality of the product from customer side. Forming time is mostly related to

feasibility of the process, since if it has such a long time it can be unacceptable. (Cappetti et al., 2010)

2.2.4 Technological and Economical Aspects of SPF Process

In a superplastically formed part, hardening of material does not exist and spring-back is zero, furthermore neck free and very large elongations are possible with SPF process. SPF process enables to produce very complex parts in one step, this removes many assembly processes, joints thus decrease part weights. These properties of product make it a very good finished product which has high dimensional accuracy that obstructs extra finishing treatments. Furthermore, it reduces metal consumption from 2-5, labour of machining is also decreased with this process, it also enables to reduce manufacturing costs because lower power equipment can be used and their service costs are less compared to other processes. SPF process is being used in aerospace and automotive industry, medicine and ship building where material savings are very crucial. Especially product quality, weight reduction, service lives are very important for aerospace industry since product costs are high and quality of product is very important for safety requirements. (Ermachenko et al., 2011)

Low flow stresses and large elongations during SPF process make it to be used as a manufacturing process like thermoforming of plastics. (Ceschini and Afrikantov, 1992) SPF is expensive, because process temperature is high which is more than 60% of material melting temperature, grain size in average should be less than 10 μm , and strain rate required is very small. (less than 10^{-2} 1/sec.). Small grain size requires very expensive material treatments; furthermore, different heat treatments can be required to advance material mechanical properties. SPF is being used in aerospace industry for more than 30 years for production of such as blades, discs of gas turbine, cylinders and flanges. For example, fan blades are used to be manufactured with conventional method fabricating. Fabricating of fan blades required labour-intensive mechanical working and utilization of metal was very low. Furthermore, deformation of part is very high and hot blank faces into contact with cold die which causes plasticity to decrease and local zones with different properties are created. These handicaps of conventional process lead to manufacture fan blades with SPF process. (Ceschini and Afrikantov, 1992)

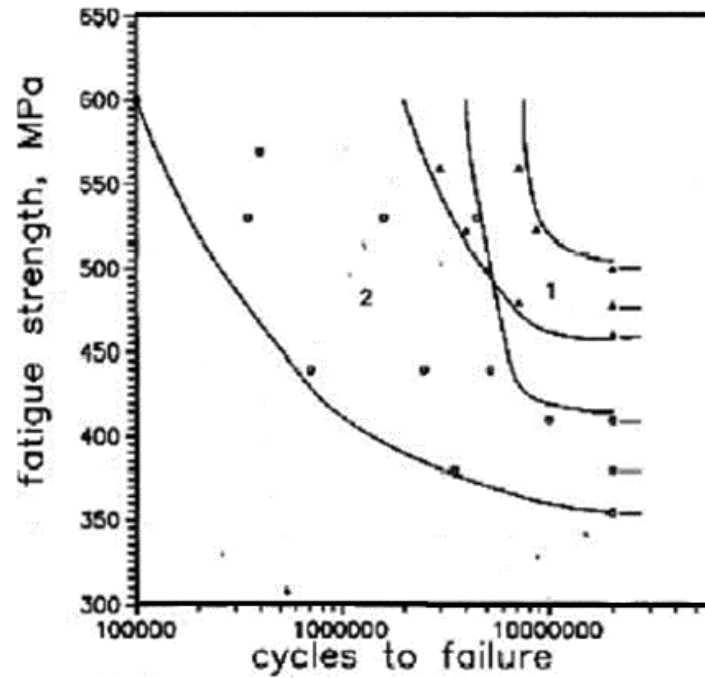


Figure 2.13: Fatigue curve comparison for fan blades for SPF (1) and conventional (2) methods (Afrikantov, 1992)

Comparison of fatigue strength versus cycles to failure diagram for both methods is illustrated in **Figure 2.13** and it proves that SPF process significantly improves fatigue strength properties compared to conventional method. Furthermore, it creates more near-net shape product under superplastic conditions. (Afrikantov, 1992)

Forming limit diagram (FLD) for materials are defined with a curve of major strain versus minor strain, FLD expresses the boundary within elastic or plastic deformation, failure possibility is expressed by the distance between actual strain condition in the forming process and the forming limit curve. Usage of SPF process is restricted by slow strain rates, this is elemental feature of the process and needs to be localized to the area which has forming risk, here strain needs to be small which makes process time long. Although SPF process has excellent features which make it very advantageous over conventional forming processes, handicaps mentioned above need to be considered before deciding to use this method for production of a part, both technological and economic factors should be considered. (Marinho et al., 2012)

When selecting a process and material for manufacturing purpose main considerations are minimum cost and maximum structural efficiency. Weight and cost savings drive to select SPF for manufacturing process.

2.3 Information about Superplastic Titanium Alloys

Ti alloys are one of the most important materials in high strength materials, especially in aerospace industry. Mostly, aircrafts are manufactured by Al alloys, for the high temperature exposure and unyielding strength necessary places Ti alloys are preferred. Al has lower density compared to Ti alloy, but Al alloys do not have high strengths at elevated temperatures. Furthermore, Ti alloys have also corrosion free features while Al not. Cost of a Ti alloy is nearly 8 times more expensive than an Al alloy. In these days, it is really significant in aerospace industry to have advancement in technology from design, production sides. SPF is an advanced technology that supplies reductions in both procurement and life cycle costs. (Sieniawski and Motyka, 2007)

In this section, SPF characteristics of Ti alloys will be investigated, since they are irreplaceable materials of aerospace industry.

Superplastic alloys are mostly two-phase alloys such as Al₆Cu_{0.4}Zr, Ti₆Al₄V, Ni₉Si_{3.1}V₂Mo, since grain size stability is provided by one phase, as a result material becomes less prone to grain growth. Ti and Ti matrix composites are generally interest by manufacturers and researchers. Especially, Ti₆Al₄V alloy is utilized and investigated in recent years. At 70's years, ultimate tensile elongation of this alloy was approximately 1000% at 10⁻⁴ 1/sec. strain rate, but it has been improved by the recent develops. For instance, applied thermomechanical methods doubled tensile elongation and increased strain rates nearly 100 times. TiAl or Ti₃Al are intermetallic alloys which are relatively new group in superplastic Ti alloys. Intermetallic based alloys are known with their high temperature creep resistance and high relative strength. (Sieniawski and Motyka, 2007) As seen from **Figure 2.14**, extremely high elongations are possible with Ti₆Al₄V compared to other commercial superplastic alloys.

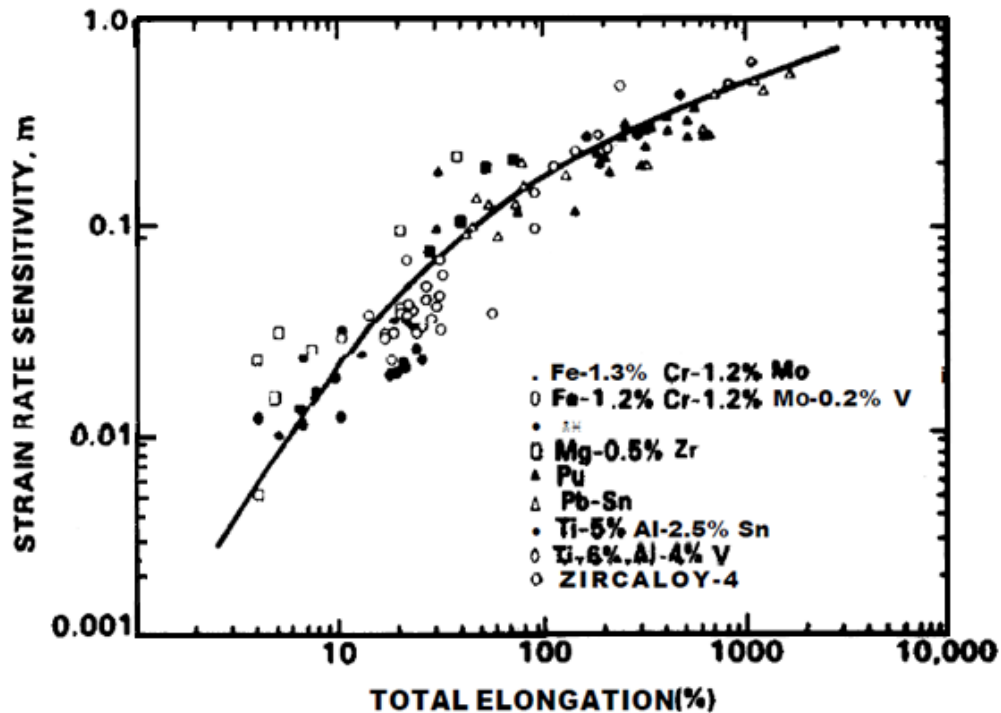


Figure 2.14: Strain rate sensitivity diagram of superplastic materials (Ghosh and Hamilton, 1986)

Optimum conditions for Ti6Al4V is at a temperature between 870°C and 927°C and 4-8 μm grain size. Strain rate intensity is investigated by many researchers and values in the range of 0.5-0.8 showed increased elongations. (Miller et al., 1979)

2.4 Finite Element Formulation of SPF Process

FEM is a numerical procedure to analyse many problems which are mostly very complicated to be able to be solved by classical analytical methods, and FEA is a very useful method to solve engineering problems. (Deshmukh, 2003)

Since the early one dimensional membrane analysis of Ghosh and Hamilton (Ghosh and Hamilton, 1986), many innovations have been done to obtain more realistic nonlinear finite element models of SPF process. It is now achievable to get more accurate thickness predictions of complex 3d shapes and gas pressure profiles which can be later directly applied to gas management systems. Furthermore, it is possible to visualize sheet movement while the whole forming process. It is also possible to see wrinkles and study on how to obstruct them, then it is possible to develop real tool with the desired properties. By the usage of commercially developed software and powerful computers,

in just a few central processing unit (CPU) hours, it could be possible to validate tool design and optimization of process parameters. It has still challenges to have a successful SPF modelling which can be summarized as;

- Selecting explicit or implicit analysis codes
- Having sensible constitutive equations for interested materials
- Reliable modelling of tool and dies (Marinho et al., 2012)

In order to simulate a forming process by finite elements method, first model of the sheet-die assembly is created, according to problem, 2D, 3D, axisymmetric or symmetric models can be created. Best model should be decided according to computational costs, then model is divided by finite elements by choosing convenient element type and appropriate element size. Choosing the material model is one of the most important steps of forming analysis, because it specifies the strain and stress behaviour of the parts during analysis. Finally, boundary conditions and loads are applied to the model, here loads simulate the releasing the plunger to the clamped sheet. It is possible to model irregular shaped structures, handle various boundary conditions, process parameters easily and cheaply compared to testing in a real condition. Advantages of FEM make it an ideal tool to analyse SPF processes. (Deshmukh, 2003)

Most of the researches of SPF has been done since now is to develop an optimum pressure algorithm in order to reduce forming time and to obtain uniform thickness distribution.

2.4.1 Implicit and Explicit Approaches

Explicit and implicit methods are approaches used in numerical analysis for obtaining numerical solutions of time-dependent ordinary and partial differential equations, as is required in computer simulations of physical processes. Metal forming processes are classified as quasi-static or high strain rate phenomena. In a quasi-static problem, kinetic energy is an unimportant part of total energy, SPF is in this category, while in high strain rate problems kinetic energy constructs an important role and they are generally dynamic processes.

Implicit approach is a method that gives full static solution of the deformation with control of convergence, this method enables large time increments, but when contact occurs, it obstructs high time increments. Computation time can increase 4 times with increase in elements. Also, at bifurcation points (for instance at beginning of wrinkling) there is singularities in the stiffness matrix. Central time differentiation scheme is utilized by dynamic explicit method, and time step is calculated by **Equation (2.7)**.

$$\Delta t \approx \frac{L}{\sqrt{\frac{E}{\rho}}} \quad (2.7)$$

Here, L is the length of the element, E is the Young's Modulus and ρ is the density. For a SPF analysis, a time step is very small and this causes high number of time steps, this makes this method disadvantageous for SPF analysis. Increasing density of material is a method to decrease the required number of time step. (Deshmukh, 2003)

Both method can be successful in SPF analysis, hence implicit method is a better choice for SPF from time perspective and enables full static solution of problem with control of convergence, so implicit method is preferred in this study.

2.4.2 Finite Element Analysis of SPF Process in ABAQUS Software

In this study, commercial finite element solver ABAQUS 6.13.1 which is a FE code includes direct implicit integration time integration by Hilber-Hughes operator is used. This program is selected generally for SPF processes, because it permits a full static solution of deformation problems with a convergence check. Furthermore, time increment size could be arranged practically. However, in an explicit analysis method, stability criterion makes the time steps very small and it can require thousands of time steps. Quasi-static implicit method is a better choice than explicit dynamic method for a SPF process. (Nazzal and Khraisheh, 2005)

SPF process is a complex forming procedure that has large strain, deformation, nonlinearity of materials and boundary conditions generally depend on material nonlinearity. As a result, numerical analysis of such a complex and nonlinear problem is really difficult. However, SPF can be expressed by flow stress which is a function of strain rate, this permits the material to be described as rigid viscoplastic. Consequently,

FE analysis of SPF process can be achieved using the creep strain rate control scheme within ABAQUS.

Constitutive behaviour of the specimen is very crucial to predict thickness distribution behaviour accurately during the forming process. In this study, material behaviour is expressed by the **Equation (2.8)**.

$$\sigma_e = K \cdot \dot{\varepsilon}^m \quad (2.8)$$

Here, σ is flow stress and $\dot{\varepsilon}$ is the strain rate, K is material constant and m is strain rate sensitivity index. In the FE analysis, this equation can be implemented by usage of creep material model in ABAQUS. (Chen et al., 2001)

2.4.3 Modelling of SPF Process in ABAQUS Software

SPF can require modelling of very complex components, so it is very important to model shape of die surface accurately and generate an adequate mesh quality. It is possible to use advantage of symmetry, which can be reflective, skew, axial or cyclic. Here, symmetry means having symmetry in geometry, material properties and boundary conditions. Modelling assemblies partially is very advantageous, it decreases solution time. In a SPF analysis, more than quarter of the die needs to be modelled, because it is crucial to avoid points fall off the die surface during course of the analysis, and it obstructs contacting nodes to slide off over master surface. Die geometry can be meshed with three dimensional rigid elements, for a good convergence it is necessary to create rigid surface representation. Rigid elements are defined with R3D3 triangular elements, and ABAQUS automatically smooths any discontinuous surface normal transitions between the surface facets. (Nazzal and Khraisheh, 2005)

Mesh of the sheet is the main concern when doing FE analysis of SPF process. Sheet can be meshed with a membrane element or a shell element. In this analysis membrane element is preferred, because it is efficient from computing time and contact behaviour is handled easier. Membrane elements are type of surface elements and they only transmit in plane forces and they do not transmit moments, they don't have bending stiffness. In SPF, bending effect could be ignored because thickness of sheet is very small regarding to other dimensions. Membrane elements have 3 degrees of freedom.

In a nonlinear analysis, cross section of the sheet changes with time. As seen in **Figure 2.15**, positive normal direction of a membrane element is expressed by right hand rule, and top surface of the membrane element is named SPOS face for contact definition and bottom surface is called as SNEG face for contact definition. (Hibbit and Hibbit, 2001, Deshmukh, 2003)

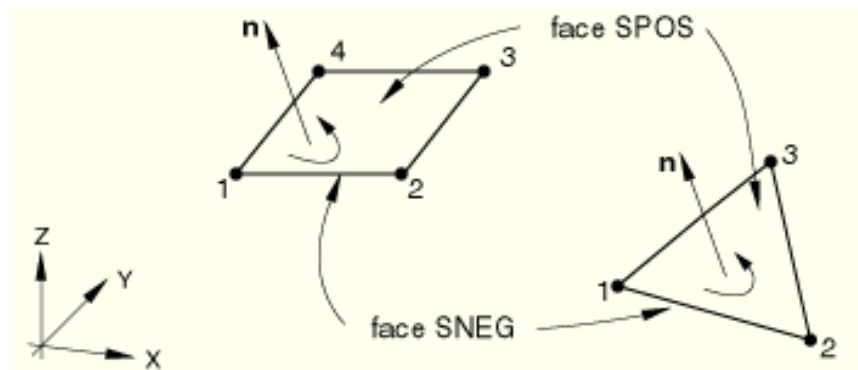


Figure 2.15: Positive normals for general membranes (Hibbit and Hibbit,2001)

In this study, M3D4 element typed membrane elements are used which are fully integrated bilinear membrane elements. In a SPF analysis, very large displacements occur and this can lead to buckling of sheet material when it is subjected to compressive loads. This condition can be handled by application of a small biaxial initial stress, the value of that stress should be in a value that final solution is not affected.

After meshing of the die and sheet metal part, another concern is definition of the contact behaviour between them. Contact problem in a SPF process is little complicated because sheet is not in contact with die at early stages and which parts are in contact in any stage is not clear, as a result contact is nonlinear because of asymmetry. A node could be in contact or rigidly constrained. In SPF analysis, classical ABAQUS coulomb friction model could be used, two surfaces are defined as contact pair which can have contact, there is master and slave surfaces. Node of the slave surface tries to find the closest node on master surface during analysis. In SPF analysis, rigid surface needs to be defined as master surface and deformable body should be defined as slave surface.

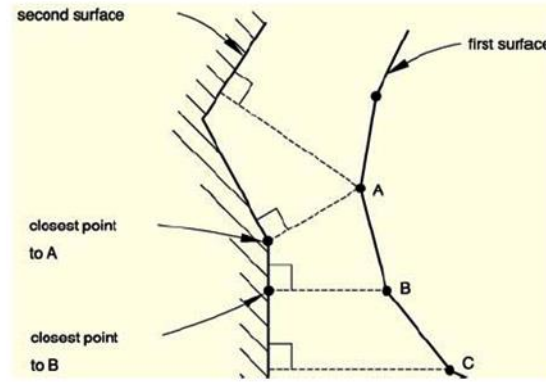


Figure 2.16: Coulomb friction in ABAQUS (Deshmukh, 2003)

Loading and controlling of the load is very important while realizing a SPF analysis. Controlling process parameters is one of the main difficulties of such an analysis. Temperatures and strain rates of the work piece should be in certain range that superplastic deformation can continue. Process should be realized as soon as possible and strain rates should not be more than maximum allowable strain rates at any location of the sheet. For this concern, ABAQUS has a component which helps to control loading with a solution dependent amplitude and a target maximum creep strain rate. This is activated by using the creep module of ABAQUS while material properties definition. When preparation of the analysis, user should define the reference value. When defining the amplitude, user should give initial, minimum and a maximum load multiplier. During the quasi static analysis, ABAQUS compares the maximum creep strain rate with target value, and load application is done based on this comparison. (Hibbit, 2001)

Solution dependent amplitude pressure varies while simulation to maintain strain rate at a target strain rate. While any increment, ABAQUS calculates ratio of maximum equivalent strain rate to the target strain rate ($\varepsilon_{opt}^{\circ}$) which is specified by user. For any integration point for a specified element set. (see **Equation (2.9)**.)

$$\gamma_{\max} = \frac{\varepsilon^{\circ}}{\varepsilon_{opt}^{\circ}} \quad (2.9a)$$

At an increment n , the pressure algorithm is progressed as below;

$$\text{If } \gamma_{\max} < 0.2 \text{ then } P_{r+1} = 2.0P_r \quad (2.10a)$$

$$\text{If } \gamma_{\max} > 3 \text{ then } P_{r+1} = 0.5P_r \quad (2.10b)$$

$$\text{If } 0.2 \leq \gamma_{\max} < 0.5 \text{ then } P_{r+1} = 1.5P_r \quad (2.10c)$$

$$\text{If } 0.5 \leq \gamma_{\max} < 0.8 \text{ then } P_{r+1} = 1.2P_r \quad (2.10d)$$

$$\text{If } 0.8 \leq \gamma_{\max} < 1.5 \text{ then } P_{r+1} = P_r \quad (2.10e)$$

$$\text{If } 1.5 \leq \gamma_{\max} \leq 3 \text{ then } P_{r+1} = 0.5P_r \quad (2.10f)$$

Here, P_{r+1} is the new calculated pressure to be applied at iteration number $r+1$, while P is applied pressure value of previous iteration whose number is r . Calculated pressure is applied to the free forming region of the sheet at each increment and clamped region is constrained from all degrees of freedom. (Hibbit, 2001)

SPF analysis in ABAQUS could be realized in two steps, first step is considered as elastic, the pressure is applied in a very short time and so the response is purely elastic. At second step, creep response is developed by usage of quasi-static procedure. During quasi-static step, an accuracy tolerance is specified and this controls the time increment so accuracy of the creep solution. When comparing the creep strain rate at the beginning and end of an increment, ABAQUS considers the difference and it should not be more than the tolerance divided to time increment. If it is higher, this step is repeated with a smaller time increment. Specification of this tolerance value is important, since it affects the stress and strain results. Lower tolerances end with good analysis results close to real values but they require more computation efforts. (Nazzal et al, 2004)

SPF analysis by using creep module in ABAQUS could be realized by using the creep definition available in ABAQUS, by application of time hardening power law. Time hardening power law is defined as the formula below;

$$\sigma_e = K \cdot \varepsilon^m \quad (2.8)$$

$$\varepsilon^{\circ} = C \sigma^n \quad (2.11)$$

Here, n is creep stress exponent and C is the power law multiplies, n and C should be from an experimentally determined study. (Deshmukh, 2003, Hibbit, 2001)

2.5 Machine Learning and Data Mining

High performance computing and developments in information technology which are used in engineering simulations lead to having large data sets. Increasing data set is due to analysing them manually, hence there is information hidden in the available large data

sets and they are generally cannot be discovered manually, at this point, data mining techniques are required. (Twin, 2016)

Data mining is a sub-branch of computer science and utilized to find out patterns in huge data sets by using methods such as machine learning, statistics, artificial intelligence and database systems. Data mining in overall desires to get information from available data sets and create a structure which could be used in future. Data mining techniques are significant in design processes for engineering like structural, thermal flow design problems. When discovered problem gets more complicated, parameters and obtained data sets become huge and difficult to overcome. (Twin, 2016)

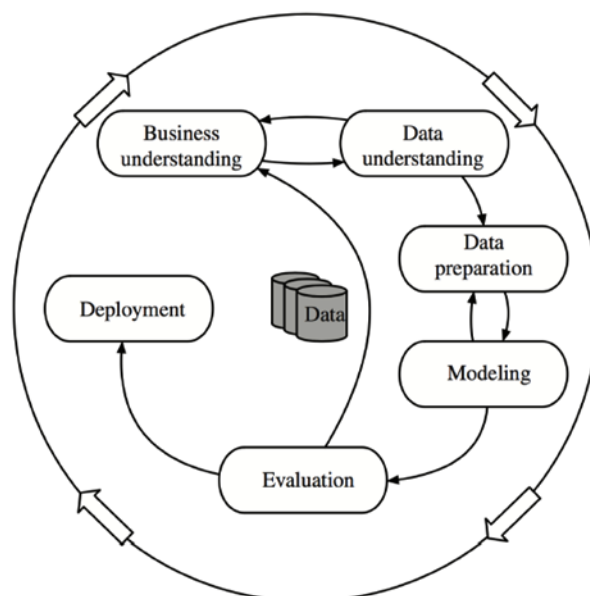


Figure 2.17: Illustration of data mining process cycle (N.N., 2016)

Figure 2.17 illustrates the data mining process cycle, it firstly started with business understanding which requires understanding objective of business and finding the needs. Later, data understanding starts in which initial data collection is done to be familiar with data, here data is explored, visualized and understood, and users ask themselves if the data has enough quality and required data collection is complete. Then, data preparation phase initiates which is the most time consuming phase of the data mining process. User needs to explore all available data set, if they make sense, if some of them should be cleaned or new data should be added. Later, they are formed into desired form according to which result is aimed to obtain. After data preparation phase, modelling

phase starts. Here, according to problem type modelling techniques is selected by thinking about required quality and validity of the model, then model is evaluated. Model results are evaluated in the evaluation phase, if they meet the business requirements. If the results are not adequate, users need to return to business understanding phase, else deployment phase starts, in the deployment phase obtained results are presented and documented to be used in further. (Waikato, 2016)

Machine learning is a sub-branch of computer science and one of the methods used for data mining which can make computers learn without explicitly programmed. Machine learning investigates the current study and builds the algorithms to learn from data and make predictions based on that. Machine learning is a method used in many fields in order to construct complicated models and algorithms for prediction. Analytical models used for machine learning enable researchers, engineers, analysts and data scientists to obtain reliable, repeatable decisions and results by learning from trends and historic relationships in the data. (Simon,2013, Britannica,2009)

Machine learning and data mining are wide topics and this study will not go into detail. This study uses machine learning technique for data mining in order to create a learning from available data sets created from investigation of process parameters for SPF process analysis.

2.5.1 Regression Technique for Machine Learning

Machine learning has variable algorithms for predictions. Regression is one of the most popular algorithms used in machine learning. Regression is a method for predictive modelling which explores the relationship between a target (dependent variable) and predictor (independent variable).

Regression technique is important in order to investigate data and it fits a curve or line to data points to represent general behaviour of given data. **Figure 2.18** illustrates an example of simple linear regression; red line represents fitted line for given data points.

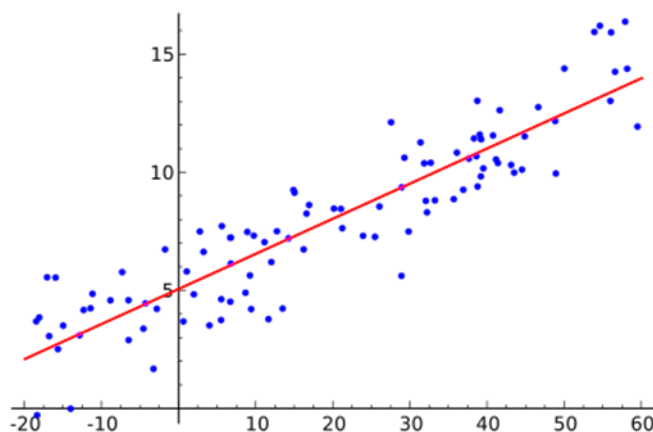


Figure 2.18: Representation of simple linear regression (Analyticsvidhya, 2016)

Regression method could both indicate relationship between dependent and independent variables, also strength of impact of different independent variables for a dependent variable. Regression technique includes many different types to make predictions and usage of each method can be decided according to number of independent variables, type of different variables and shape of regression line. (Analyticsvidhya,2016) Only limited versions of regression techniques are mentioned in this study.

2.5.1.1 Linear Regression

Linear regression is one of the most used and known prediction modelling technique. In linear regression technique, dependent variable is continuous and independent variables can be continuous or discrete, also regression line is linear. Linear regression aims to find relation between dependent variable (Y) and independent variable (X) by creating a line which fits variables.

Linear regression line represents an equation below, here a is intercept, b is slope of line and e is the error terms, so this formula enables to predict dependent variable. (Analyticsvidhya,2016)

$$\mathbf{Y = a + b * X + e} \quad (2.12)$$

2.5.1.2 Least Square (LS) and Least Median of Squares (LMS) Regression

LS regression is a regression technique whose solution minimizes sum of squares of errors occur at result of each equation.

$$Y_i = \beta_0 + \sum_{k=1}^p \beta_k X_{ik} + \varepsilon_i \quad k = 1, \dots, p \quad (2.13)$$

LS regression is expressed with above formula, here Y is dependent variable, X_1, \dots, X_p is independent variables, β_0, \dots, β_p are regression coefficients, finally $\varepsilon_1, \dots, \varepsilon_n$ are independent set. Best fit of data occurs when this method minimizes the residuals which is defined as differences between observed and predicted response to solve set of equations. Least square regression method is notorious when there are uncertainties in the independent variables. In this case better models are required, because sometimes sacrificing to fit bulk of data occurs to obtain large advance to fit outliers. In order to prevent these problems robust regression techniques are developed. One of them is LMS regression which minimizes the median of squared residuals, since they are not changed by outliers, so response outliers do not affect or distort fitted line and easily identified in residual plots. **Figure 2.19** illustrates robustness comparison of two methods. (Analyticsvidhya, 2016 and Dallal,1992)

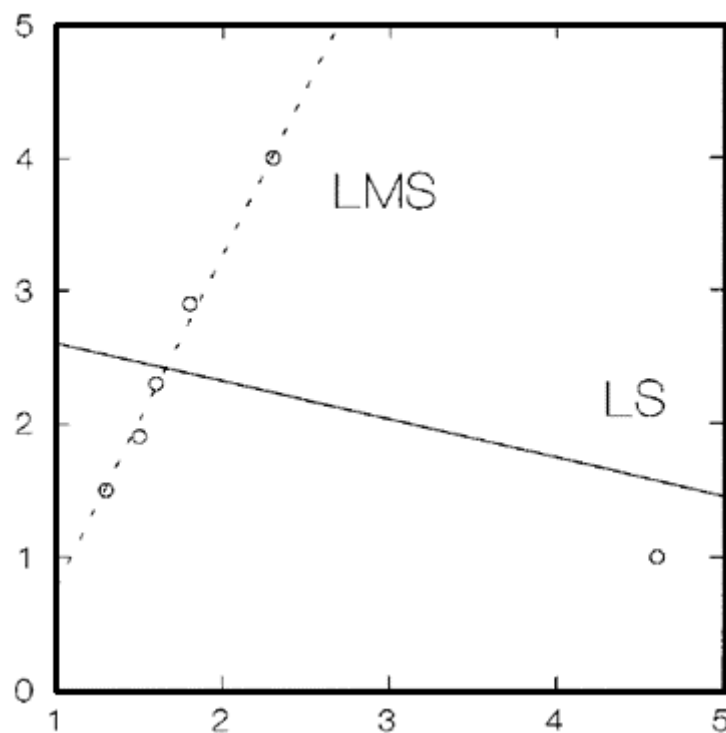


Figure 2.19: Robustness comparison of LS and LMS regression methods
(Dallal,1992)

3 Aim and Scope of the Thesis Work

SPF process is widely used in Aerospace industry for its many advantageous features. The company TEI also aims to add SPF process capability to its production abilities to be able to compete with other suppliers. Cold forming and hot forming could also be preferred as manufacturing method, but it could only succeed elongations until 200% while SPF can achieve elongations until 1000%, furthermore TEI aims to decrease weight of components by removing joints that are used in conventional processes for assembly purpose, because SPF enables to produce parts in one step. (Shojaeefard et al., 2014) Furthermore, increasing service lives and saving cost are another reasons for preferring this method as an alternative approach. (Ermachenko et al., 2011) In order to compete with other suppliers for aviation industry, TEI needs to include SPF to its current capabilities.

Before producing aerospace parts with SPF method, TEI aims to deeply learn the process by investigating process parameters for simple geometries like rectangular and conical parts for Ti6Al4V material which is the most popular material for aerospace industry. Since, experiments for many process parameters are expensive especially because of high cost of raw materials, process parameters are aimed to be investigated by a commercial finite element program, ABAQUS. Due to experimenting limitations, analysis method is compared with experiments of Moscow State University which is available in literature. Later, process parameters are investigated for rectangular and conical shaped specimen and results are evaluated for time and quality perspective. A handicap encountered while investigation of process parameters of SPF process is the process time which is an input to the program and needs to be estimated, and this forces the user to make many analyses. For this purpose, an equation is developed in order to estimate process time of SPF process by entering process parameters for a rectangular box, and a software is developed to utilize this equation to be used in the factory. Later, in order to use the information obtained from simple geometries, an industrial product, which is an aircraft blowout door, is shaped with SPF process using finite element simulation for different process parameters. It is aimed to optimize the process and to cross check if the obtained information obtained for simple parts is also compatible to

complex industrial parts. Finally, a cost analysis study is conducted for this project in order to estimate the profit gain by this approach. Process chart of the thesis is illustrated in **Figure 3.1** in order to show steps of the study.

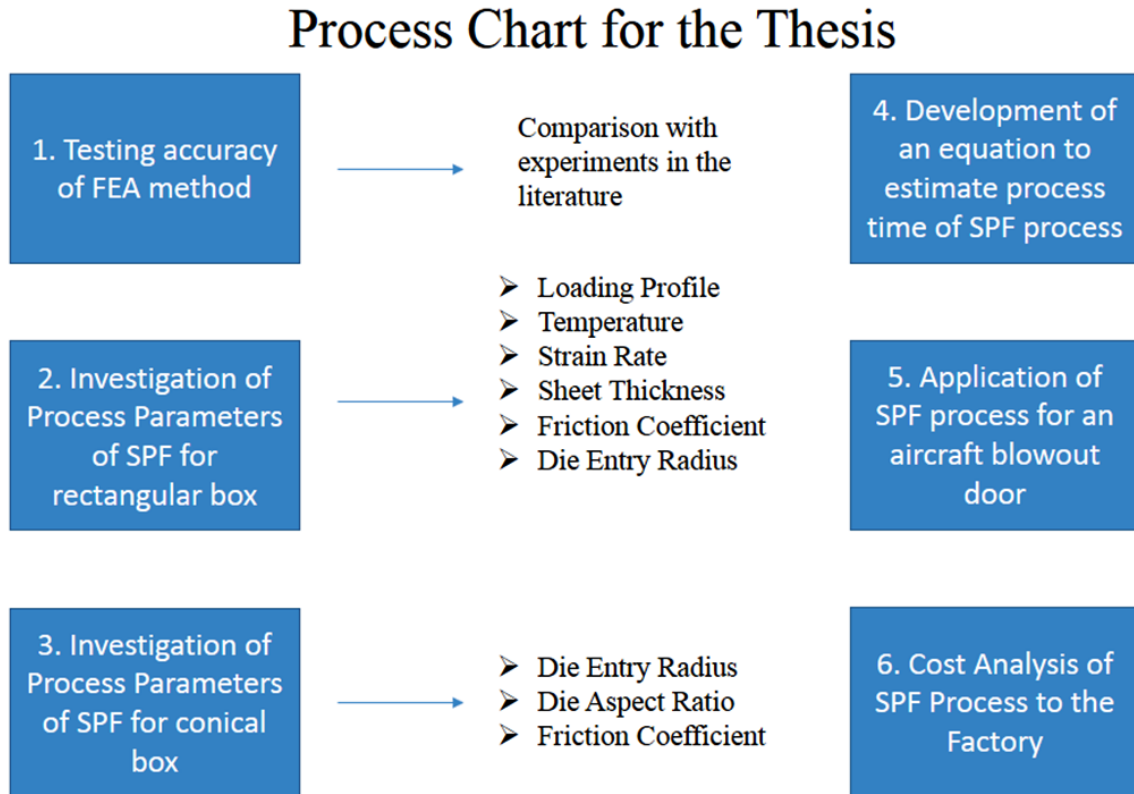


Figure 3.1: Process chart for the thesis

4 Investigation of Effect of Process Parameters to SPF Process

In this section, FE model of SPF process is realized and effects of process parameters to the forming procedure are investigated. Simulations for SPF are achieved with a commercial FEA program ABAQUS, and CREEP module in ABAQUS is used for SPF process which enables the user to define superplastic material properties. Details are explained in Chapter 2.4.2 and 2.4.3.

Power law for SPF process could be defined in ABAQUS under creep properties. Power law is defined in ABAQUS with the following formula;

$$\dot{\varepsilon} = C\sigma^n \quad (2.12)$$

In order to find out applicability of CREEP module in ABAQUS, FEA results are compared with experimental data obtained from study of Moscow State University, then process parameters are investigated for a rectangular and conical parts.

Pressure application at the beginning of SPF process is accepted to occur quickly and specimens' response is elastic. Because of that, initial of the process is analysed with a static procedure, later at second step quasistatic step is analysed with an accuracy tolerance. Time increment at that step is decided according to this tolerance, and it is important to decide an acceptable tolerance to get true results. Equivalent creep strain is compared at the beginning and at the end of each increment, the difference need to be smaller than the tolerance value division to time increment, or else same time step is realized again with smaller time increment. (Nazzal et al, 2004)

4.1 Comparison of Finite Element Analysis Study with Experimental Results

To test the accuracy of the ABAQUS creep module for modelling of SPF process, the experimental data in literature is compared to the obtained FEA results throughout this thesis. For this purpose, a study conducted in Moscow State University for mathematical modelling of SPF of a long rectangular sheet is investigated. Firstly, constant gas pressure is applied to a 1.0 mm Ti6Al4V alloy into a rectangular die which has a 15 mm depth, 30 mm width and 120 mm length at 900°C temperature. Experimental data obtained are given in **Table 4.1** for application of constant gas pressure to the sheet material.

Table 4.1: Experiment results for application of constant gas pressure to the sheet

Applied pressure (MPa)	Experiment time (sec.)
1	2
0.6	2550
0.8	1290
1.0	940
1.2	550
1.4	400

Material properties are investigated according to experimental results of Moscow State University. The following values of material constants are used as given in the study $m=0.470$ and $K=645 \text{ MPa s}^m$. Therefore,

$$\sigma_e = K \cdot \varepsilon^m \quad (2.8)$$

$$\varepsilon^\circ = C \sigma^n \quad (2.12)$$

it is assumed in calculations:

$$n=1/m=2.13;$$

$$C=1/K^n=1.8 \times 10^{-19} \text{ s}^{-1} \text{ Pa}^{-n}$$

the results obtained by taking into account the values of elastic constants have been chosen as;

$$E = 1.0 \times 10^9 \text{ Pa};$$

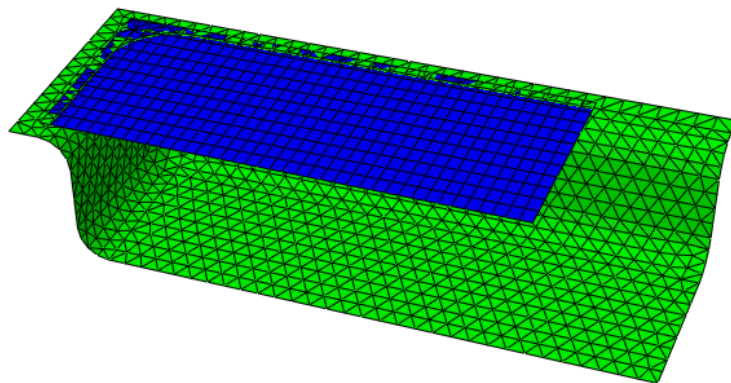
$$v = 0.49.$$

Here, E is elasticity modulus and v is poisson's ratio.

Table 4.2: Material properties for Ti6Al4V (Vasin et al., 2003)

Material properties	Values
Elasticity modulus, E (Pa)	10^9
Strain rate sensivity index, m	0.470
Material constant, K ($s^{-1} Pa^{-n}$)	1.8×10^{-19}
Poison ratio, ν	0.49

In order to compare analysis results with the experimental results, FE model for die and sheet are created in HYPERMESH program. Mesh for die and sheet could be seen in **Figure 4.1**. Material properties, boundary conditions and FEA is achieved in ABAQUS. Sheet is clamped to die to form a cavity of desired shape. Material properties given in **Table 4.2** are used as inputs for the simulations. Quarter of die and sheet are modelled in order to decrease simulation time by taking advantage of symmetry.

**Figure 4.1:** FE model for SPF process

A mesh convergence study is conducted, before comparing analysis results with the experimental data gained in literature. First, rectangular sheet metal is meshed with different element sizes starting from 2 mm to 0.6 mm and 1.4 MPa constant pressure is applied for 400 seconds and stresses and minimum sheet thicknesses obtained are compared for each element size. This mesh convergence study aims to find an optimum element size for both analysis accuracy and analysis time perspective. As seen in **Table 4.3** there is not a significant difference for analysis results, but for element size 1 mm,

results change less according to element sizes 2, 1.8, 1.6, 1.4 and 1.2 mm. Since analysis time is also one of the most important concerns, and smaller element sizes require more time for analysis, 1 mm element size is chosen for further analysis.

Table 4.3: Analysis results for different element sizes

Element size <i>(mm)</i>	Maximum von misses stress <i>(MPa)</i>	Final minimum sheet thickness <i>(mm)</i>
2.0	18.725	0.625388
1.8	18.7529	0.634236
1.6	18.7563	0.63435
1.4	18.7993	0.637205
1.2	18.7468	0.635502
1.0	18.9329	0.647104
0.8	18.8757	0.636303
0.6	18.9305	0.649478

Female die is modelled with 1767 rigid elements using R3D3 element type. To prevent sliding off contacting nodes from master surface female die is extended from axis of symmetry. Sheet is clamped on all its edges. 1765 M3D4 type elements are used for modelling of the sheet part. Rectangular box formed from a rectangular sheet after the forming process in ABAQUS could be seen in **Figure 4.2**.

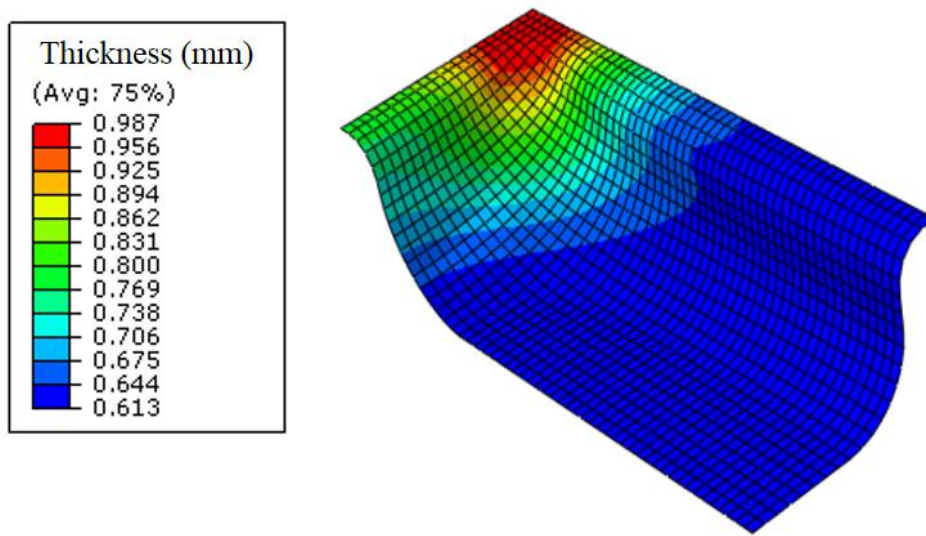


Figure 4.2: Rectangular box formed in ABAQUS for the application of 1.4 MPa constant pressure application

Table 4.4: Comparison of analysis time with experiments

Applied pressures (MPa)	Time in experiment (sec.)	Time in ABAQUS (sec.)	Difference (%)
0.8	1290	1400	8.5
1	940	850	9.5
1.2	550	570	3.6
1.4	400	430	7.5

Table 4.5: Comparison of analysis results with experiments

Applied pressures (MPa)	Min. Sheet thickness in experiment (mm)	Min. sheet thickness in ABAQUS (mm)
0.8	0.62	0.6133
1	0.62	0.6152
1.2	0.62	0.6157
1.4	0.62	0.6127

Table 4.4 and **Table 4.5** compare analysis results with experiment data given in case of time and obtained sheet thicknesses. Results are consistent for constant pressure application, since a maximum of 9.5 % error for forming time between the ABAQUS FE model and the experiment results have been achieved. In general, ABAQUS forming times are greater than those obtained in the experiments. The reason for that might be that the material model has some properties which are not inputs of ABAQUS model, and therefore it may not model forming process as realistically as real forming process.

In industrial applications, manufacturing process needs to be designed to be as fast as possible, and it should not exceed allowable maximum strain rate for formed part. Controlling the process parameters in a SPF process is one of the main challenges. Temperature and strain rate that material exposure during forming should be in a certain range to sustain superplasticity. Forming the part with application of constant pressure makes the control of process difficult from strain rate perspective. Another approach is the determination of gas pressure according to a target constant strain rate. This method is widely preferred in current studies and industrial applications, since target strain rate is predetermined to obtain maximum ductility and it also inhibits premature failures. (Vasin et al., 2003) Here, loading is controlled according to maximum equivalent creep strain rate found in the whole deformed sheet., the maximum rate is seen at the middle of the sheet, but when it has contact with die, maximum location is shifted until the whole sheet is deformed. (Nazzal and Khraisheh, 2005)

Current study also includes experimental results for application of constant strain rates. In this case, the value of the applied gas pressure (p), is varied in accordance with the pre-determined program with the aim to satisfy the following condition. (Vasin et al., 2003)

$$\dot{\varepsilon} = \dot{\varepsilon}_{opt} = \text{constant} \quad (4.1)$$

where $\dot{\varepsilon}_{opt}$ is the optimum strain rate. In this method target strain rate controls the pressure to be applied to the system.

Literature study realized in Moscow State University also applies pressures calculated analytically which are to be applied to the sheet to obtain constant strain rate.

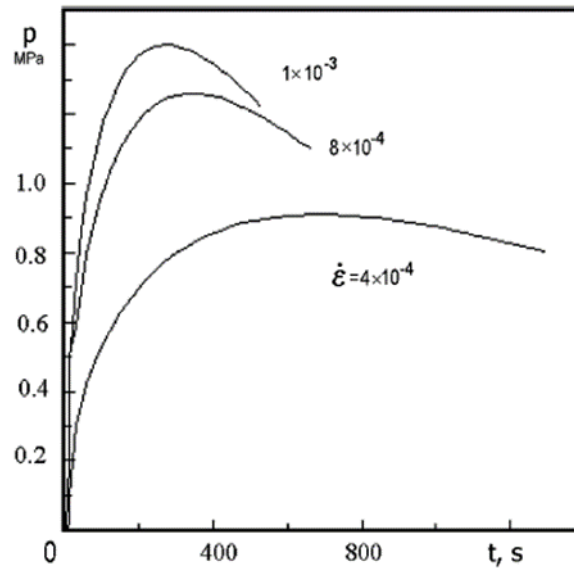


Figure 4.3: Pressure-time cycles applied in experiment for different constant target strain rates (Vasin et al., 2003)

The pressure values shown in **Figure 4.3** are applied to the workpiece in experiment to obtain constant strain rate. Experiments are realized for different target constant strain rates. ABAQUS also enables to control strain rate which means target strain rates could be obtained during forming process. User needs to supply constant target strain rates and the pressure to be applied to the system is selected by program to sustain current strain rate. ABAQUS calculates the pressure to be applied according to constant strain rate, user can set limits of pressure but pressure is not defined by user as in the experiment. Pressure is solution dependent in the analysis. User has ability to define initial, minimum and maximum multipliers for pressure, but how the pressure changes during forming is arranged according to program to get a constant strain rate.

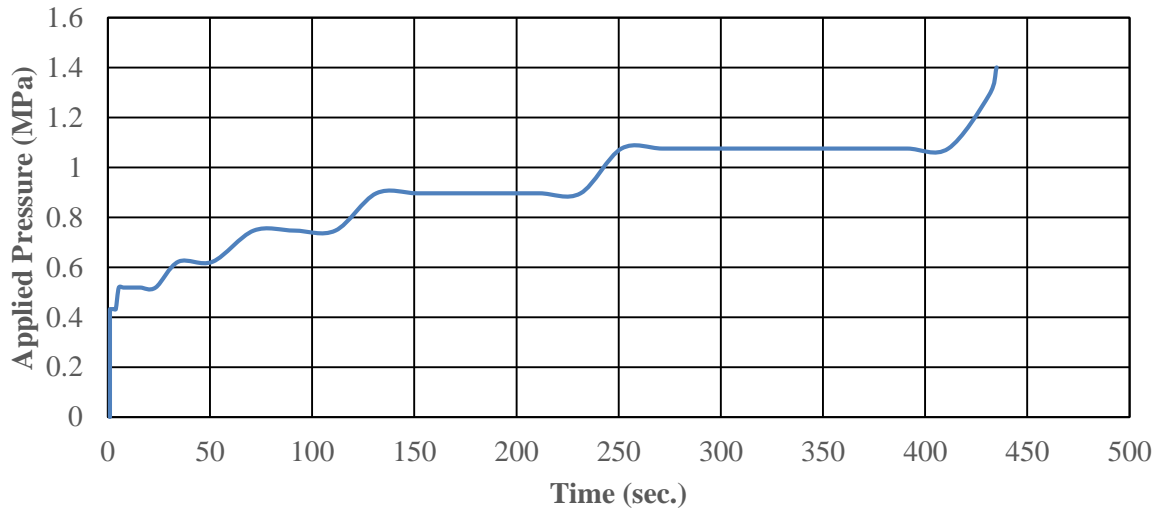


Figure 4.4: Pressure scheme applied to the workpiece for FE simulations

Analysis is realized for constant target strain rate of 10^{-3} 1/sec. and results are compared with analysis results.

Table 4.6: Comparison of analysis results with experimental data for different target strain rates

	Strain rate	Time (sec.)	Dome height (mm)	Minimum sheet thickness (mm)	Stress (MPa)
Experiment	10^{-3}	434	14.5	0.65	25.1
ABAQUS	10^{-3}	434	13.7	0.69	24.19
Difference	-	-	0.8	0.04	1.09
Difference (%)	-	-	5.5	6.15	4.34

Table 4.6 shows comparison of analysis results with experimental data obtained from dome height, minimum sheet thickness and maximum stress which occurs in the workpiece for the same forming time. For the same forming time, ABAQUS produces a part which has less dome height and sheet thickness is changed less and stress occurring in the specimen is smaller compared to experiment results.

Differences between experiment and analysis are thought to be based primarily on the loading scheme. Both method uses constant strain rate method but loading scheme is

different. In experiment, calculated pressure is applied to the workpiece to obtain target constant strain rate. In experiment, there exists a predetermined pressure cycle. In the FE study, pressure is determined by the program. **Figure 4.3** and **Figure 4.4** illustrate pressure schemes for experiments and FE analysis. In the end, they both reach the same maximum pressure value but how they are applied during the experiment and analysis is different. Another reason could be is that, the material properties are obtained from constant pressure application experiments, but these material properties are applied to the experiments for constant strain rate which can cause the difference between analysis and experiment.

This thesis aims to investigate process parameters to SPF process, in the end, TEI desires to add this process to its available process portfolio, that is why it is desired to investigate process parameters on a simple part in FE program without an experiment. In order to see applicability of creep module in ABAQUS for SPF process, results of the FE study are compared with experimental results of study mentioned above which is conducted for application of constant pressure and constant strain rate. Application of constant pressure in ABAQUS has a maximum of 9.5 % error compared to the experiments for forming time, while application of constant target strain rate can form 95% of part at the same time. This is mostly because of pressure application difference between experiment and analysis and other possible reasons mentioned above.

Although, there are differences for both methods between experiment and analysis, ABAQUS creep scheme to simulate SPF process can be used as a very useful method to investigate process parameters, which will save time and resources by eliminating experiments for expensive materials.

4.2 Investigation of Process Parameters for SPF Process for a Rectangular Part

In this section, SPF of a rectangular box is analysed with ABAQUS FEA program, a Ti6Al4V sheet material is formed into a rectangular box by application of an inert gas pressure. Sheet is clamped to die which forms a cavity of the shape required. Assembly of the die-sheet is showed in **Figure 4.6**.

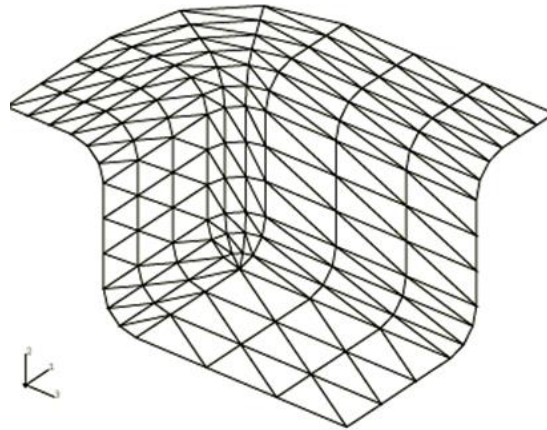


Figure 4.5: Rigid surface for the rectangular die

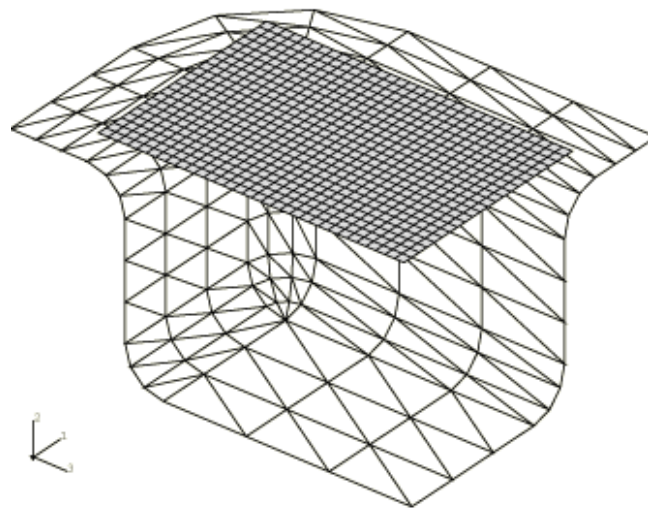


Figure 4.6: Assembly of sheet metal and die

Rectangular box simulated is 60 mm long, 40 mm wide and 20 mm deep and has 4 mm flanges around of box. The box is formed by application of a uniform fluid pressure. Advantage of symmetry is utilized here and quarter of blank is modelled with 704 M3D4 typed membrane elements which are fully integrated bilinear elements. Symmetry boundary conditions are applied to the model. Sheet dimensions are 64 mm by 44 mm and the thickness is 1 mm. Sheet is clamped on all edges, membrane model is singular in normal direction. If it is not stressed in biaxial tension, which could have caused problems and it is prevented by application of a small biaxial initial stress of 0.01 MPa by initial stress conditions. Female die is modelled with 231 rigid elements using R3D3

element type. To prevent sliding off the contacting nodes from master surface, female die is extended along the axis of symmetry.

By simulation of SPF of a rectangular box, investigation of the effect of applied pressure, process temperature, friction coefficient between die and sheet, sheet thickness, and die radius on forming process are aimed.

In order to simulate the SPF process in ABAQUS, ABAQUS creep module is used with the following formula;

$$\dot{\varepsilon} = C\sigma^n \quad (2.12)$$

Here, n is creep stress exponent and C is the power law multiplier. n and C are taken from an experimentally determined study. **Table 4.7** shows creep stress exponent and power law multipliers at different temperatures.

Table 4.7: Experimentally determined power law creep properties (Warren and Wadley, n.d.)

Temperature (°C)	Creep stress exponent, n (strain rate sensitivity: $m = 1/n$)	C (1/sec MPa ^{n})
840	1.34	1.9×10^{-5}
900	1.70	1.2×10^{-5}

ABAQUS enables to apply a constant load or the load schedule can be arranged by ABAQUS according to a target strain rate. In this section, SPF of a rectangular box is investigated first with a constant, later with the application of automatic pressure.

4.2.1 Investigation of the Effect of Loading Profile

ABAQUS enables to apply forming pressure as a constant load and solution dependent amplitude. In this section, these two different loading profiles are compared. Material properties at 840 degrees are used to determine the effect of loading profile.

Prestressed blank is formed by a rapidly applied external pressure of 1 MPa and then it is held constant for 1000 seconds until the box is formed. Before investigation of process parameters, a mesh convergence study is conducted to check if mesh quality is adequate. Different meshes are created from 1.4 mm to 0.6 mm element sizes and results are

compared. All sheets for different element sizes are applied to a constant pressure value of 1MPa for 1000 seconds.

Table 4.8: Analysis results for different element sizes

Element Size <i>(mm)</i>	Maximum von misses stress <i>(MPa)</i>	Final minimum sheet thickness <i>(mm)</i>
1.4	13.5624	0.41582
1.2	13.5954	0.41542
1.0	13.6394	0.41725
0.8	13.722	0.41435
0.6	13.7454	0.41372
0.4	13.7491	0.41408

This mesh convergence study aims to find an optimum element size for both analysis accuracy and time perspective. As seen from **Table 4.8** there is not a significant difference for analysis results, but for element size 0.8 mm results change less according to element sizes 1.4, 1.2 and 1.0 mm. Since, analysis time is also one of the most important concerns, and smaller element sizes require more computation time, 0.8 mm element size is chosen for further analysis.

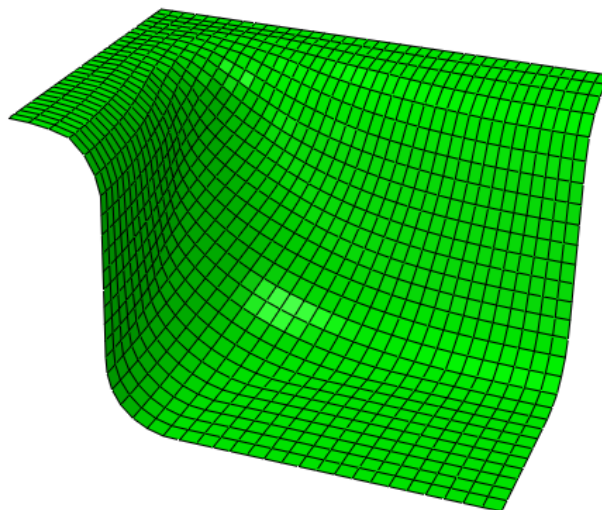


Figure 4.7: Deformed shape of sheet metal after 1000 second for constant pressure application for element size 0.8 mm

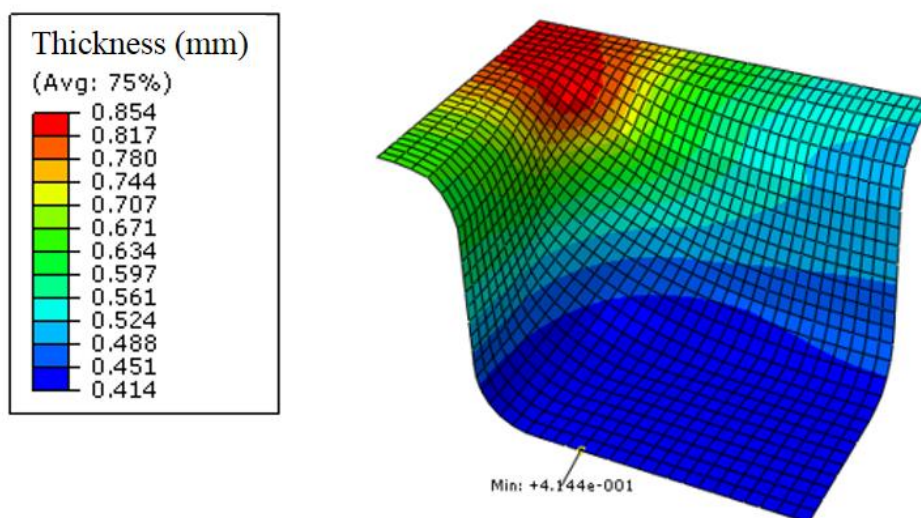


Figure 4.8: Sheet thickness distribution at blank for constant pressure application

Figure 4.8 shows sheet thickness distribution on blank after forming ends, maximum thickness reduction occurs at bottom of box which decreases to 0.4144 mm from 1 mm. Forming process needs to be as fast as possible, and in order to avoid premature failures, maximum allowable strain rate should not be exceeded. Process parameter control in a SPF process is one of the challenges. In order to sustain superplasticity, temperature and strain rate require to be in a certain range. If forming is done with application of a

constant pressure, controlling the strain rate could be difficult. Application of gas pressure according to a target strain rate is another approach, and this approach is widely preferred in current studies and industrial applications, since target strain rate is predetermined to obtain maximum ductility and it also inhibits premature failures. (Vasin et al., 2003)

In order to see effect of loading profile, same sheet is formed for a constant strain rate value of 10^{-2} 1/sec. Target strain rate is achieved by controlling the deformation at the corner node of the sheet since this is the region of maximum deformation. Pressure to be applied to the system is decided by program to obtain target constant strain rate. Pressure is solution dependent in the analysis, user has ability to define initial, minimum and maximum multipliers for pressure, but how the pressure changes during forming is arranged according to program to continue constant strain rate.

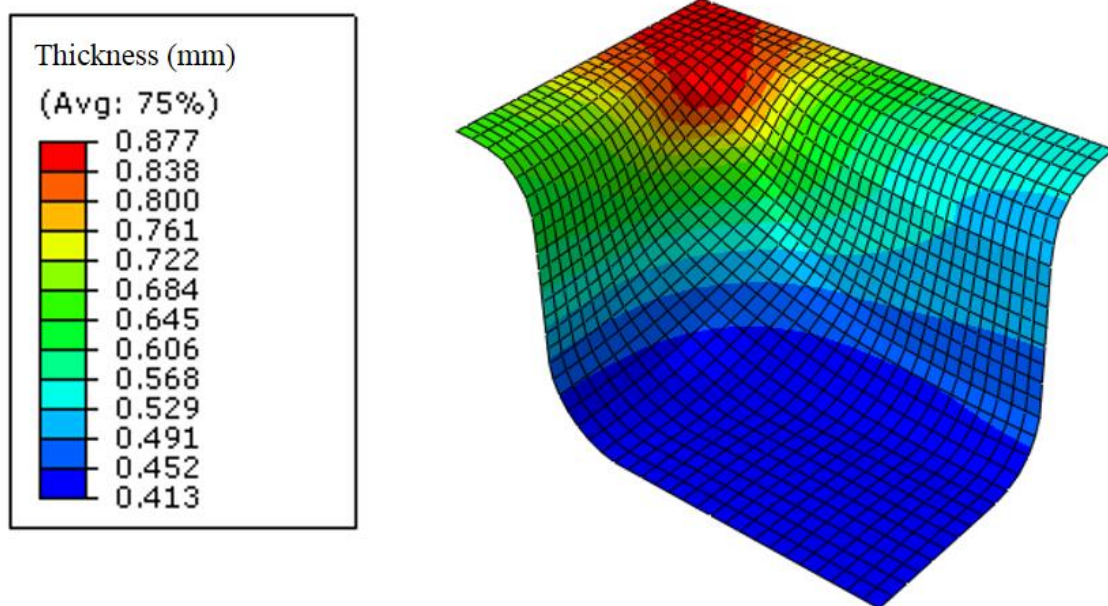


Figure 4.9: Sheet thickness distribution at blank for constant strain rate application

For application of constant strain rate, current process takes 88.8 seconds which is less compared to the time for constant pressure application to get the sheet formed.

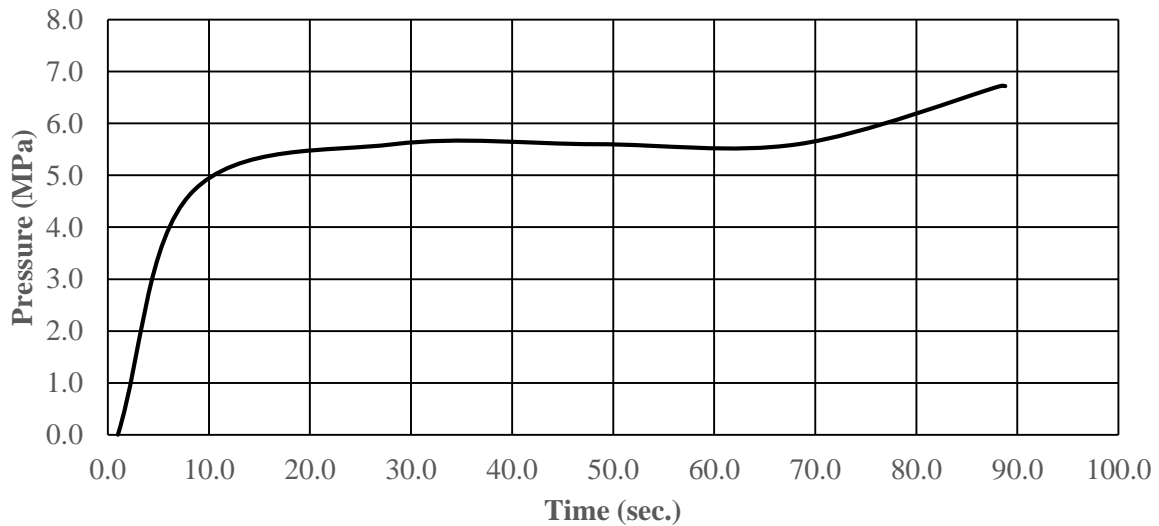


Figure 4.10: Pressure schedule for automatic pressure application for strain rate 10^{-2} 1/sec.

Figure 4.10 illustrates the necessary pressure to obtain desired constant strain rate. Required maximum pressure value for this approach is calculated by program as 6.7 MPa. This approach enables to control strain rate in a process to prevent sudden failures during application of constant pressure. Furthermore, required shape could be obtained in a shorter time. In the further analysis in this thesis, constant strain rate approach will be used.

4.2.2 Investigation of Effect of Process Temperature

Temperature is one of the most significant parameters of a SPF process, because mechanical properties of the materials change with respect to temperature, as a result of which the forming process is affected by the temperature. In Table 4.7, the mechanical properties of the material at different temperatures is illustrated. To investigate the effect of temperature on mechanical properties, two analyses are conducted at 840 and 900 °C at the constant strain rate of 10^{-2} 1/sec.

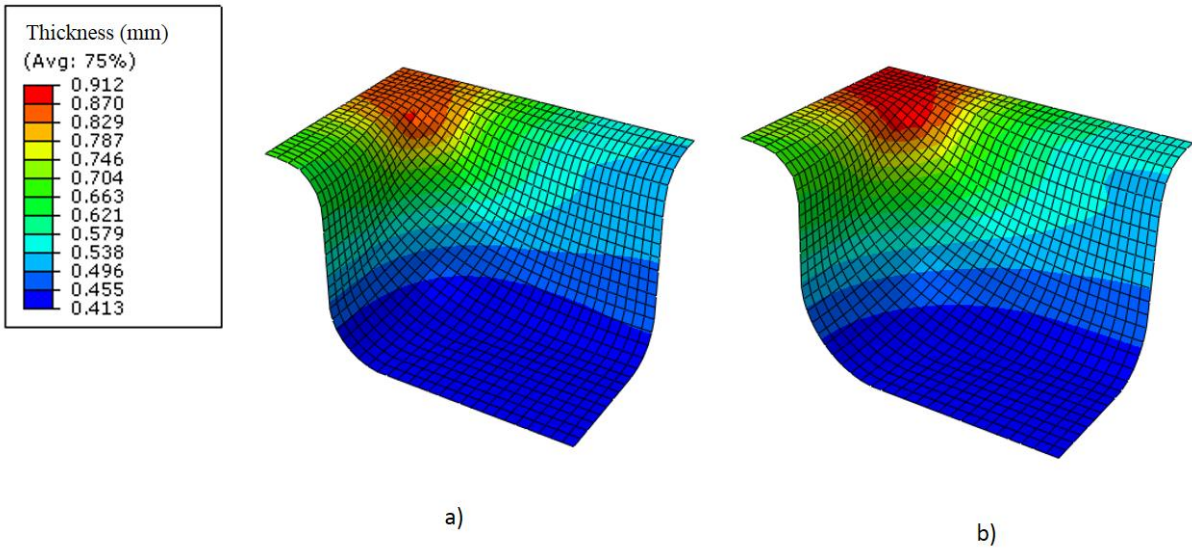


Figure 4.11: Sheet thicknesses comparison a) for 840° and b) for 900° process temperatures

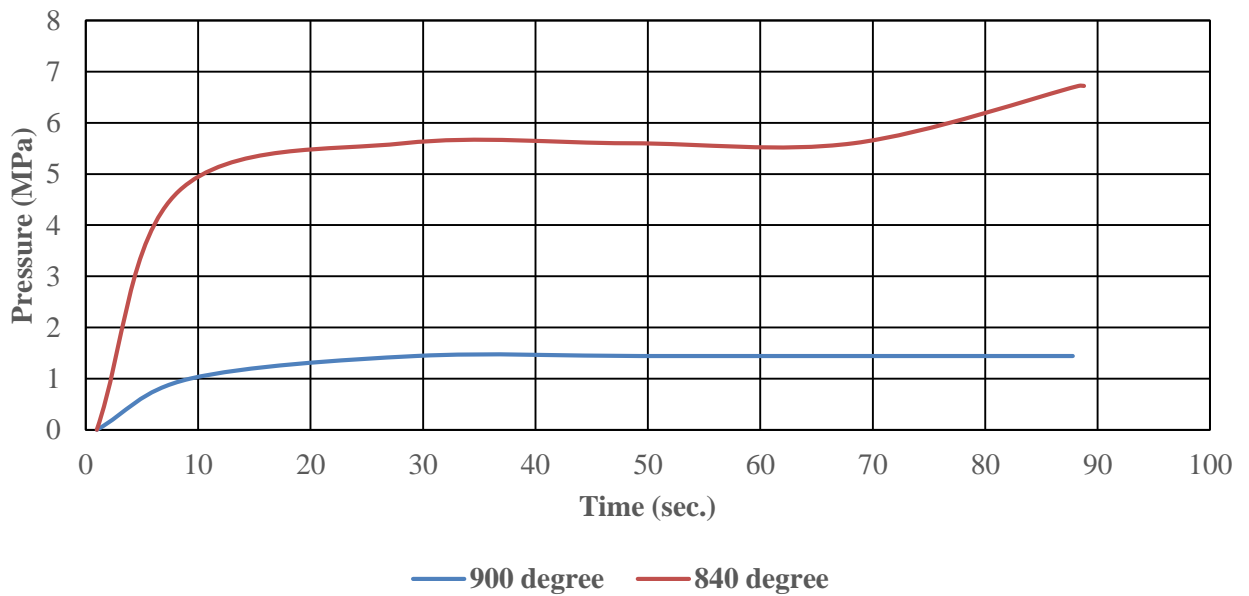


Figure 4.12: Comparison of applied pressure for 840 and 900 degrees

Table 4.9: Summary of results obtained for process temperatures of 840 and 900 degree

Applied pressure type	Forming temperature ($^{\circ}C$)	Target strain rate ($1/sec.$)	Applied max. pressure (MPa)	Process time (sec.)	Maximum equivalent creep strain	Final min. thickness (mm)	Max. eqv. stress (MPa)
Auto scheduled pressure	840	10^{-2}	6.72	87.8	0.774	0.413	97.09
Auto scheduled pressure	900	10^{-2}	1.44	86.8	0.833	0.413	47.36

Table 4.9 summarizes results obtained during two analyses, application of pressure by entering a target creep strain rate to the program enables to arrange applied pressure according to target creep strain rate. Process temperature is also an important parameter which affects power law material constants, as seen from Table 4.9, increasing process temperature enables to get sheet to be formed with a smaller applied pressure. Increasing the temperature activates and balances GBS and decreases strain hardening, since GBS sliding contributes to final elongation, so effective stress occurring on the specimen decreases significantly. (Cappetti et al.,2010)

In industrial applications, changing process temperature is an important opportunity to decrease process time by application of similar pressure, same product can be obtained in a shorter time. Furthermore, less forming pressure means less energy required for presses, and because less stresses occur on the final product, it enables to use parts with more service lives. Also, higher temperatures enable to obtain have a product which has more uniform thickness distribution, because less difference is seen in maximum and minimum thicknesses for $900^{\circ}C$. While increasing process temperature, it should also be considered that life time of dies and presses decrease because of exposure to high temperatures, as a result of this temperatures, presses operating at higher temperatures

should have better mechanical properties, so more expensive materials. Because of time, stress, applied pressure and uniform thickness perspective, 900 °C is a better choice for the process temperature, further analysis is realized with it.

4.2.3 Investigation of Effect of Strain Rate

One of the most challenging handicaps of SPF process is process time, and all efforts from this point of the study aim to shorten process time and obtain an optimum forming process which has both short process time and acceptable product quality, because SPF has never been convenient for mass production. Strain rate is a very important criterion for SPF analysis, so in this section effect of strain rate to the forming process is investigated. Same FEM models are tested at 900 °C for 10^{-4} , 5×10^{-4} , 10^{-3} and 10^{-2} strain rates, in these test runs all of the boundary conditions, material properties, mesh type, element size are same except for the strain rates. In all simulations, forming is continued until the sheet has the form of the die.

Forming pressure profiles obtained at the end of the simulations for different strain rates are shown in **Figure 4.13**, It can be observed that, there is a gradual increase in applied pressure for 20% of the total forming process time, later pressure seems to be constant, finally, there is a gradual increase in applied pressure to the sheet.

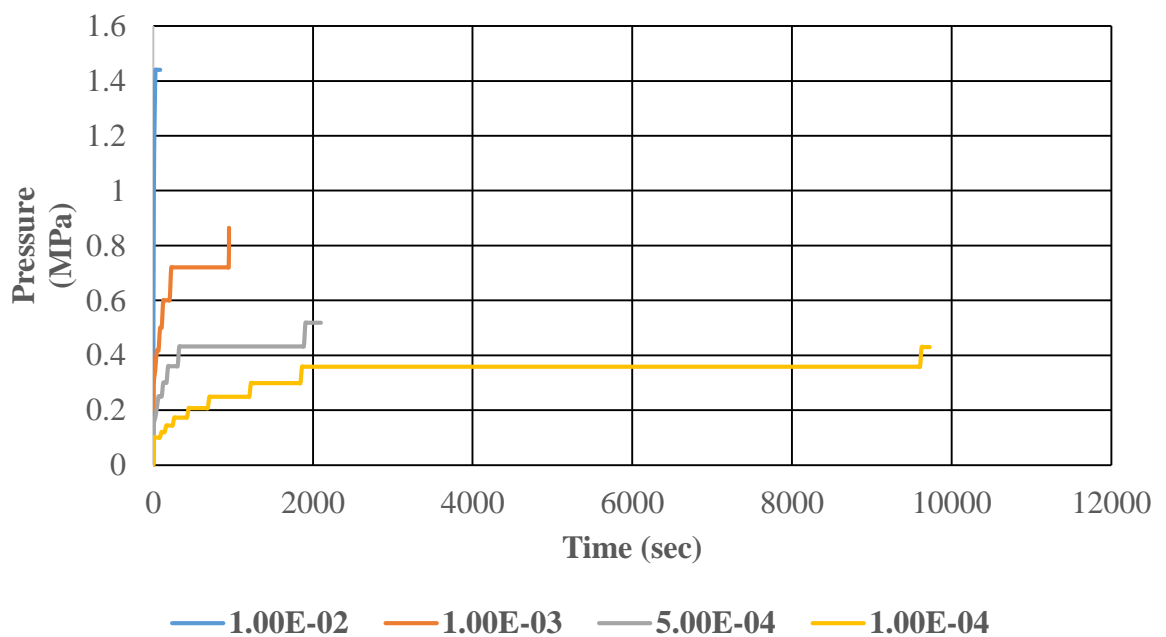


Figure 4.13: Pressure time profiles at different target strain rates

Instant increase at the early stages of forming process is because of increase in stresses, isotropic hardening and grain growth of sheet material, after that, thinning effect and hardening can balance each other and pressure becomes to be steady. At the final stages of process, sheet has contact with bottom part of the die, deformation is obstructed and effective area which pressure is applied becomes smaller, hence target strain rate has to be maintained, therefore, more pressure is required for this reason. (Deshmukh, 2003)

From Figure 4.13, it can be concluded that, higher pressures are required for higher target strain rates, because higher flow stresses occur with higher strain rates, for lower strain rates process time takes more time. For instance, forming time for 10^{-4} target strain rate takes 9725 seconds.

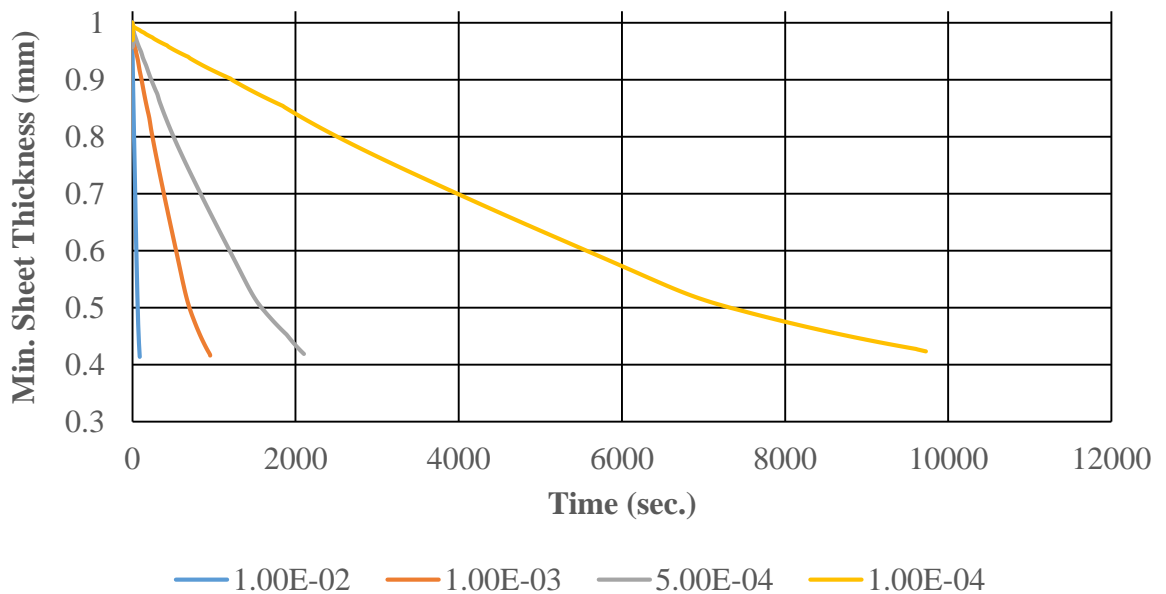


Figure 4.14: Minimum sheet thickness-time profiles at different target strain rates

Figure 4.14 illustrates minimum thicknesses achieved during the forming process for different target strain rates, most uniform thickness distribution is obtained for 10^{-4} target strain rates, but it took 9725 seconds to complete the forming process, while forming process took 87.5 seconds for 10^{-2} target strain rate. With increasing strain rate, strain hardening rises and it causes worse mechanical properties of product. (Cappetti et al., 2010). **Table 4.10** summarizes the final maximum and minimum sheet thicknesses and required process times for different target strain rates.

Table 4.10: Summary of the results obtained for different target strain rates

Strain rate (<i>1/sec.</i>)	10^{-4}	5×10^{-4}	10^{-3}	10^{-2}
Forming time (<i>sec.</i>)	9725	2100	950	87.8
Original thickness (<i>mm</i>)	1	1	1	1
Max. thickness (<i>mm</i>)	0.899	0.900	0.901	0.912
Min. thickness (<i>mm</i>)	0.423	0.418	0.415	0.413
Max. eqv. stress (<i>MPa</i>)	3.6	8.487	14.18	47.36
Max. required pressure (<i>MPa</i>)	0.429	0.5184	0.864	1.44

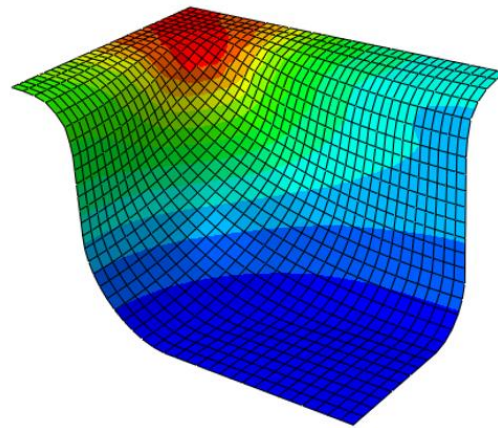
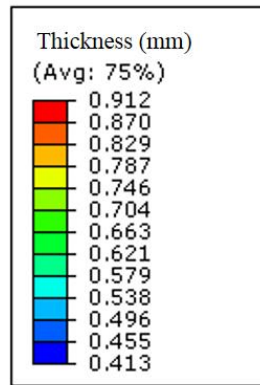
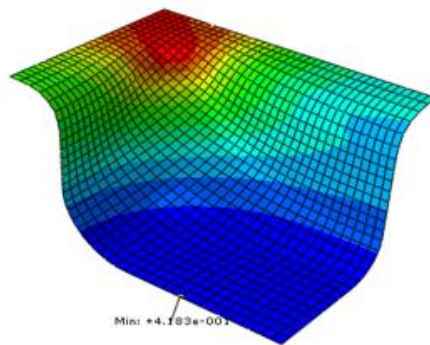
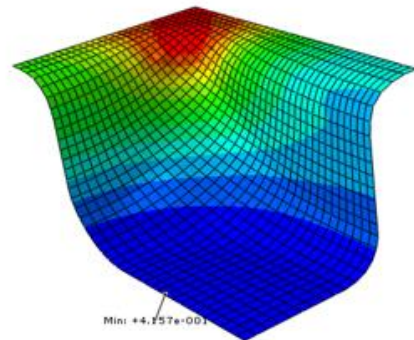
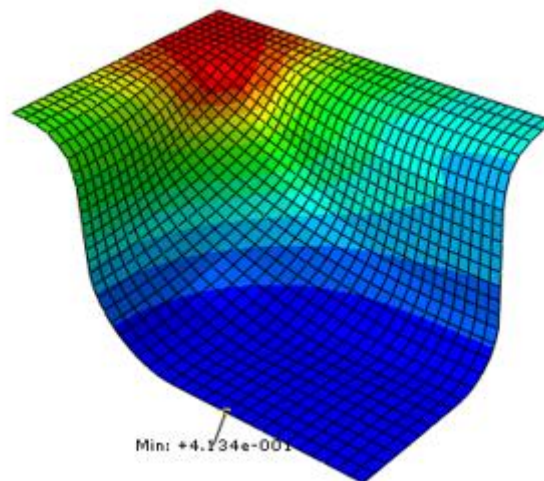
a) 10^{-4} 1/sec.b) 5×10^{-4} 1/sec.c) 10^{-3} 1/sec.d) 10^{-2} 1/sec.

Figure 4.15: Sheet thickness distribution at the end of the forming process for a) 10^{-4} 1/sec., b) 5×10^{-4} 1/sec., c) 10^{-3} 1/sec., d) 10^{-2} 1/sec. strain rates

4.2.4 Investigation of Effect of Sheet Thickness

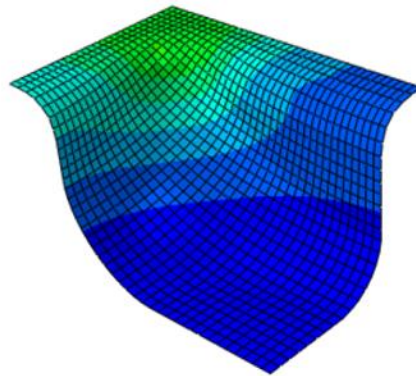
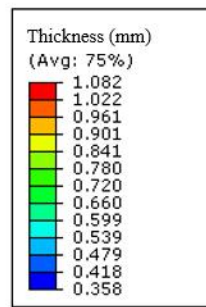
One of the other effecting parameter to the SPF process is thicknesses of the sheet specimens, for that reason analyses are conducted for sheet parts with different thicknesses. 0.80, 1.00 and 1.20 mm sheet materials are formed with SPF in ABAQUS, rather than sheet thicknesses other parameters are held constant to find out effect of sheet thickness. Analysis are conducted for 10^{-3} 1/sec strain rates.

Table 4.11: Summary of the results obtained for different sheet thicknesses

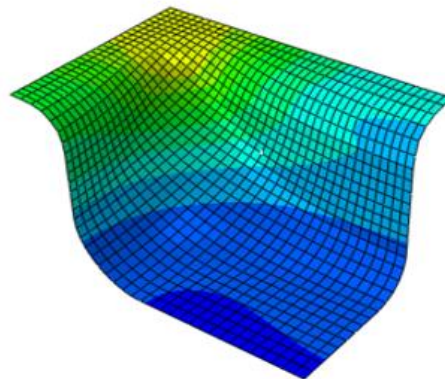
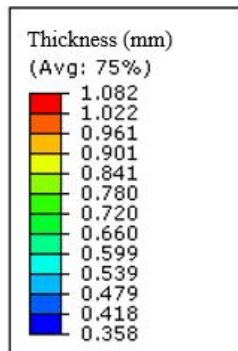
Sheet thickness (mm)	Strain rate (1/sec.)	Min. thickness (mm)	Reduction in sheet thickness (%)	Forming time (sec.)	Max. required pressure (MPa)	Max. eqv. stress (MPa)
0.8	10^{-3}	0.358	55.25	950	0.622	14.18
1	10^{-3}	0.433	56.73	950	0.864	14.18
1.2	10^{-3}	0.498	58.50	950	1.0368	14.18

As illustrated in **Table 4.11** minimum sheet thickness could be obtained with 0.8 mm sheet thickness with a less required pressure and it is possible to obtain similar final maximum stress values for all three specimens. As mentioned before, higher required pressures mean higher energy requirements, and higher pressures also decrease life of forming tools, when forming a sheet metal, sheet thickness should be considered as an important criterion, because higher sheet thicknesses require more forming time and forming pressure in order to obtain same final thicknesses. On the other hand, higher sheet thicknesses show more % reduction in thicknesses at the same time because of higher applied pressure values.

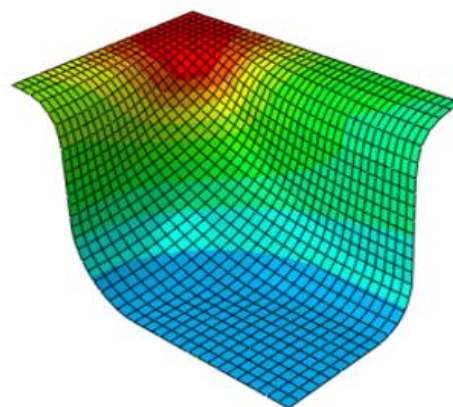
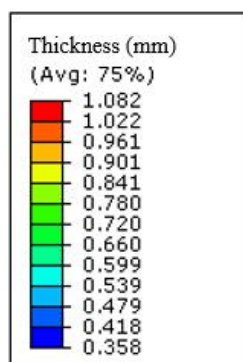
Figure 4.16 illustrates the sheet thickness distribution after forming process and it could be concluded that sheet which has 0.8 mm initial thickness shows more uniform thickness distribution at the end of the forming process.



a) 0.8 mm



b) 1 mm



c) 1.2 mm

Figure 4.16: Sheet thickness distribution for a) 0.8 mm, b) 1 mm and c) 1.2 mm sheet thicknesses

4.2.5 Investigation of Friction Coefficient

One of the parameters affecting the SPF is friction which is related to the lubrication type used between die and specimen (sheet material). When components have contact between each other, a force normal to the interacting surfaces is created, and if there is a friction is defined between interacting surfaces as in the real life, shear force occurs which resist the tangential motion (sliding) of the parts. In FEA, the general aim is focusing on the areas that have or can have contact during the analysis and calculation of the contact pressures that occur during contact of each component. Contact phenomena is one of the discontinuous constrains in FEA, since there is a constrain when they are interacting and no interaction occurs when they separate. The analysis should consider the condition when two surfaces are in interaction and apply the contact constraints, and it also needs to detect when two surfaces separate and remove the contact constraints. (Hibbit and Hibbit, 2001)

When surfaces have contact with each other, they also transmit shear as well as normal forces from their interfaces, so it is required to consider friction forces that resist sliding of the surfaces. Coulomb friction is a common friction model which is also considered in this study for friction behaviour between die and sheet. Coulomb friction defines frictional behaviour by the definition of friction coefficient between die and sheet material. Tangential motion does not occur until surface physical resistance has a critical shear stress value and it is dependent on normal contact force and defined with following formula;

$$\tau_{crit} = \mu p \quad (4.2)$$

Here μ is the coefficient of friction and p is the contact pressure between interacting surfaces and τ_{crit} is the critical frictional shear stress. This equation defines the limiting frictional shear stress, and interacting surfaces do not slide relative to each other since their shear stress reaches this limiting frictional shear stress.

Figure 4.17 illustrates friction behaviour between surfaces, relative motion of surfaces does not occur when they stick to each other. (shear stresses are less than critical value). (Hibbit and Hibbit, 2001)

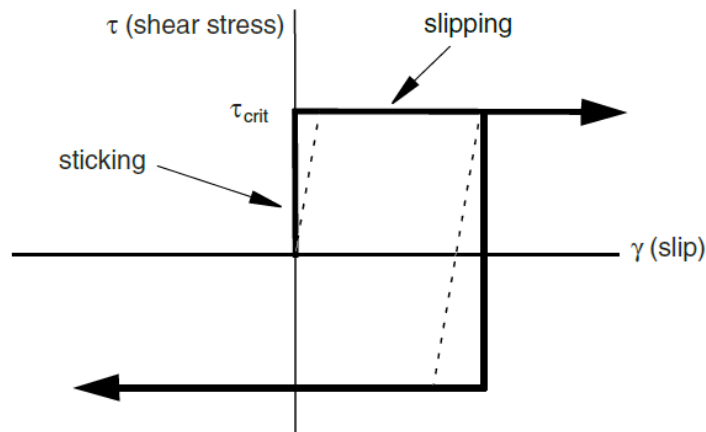


Figure 4.17: Coulomb frictional behaviour (Hibbit and Hibbit, 2001)

Sticking or slipping create discontinuity and can result in convergence problems during the analysis, friction behaviour should be considered if it is really important and affecting the analysis results. Another challenge is the definition of ideal friction model between surfaces. In most cases, penalty friction formula is preferred which has allowable elastic slip as shown in **Figure 4.17** with dotted line. Penalty friction formula for coulomb friction model gives adequate results for most of the problems such as metal forming. (Hibbit and Hibbit, 2001)

Until this point of this study, all of the analysis have been conducted without taking friction into account, in this section effect of friction coefficient to the SPF process is investigated. The analysis is surveyed for two different target constant strain rates of 10^{-3} 1/sec. and 10^{-2} 1/sec. and the coefficient of friction is changed from 0.05 to 0.5 for each analysis. Rather than friction coefficients, all of the other parameters are held constant during the process.

In SPF analysis of the rectangular box, except for clamped region of the sheet specimen, it flows into die cavity by application of gas pressure, first contact with die occurs at flange area and during time the sheet is stretched and then slides over die surface. During forming, pressure increases gradually and critical shear stress catches up with shear flow stress of the alloy, sticking occurs and flow of subsurface begins, this affects the thickness distribution in the component formed. (Nazzal and Khraisheh, 2005)

Table 4.12: Comparison of results obtained for different friction coefficients at different target strain rates

	Friction coefficient	10⁻³ (1/sec.)	10⁻² (1/sec.)
Forming time (sec.)	0.05	915	82
	0.5	1200	120
Original thickness (mm)	0.05	1	1
	0.5	1	1
Minimum thickness (mm)	0.05	0.418	0.419
	0.5	0.365	0.347
Stress (MPa)	0.05	12.41	51.03
	0.5	13.10	50.43
Applied maximum pressure (MPa)	0.05	0.72	1.44
	0.5	0.74	1.44

Table 4.12 shows results obtained for friction coefficients of 0.05 and 0.5 at different target strain rates. When the friction coefficient increases required process time to form the sheet is increasing, but in the end of the process thickness of the obtained product is decreasing significantly. With a good lubrication, process times could be decreased in industrial applications.

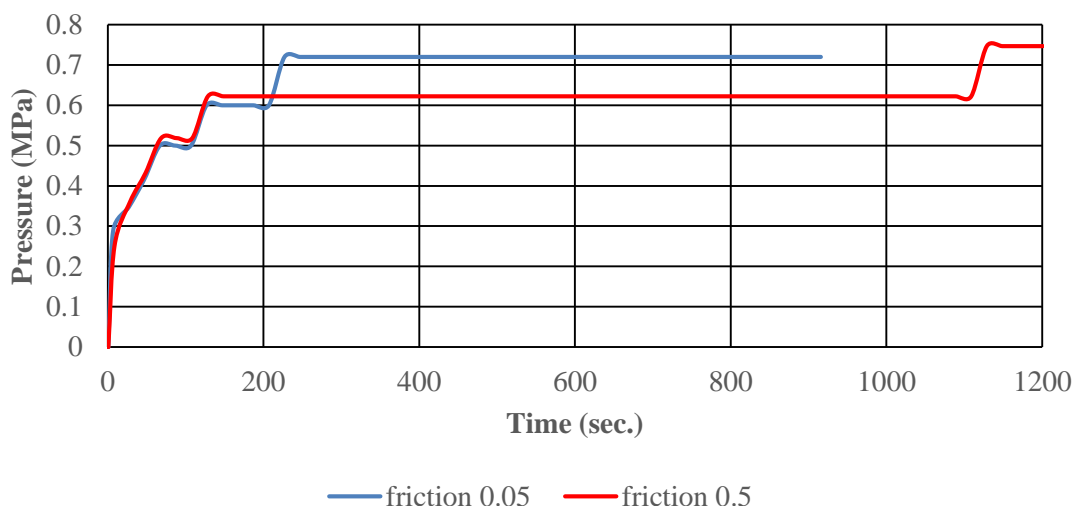


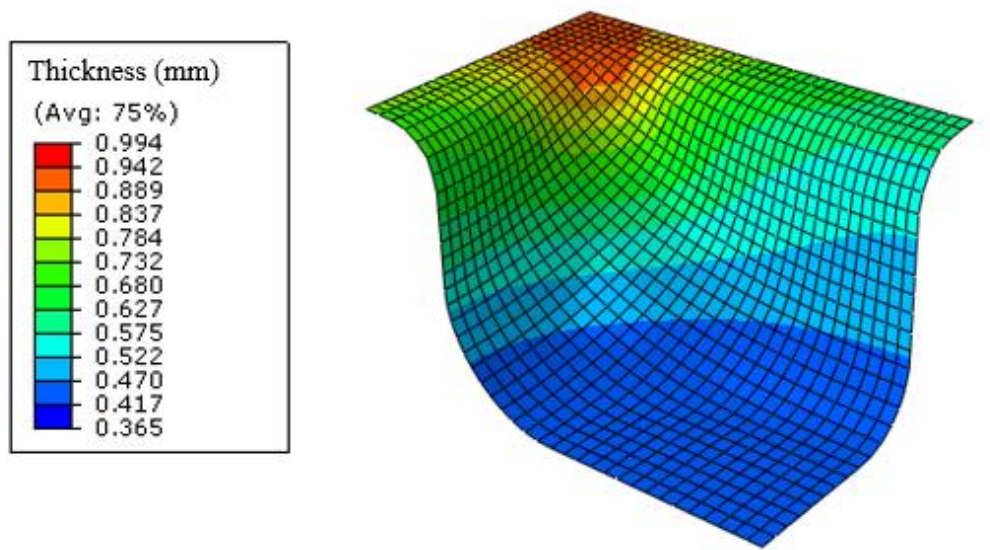
Figure 4.18: Pressure profile for different friction coefficients for a constant target strain rate of 10^{-3}

Figure 4.19 illustrates how sheet thickness profile occurs at the end of the forming process for friction coefficients 0.05 and 0.5. With increasing friction coefficient greater localized thinning occurs and necessary pressure to be applied decreases to obtain the target strain rate as seen in **Figure 4.18**. From Figure 4.18, it is proved that there is not a significant effect in early stages of forming process, since pressures for both frictions are nearly same. Hence, at later stages of deformation, contact occurs between sheet and die.

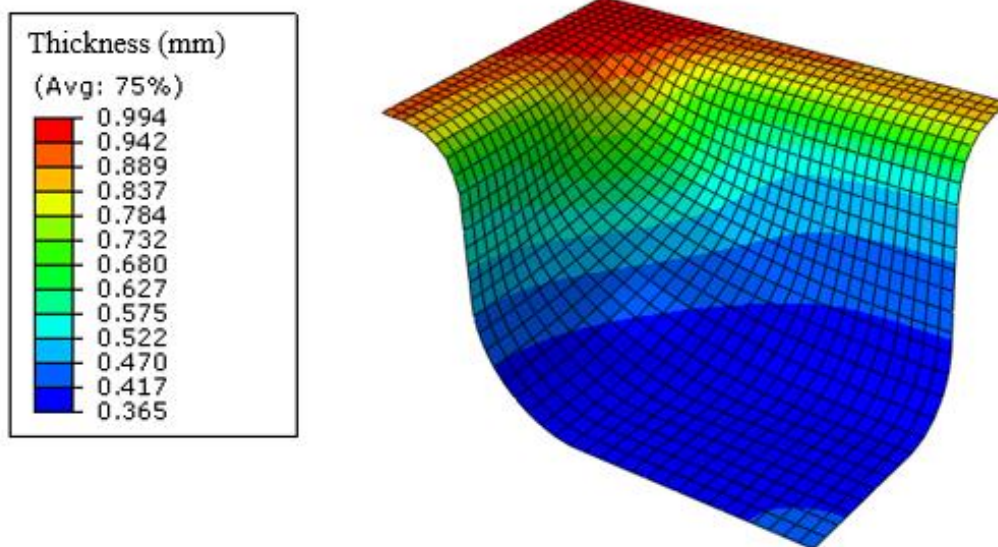
It is known that when friction coefficient increases forming pressure decreases, because friction force reduces the amount of volume that can move to free bulged region, so forming pressure decreases. When friction coefficient increases greater localized thinning occurs and necessary pressure to be applied decreases to get the target strain rate as seen in Figure 4.18. (Nazzal and Khraisheh, 2005)

It is clear that more uniform thickness distribution is obtained with smaller friction coefficient. As seen from **Figure 4.19**, thickness at the die entry is higher for 0.5 friction coefficient while thickness at the die root is less, this makes the part more nonuniform compared to the product formed under 0.05 friction coefficient.

More thinning with a higher friction coefficient can be explained as following; first contact occurs at the flange area, sheet stretches and slides over the die surface. Friction between die and sheet resists to the tensile stress and more thinning occurs for higher friction coefficient. (Deshmukh, 2003, Nazzal and Khraisheh, 2005)



a) friction coefficient: 0.05



b) friction coefficient: 0.5

Figure 4.19: Comparison of sheet thickness distribution for different friction coefficients

4.2.6 Investigation of Effect of Die Entry Radius

Die entry radius is one of the most important parameters that affect superplastic forming, since it affects thinning and breakage. In order to find out effect of die entry radius on

the SPF process and obtained product, three different analyses were conducted for constant target strain rate of 10^{-3} 1/sec for die entry radiuses of 3,4 and 5 mm. Except for die radii all other parameters and geometric properties are kept constant.

Table 4.13: Comparison of final thicknesses for different die entry radii

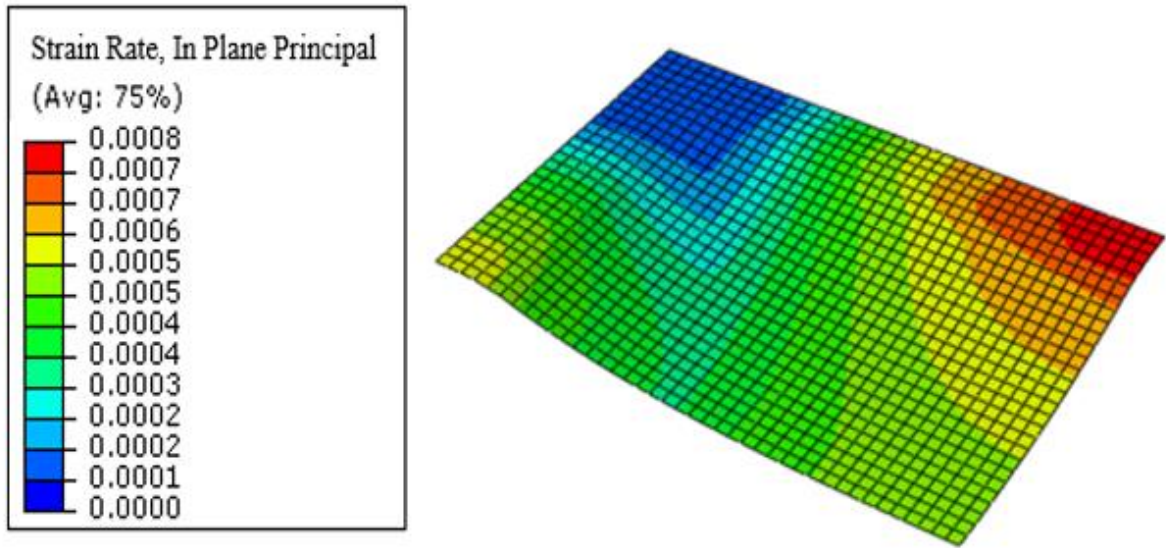
Die radius (mm)	Forming time (sec.)	Initial sheet thickness (mm)	Min. sheet thickness (mm)
3	950	1	0.4085
4	950	1	0.415
5	950	1	0.418

From **Table 4.13**, it could be concluded that, increasing die entry radii for the same forming time increases the final product sheet thickness, since a small radius at the top of die prevents material flow to the center of sheet and increases global thinning, resisting the tensile stress and as a result of that superplastic effects are reduced. (Cappetti et al., 2010)

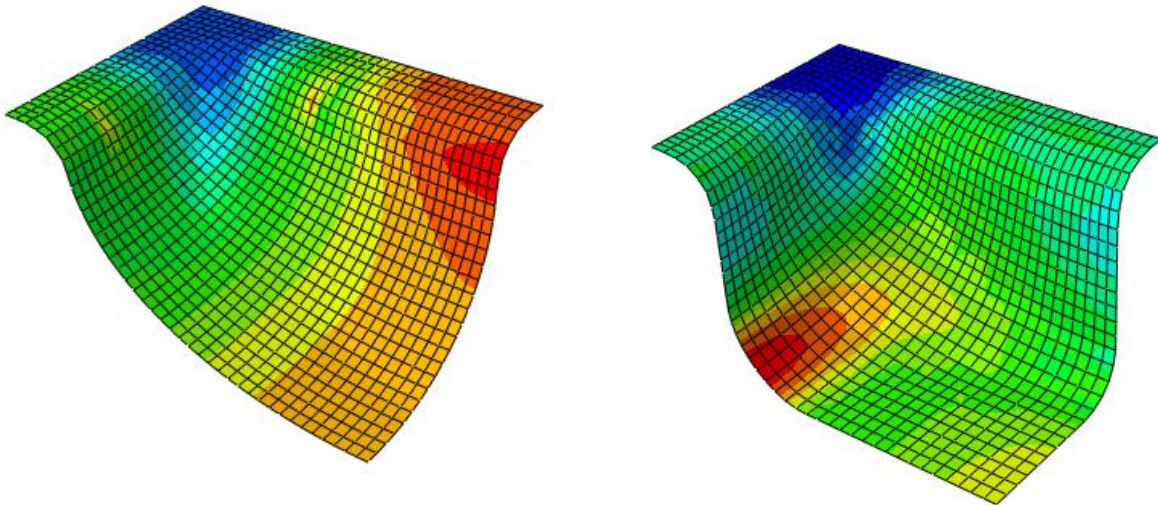
Although, final sheet thickness is reduced significantly for die radius 3 mm, forming could not be completed, it could not get the whole form of the die, it requires more time to complete the forming. It could be concluded that, smaller die radii require more forming time to finish the process, but enable to obtain thinner products. Increasing die radius increases final sheet thickness, but reduces forming time, furthermore it enables more uniform thickness distribution.

4.2.7 Investigation of Forming Behaviour for Different Time Steps

In this section, SPF process is analysed for different time steps of process in order to find out forming process behaviour. For this purpose, sheet metal investigated is formed into a rectangular box for 950 seconds at 10^{-3} 1/sec. constant target strain rate and creep strain is observed for different time points.



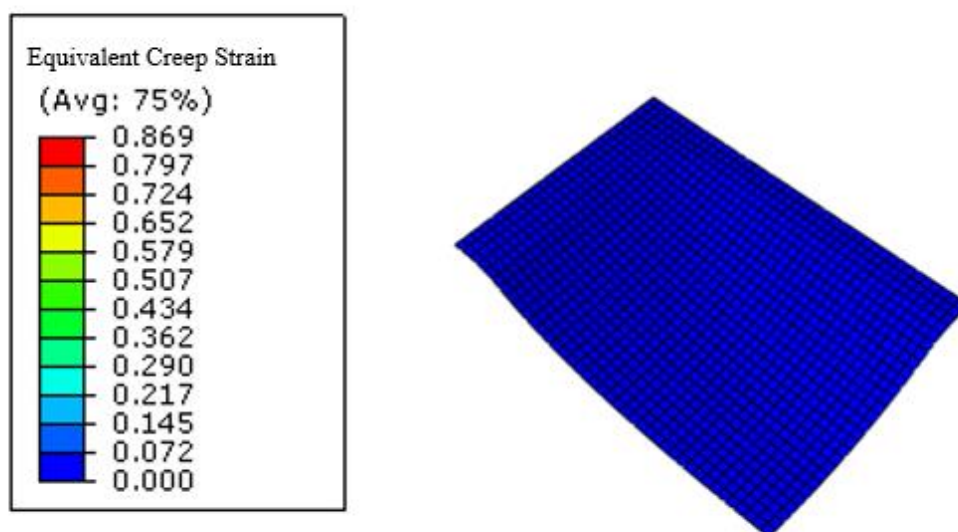
a) 45th second of forming process



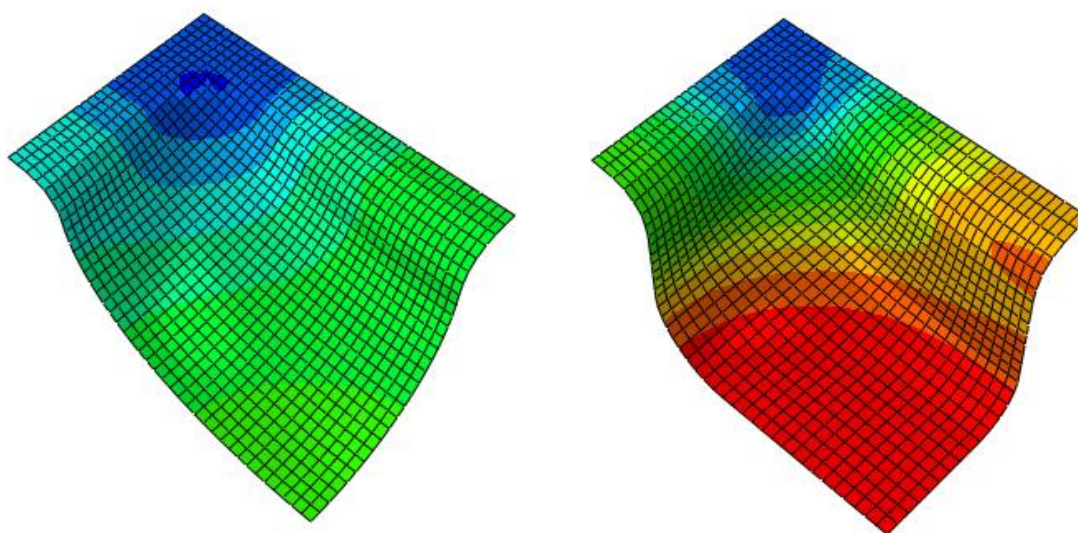
b) 495th second of forming process

c) 950th second of forming process

Figure 4.20: Strain rates occurring on the sheet metal at different stages of forming process



a) 45th second of forming process



b) 495th second of forming process

c) 950th second of forming process

Figure 4.21: Equivalent creep strains occurring on the sheet metal at different stages of forming process

Figure 4.20 and **Figure 4.21** illustrate strain rates and equivalent creep strains occurring on the part during different stages of SPF process. As illustrated, different strain rates occur at different regions of process for different time steps. At the 45th second, part tries to move from die entry and bending condition is created, at that step maximum strains

are observed at that region which is most critical at the beginning of the process. At the 495th second most critical region moves to center of the die. Maximum strains and strain rates occur at the regions close to die surface. At 950th second which is at the end of forming process, critical area is the region close to bottom radius of die because this area gets into contact with the die finally, so maximum strain rate occurs at that region.

In order to investigate forming process in more detail, sheet metal is divided into four zones as illustrated in **Figure 4.22**, and average of creep strains are calculated for nodes of each zone.

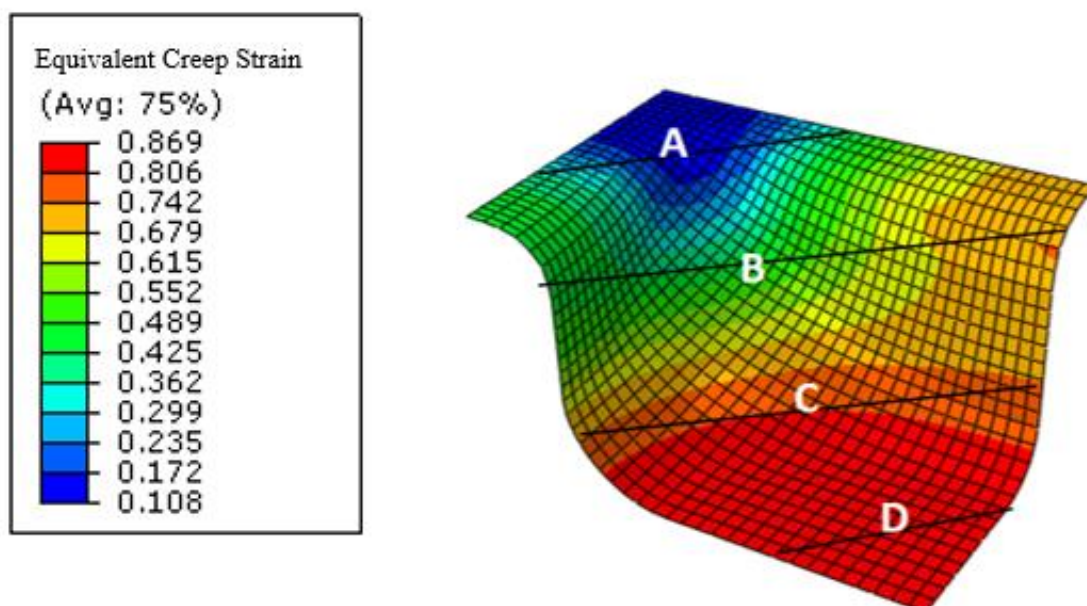


Figure 4.22: Dividing formed part to four different zones according to equivalent creep strain

Figure 4.23 illustrates equivalent creep strain change with increase of distance from the sheet initial position. It is clear that, creep strain behaviour has an increasing trend from zone A to D, since at the final stage of forming process, maximum displacement occurs in bottom region of the die, because at regions close to initial positions of sheet forming is already completed while bottom part has already contact with the die. For instance, for forming zone A, creep strain increases slowly at later stages since it cannot move or form any more when sheet metal goes into free bulged region, especially for final stages, creep strain for zone A is nearly constant. Furthermore, for forming zone D, raise of

creep strain increases tremendously for final stages since at those times pressure tries to form that region. Creep strain values at any time are getting higher when going from zone A to zone D, since the displacement that zone D is exposed to higher than the other zones. Figure 4.23 proves the fact that, bottom part of the sheet is most critical region, because highest strains occur, so possible failures are expected to happen in those regions.

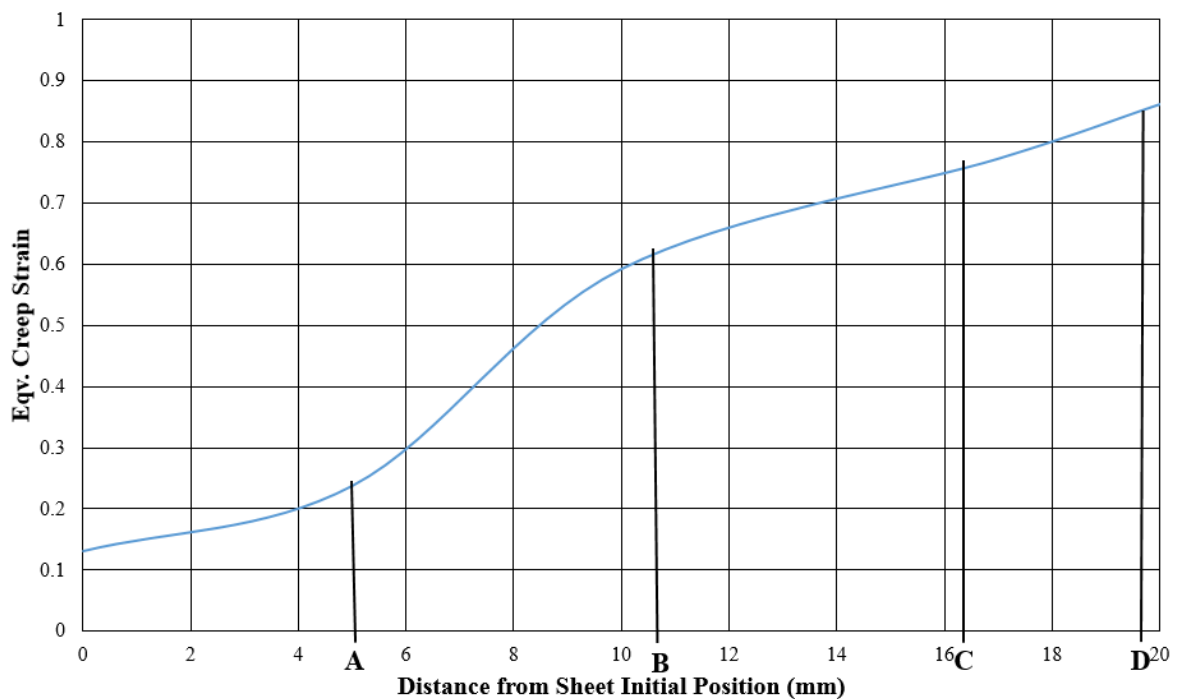


Figure 4.23: Equivalent creep strain change according to distance from sheet initial position

In a SPF process, obtaining a uniform sheet thickness at the end of the process is a very important criterion for final product, since abrupt thinning could cause premature failures. (Panicker and Panda, 2017) In order to understand and evaluate how the thinning occurs, formed rectangular box is again divided into four zones from top to the bottom of the box and thinning percent is calculated from top to the bottom of the rectangular box by taking average of thinning percent of nodes, this is shown in **Figure 4.24**.

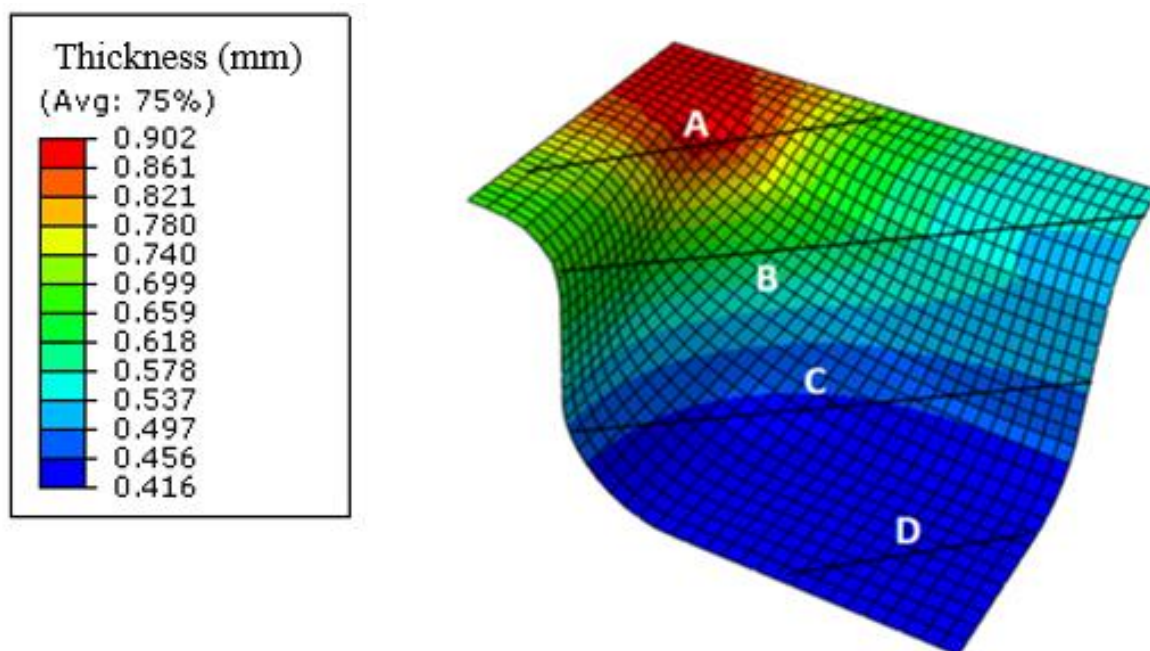


Figure 4.24: Dividing formed part to four different zones according to sheet thickness distribution

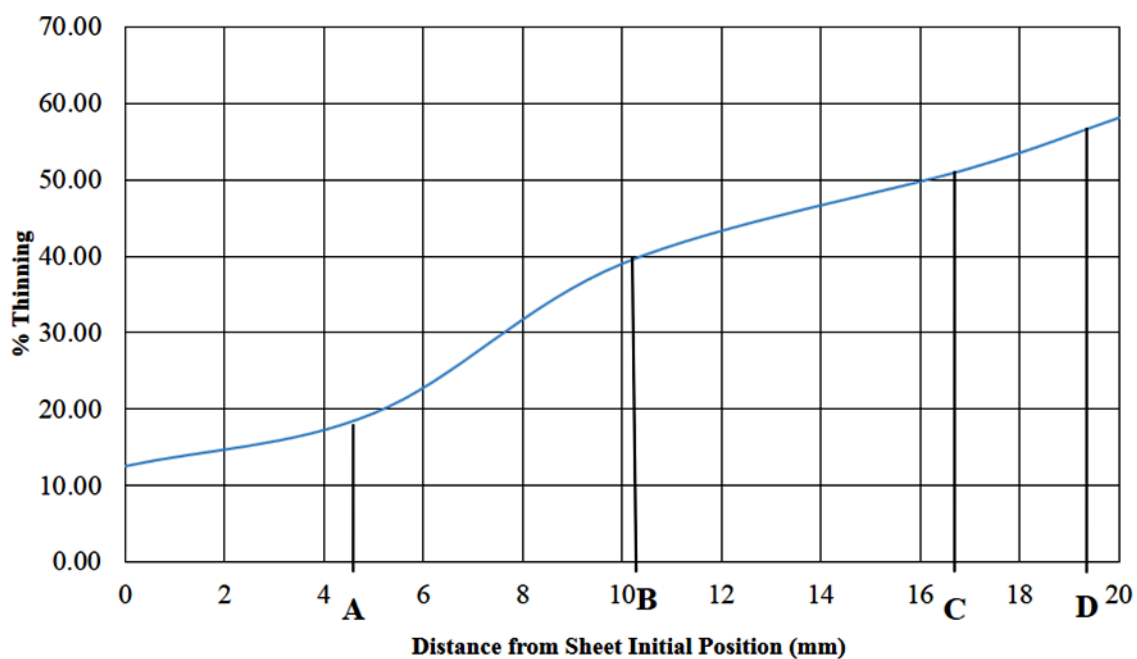


Figure 4.25: Investigation of thinning for different zones

% thinning for four zones according to distance from initial position of the sheet are illustrated in **Figure 4.25**, the most critical region of the rectangular box is seen at region D where maximum thinning occurs. Bottom part of the box might cause to failures for

a SPF process. Figure 4.25 supports Figure 4.23, too, since maximum strain and maximum thinning regions are consistent. It could be evaluated that when the box depth increases thinning percent increases also and it gets stabilized at 58.25 % thinning. When designing a SPF process, bottom part of the final product which is formed at last step, should be considered for possible failures.

4.3 Investigation of Process Parameters to the SPF Process for a Conical Part

In the real forming conditions of industrial parts, not only rectangular box type forming conditions occur, but also other type of deformation conditions could be experienced according to shape of parts. In this thesis, a sheet metal is also formed to a conical die to investigate parameters of conical die geometry to the forming process.

A conical die illustrated in **Figure 4.26** has dimensional properties as;

h : Height of the die [mm];

$d1$: Outer diameter of die [mm];

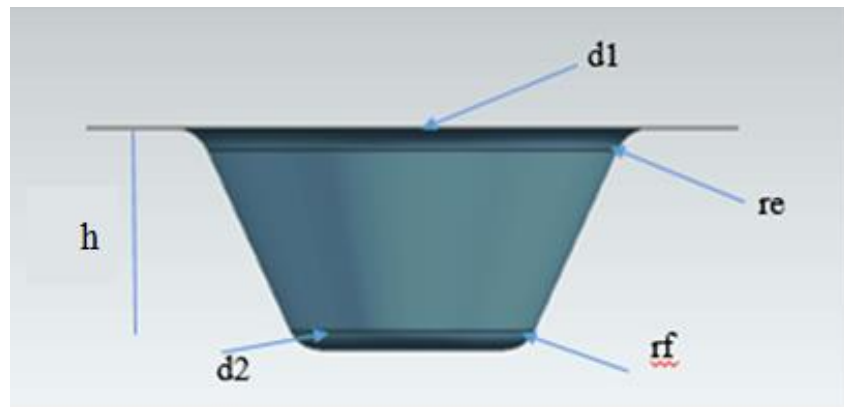
$d2$: Inner diameter of the die [mm];

re : Entry radius of the die [mm];

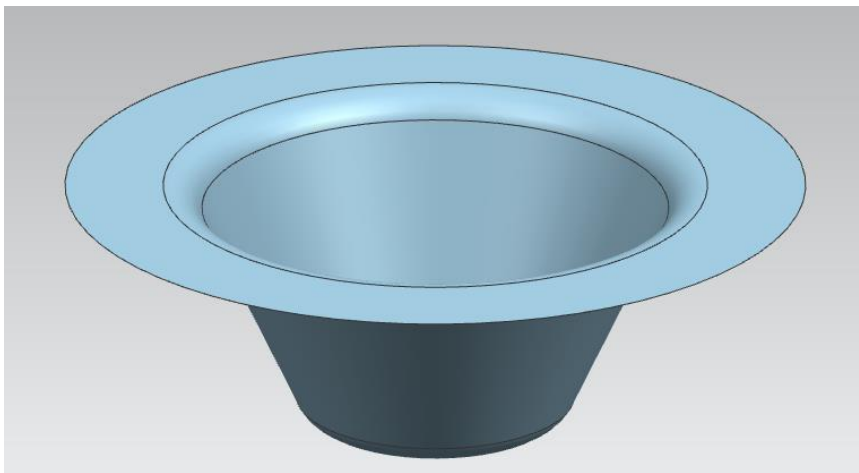
rf : Root radius of the die [mm];

α : The inclined angle of the die [-].

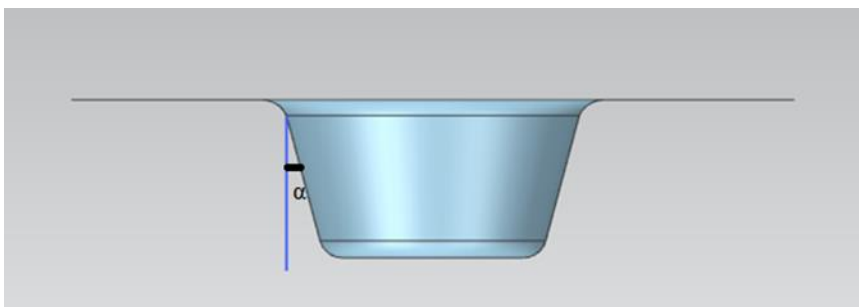
In this section, effect of $d1$, re , H and α to the forming time, forming pressure profile and final thickness are investigated.



a)



b)



c)

Figure 4.26: Geometrical schematic of conical die

4.3.1 Investigation of Effect of Entry Radius of the Die

Die entry radius of a conical die is a known parameter that could affect SPF process, to investigate that Ti6Al4V sheet material at 900 °C is formed to conical die for two different die entry radii. All dimensions of forming processes are documented in **Table 4.14**.

Table 4.14: Geometric properties of conical die for different analyses

Test number	rf (mm)	h (mm)	$d1$ (mm)	$d2$ (mm)	α	re (mm)
1	8.58	58	124	64	25	10
2	8.58	58	124	64	25	12

Sheet material has 1 mm thickness and forming is realized for constant target strain rate of 10^{-3} 1/sec. In order to decrease analysis time quarter of sheet and die are formed by utilizing advantage of symmetry.

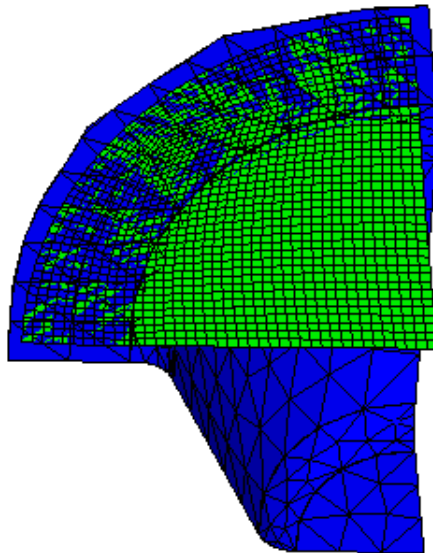
**Figure 4.27:** Mesh view for conical die and sheet

Figure 4.27 shows mesh for conical die and sheet specimen. Sheet is modelled with 1519 M3D4 element typed membrane elements. For the same geometrical and analysis conditions for model, only the die entry radius is selected as 10 mm and 12 mm, and sheets are formed to conical die geometry. For 10 mm die radius it took 975 seconds to form the sheet, and in order to find out effect of die radius a specimen which has 12 mm die entry radius is also formed for 975 seconds.

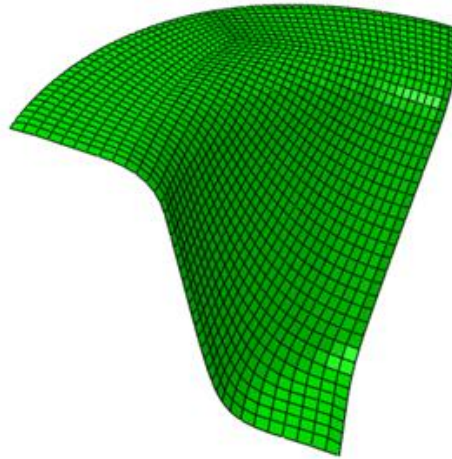


Figure 4.28: Formed configuration of sheet metal

Table 4.15: Geometrical properties of test specimen

Test number	rf (mm)	h (mm)	$d1$ (mm)	$d2$ (mm)	α	re (mm)	Strain rate (1/sec)
1	8.58	58	128	64	25	10	10^{-3}
2	8.58	58	128	64	25	12	10^{-3}

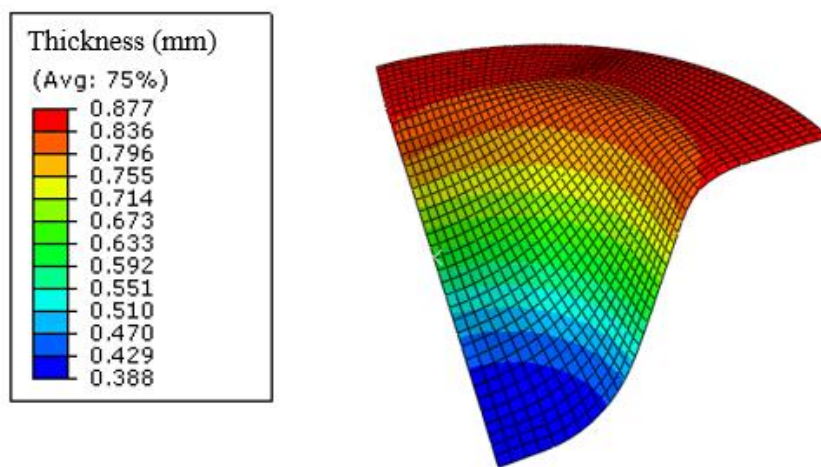
Table 4.16: Results for different die entry radii

re (mm)	Forming time (sec.)	Required max. pressure (MPa)	Minimum sheet thickness (mm)	Maximum eqv. stress (MPa)
10	975	0.432	0.388	13.79
12	975	0.432	0.393	13.92

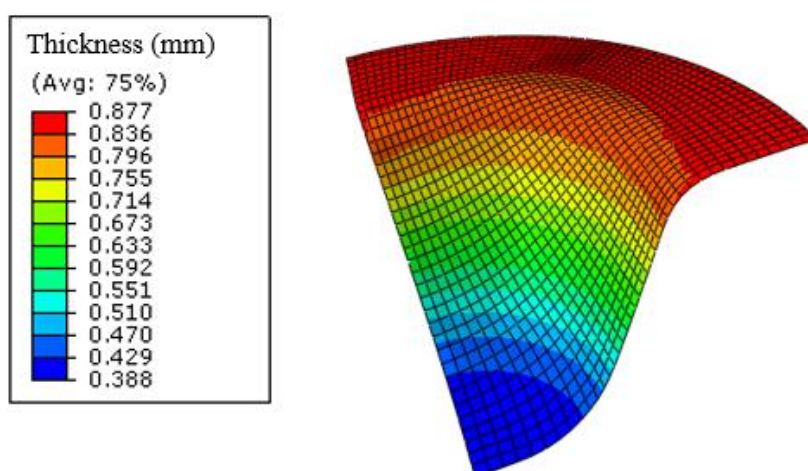
Table 4.16 illustrates analysis results for die entry radii of 10 mm and 12 mm, as seen from table for the same forming time, it requires same maximum pressure to form the part and final obtained sheet thickness decreases regarding to smaller die entry radius. Also, forming for 10 mm radius die is not finished at the same, it requires more time to complete forming. This behaviour is similar as observed for rectangular box forming.

Since, to be able to continue target constant strain rate deformation at the pole while increasing die entry radius, volume flow to the free bulged region increases and it results in an increase in required pressure. (Hwang et al., 1997)

Furthermore, higher die entry radius enables to obtain more uniform sheet thickness, since the difference between maximum and minimum sheet thicknesses are less for 12 mm radius as illustrated in **Figure 4.29**.



a) 10 mm die radius



b) 12 mm die radius

Figure 4.29: Sheet thickness distribution for a) 10 mm and b) 12 mm die entry radii

While forming, it is also known that abrupt thinning is seen at the die entry and sidewalls, because large tension occurs on elements near the junction from free bulk region, since free bulk region begins in contact with the sidewalls. Also sudden thinning decreases when the die entry radius increases. (Hwang et al., 1997)

It could be concluded that, smaller die radii require more forming time to finish the process, but enables to obtain thinner products. Increasing die radius increases final sheet thickness, but reduces forming time, furthermore it enables more uniform thickness distribution.

4.3.2 Investigation of Effect of Die Aspect Ratio

Outer diameter of conical die is another important parameter for the forming process of conical shaped part. The aspect ratio of a conical die is defined with the below formula;

$$AR = \frac{dl(1 - \sin \alpha)}{2h \cos \alpha} \quad (4.3)$$

Here dl is the outer diameter, h is the height and α is the inclined angle of the die.

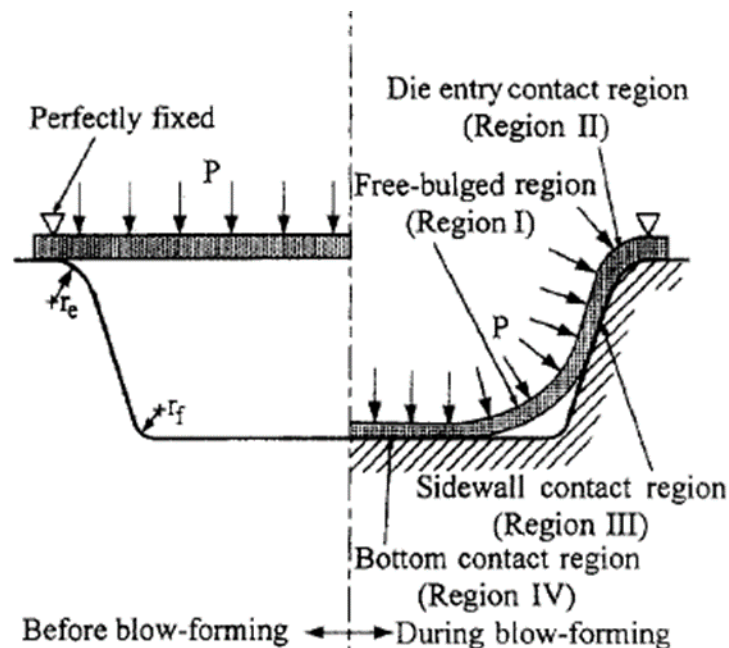


Figure 4.30: Schematic view of contact relations between die and sheet while SPF of a conical part (Hwang et al., 1997)

Table 4.17: Geometric properties of conical die for different AR values

Test number	rf (mm)	h (mm)	$d1$ (mm)	$d2$ (mm)	re (mm)	α	AR (-)
1	8.58	38	128	64	10	25	1.0733
2	8.58	58	108	64	10	25	0.5933
3	8.58	58	128	64	10	25	0.7032
4	8.58	58	128	64	10	15	0.8475

In order to see the effect of AR ratio regarding to given geometric properties, four different analyses are conducted. Geometric properties for different tests are given in **Table 4.17**.

Table 4.18: Results summary for different aspect ratio of the die

Test number	AR (-)	Forming time (sec.)	Required pressure (MPa)	Minimum sheet thickness (mm)	Maximum eqv. stress (MPa)
1	1.073359	550	0.5184	0.606	13.21
2	0.593355	1050	0.5184	0.3039	16.4
3	0.703235	975	0.432	0.388	13.79
4	0.84754	975	0.3	0.36704	13.09

Table 4.18 summarizes analysis results for different aspect ratios, it can be concluded based on the difference between test results, when aspect ratio decreases forming time increases. For test number 1, forming time is small compared to others since the die height is greater. Because die entry diameter is higher for test number 2 than test number 3, it takes less time to finish forming process, because free bulge region comes into contact with bottom earlier according to test number 2. Furthermore, increasing die entry diameter enables to obtain products which have more uniform thickness distribution as seen from **Figure 4.31**.

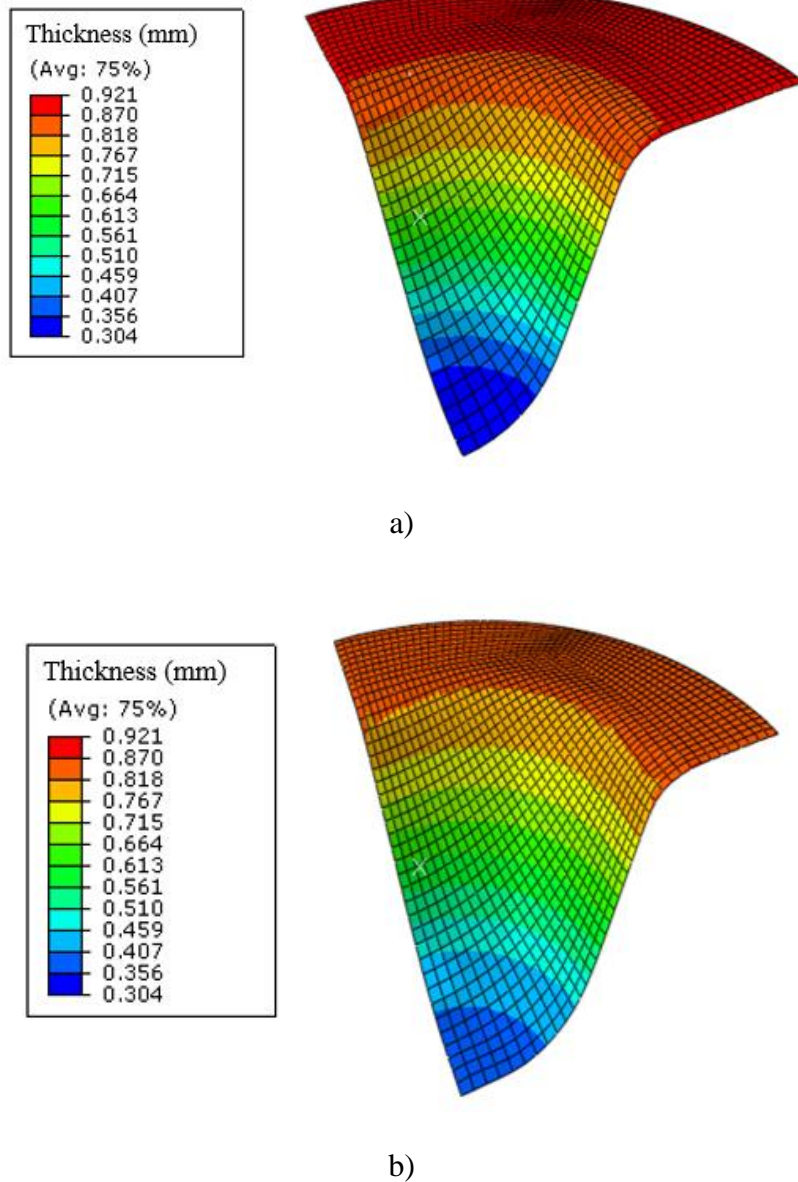


Figure 4.31: Thickness distribution for die entry diameters a) 108 mm and b) 128 mm

Another important geometric parameter affecting to the forming process is inclined angle of the die. For test condition 4, inclined angle is decreased to 15 and analysis is conducted for 975 seconds. When analysis number 3 and 4 are compared, it can be seen that higher forming pressure is required for higher die inclined angle, for the same forming time and same geometric properties except for inclined angle, because total arc length of die surface gets smaller and final thickness decreases when inclined angle decreases.

It could be concluded from the analysis results that, in order to decrease forming time and obtain better thickness distribution the outer die diameters could be increased. Aspect ratio of the die is a very important criterion for a conical shape sheet forming. Increasing AR results the forming process to complete in a shorter time. Furthermore, decreasing die inclined angle could be another solution to apply smaller required pressure resulting in smaller stress on the specimen.

4.3.3 Investigation of Effect of Friction Coefficient

Until this point of the study of conical part, all of the analysis have been done without considering friction, in this section effect of friction coefficient to the SPF process is investigated, the analysis is surveyed for target constant strain rates of 10^{-3} 1/sec. and the coefficient of friction is changed from 0.05 to 0.5 for each analysis. All of the other parameters rather than friction coefficient are kept constant during the process.

Table 4.19: Comparison of results obtained for different friction coefficients at 10^{-3} target strain rate

	Friction coefficient	Strain rate: 10^{-3} (1/sec.)
Forming time (sec.)	0.05	975
	0.5	1050
Original thickness (mm)	0.05	1
	0.5	1
Minimum thickness (mm)	0.05	0.379
	0.5	0.316
Stress (MPa)	0.05	12.653
	0.5	13.586
Applied maximum pressure (MPa)	0.05	0.36
	0.5	0.36

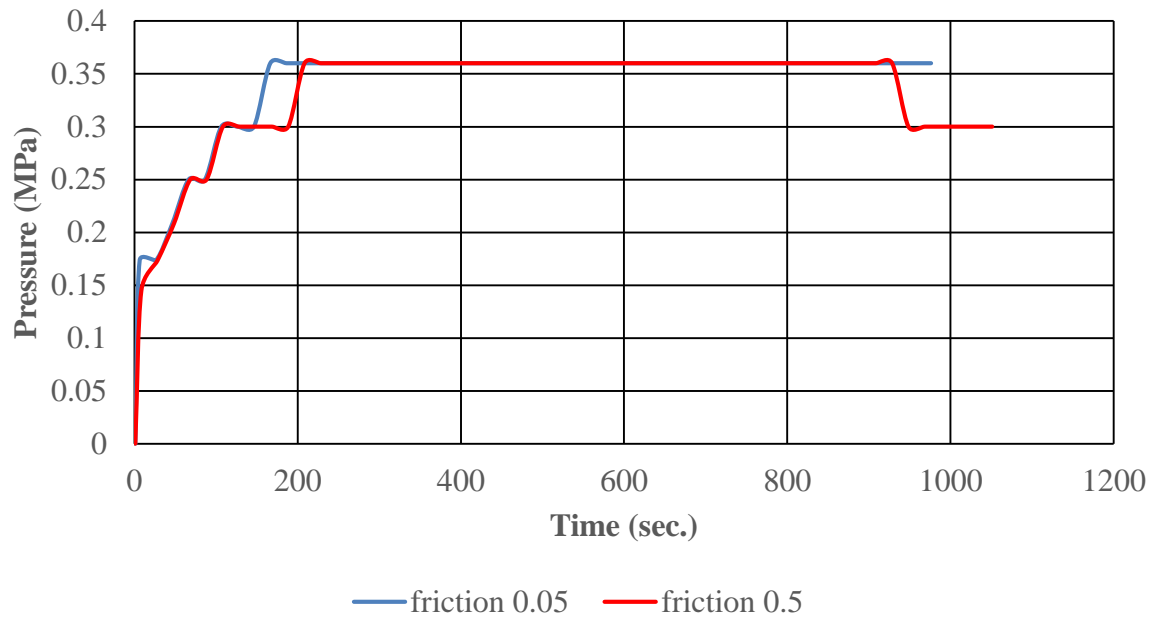
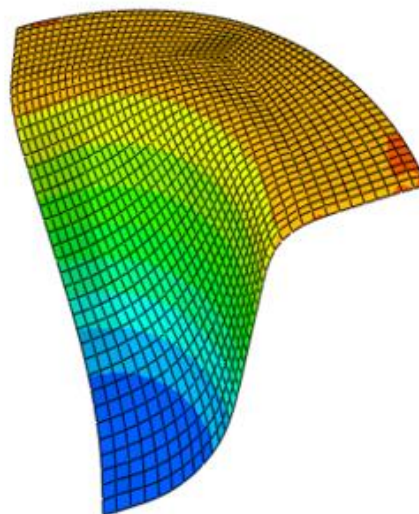
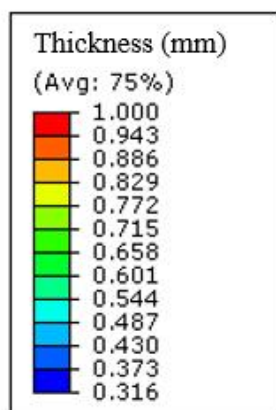
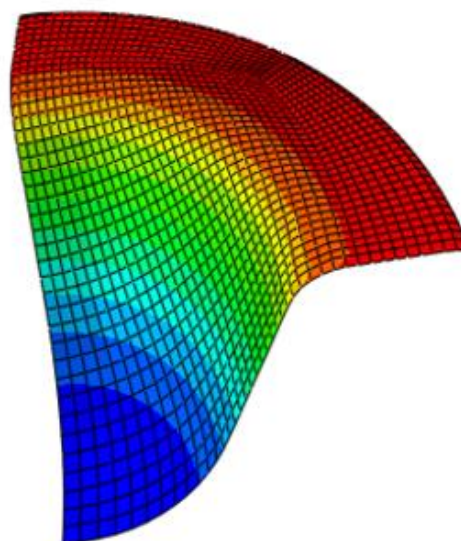
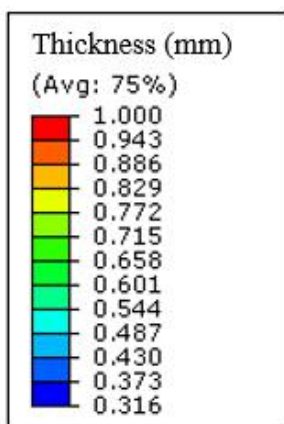


Figure 4.32: Pressure profile for different friction coefficients for 10^{-3} 1/sec. constant target strain rate

Table 4.19 shows results obtained for friction coefficients of 0.05 and 0.5 for different target strain rates. When the friction coefficient increases required process time to form the sheet is increasing, but at the end of the process thickness of obtained product is decreasing significantly. With an adequate lubrication, process times could be decreased in industrial applications.



a) friction coefficient:0.05



b) friction coefficient: 0.5

Figure 4.33: Comparison of sheet thickness distribution for different friction coefficients

Figure 4.33 illustrates how sheet thickness profile occurs at the end of the forming process for friction coefficient 0.05 and 0.5. It is known that when friction coefficient increases forming pressure decreases, because friction force reduces the amount of volume that can move to free bulged region, so forming pressure decreases. When friction coefficient increases greater localized thinning occurs and necessary pressure to

be applied decreases to get the target strain rate as seen in **Figure 4.32**. (Nazzal and Khraisheh, 2005).

It is clear that more uniform thickness distribution is obtained with smaller friction coefficients application. As seen from Figure 4.33, thickness at the die entry is higher for 0.5 friction coefficient while thickness at the die root is smaller which makes the part more nonuniform compared to 0.05 friction case. A similar behaviour was observed for rectangular box forming in Chapter 4.2.5. Friction causes more thinning for both shapes, since frictional force is created which causes thinning independent of the shape.

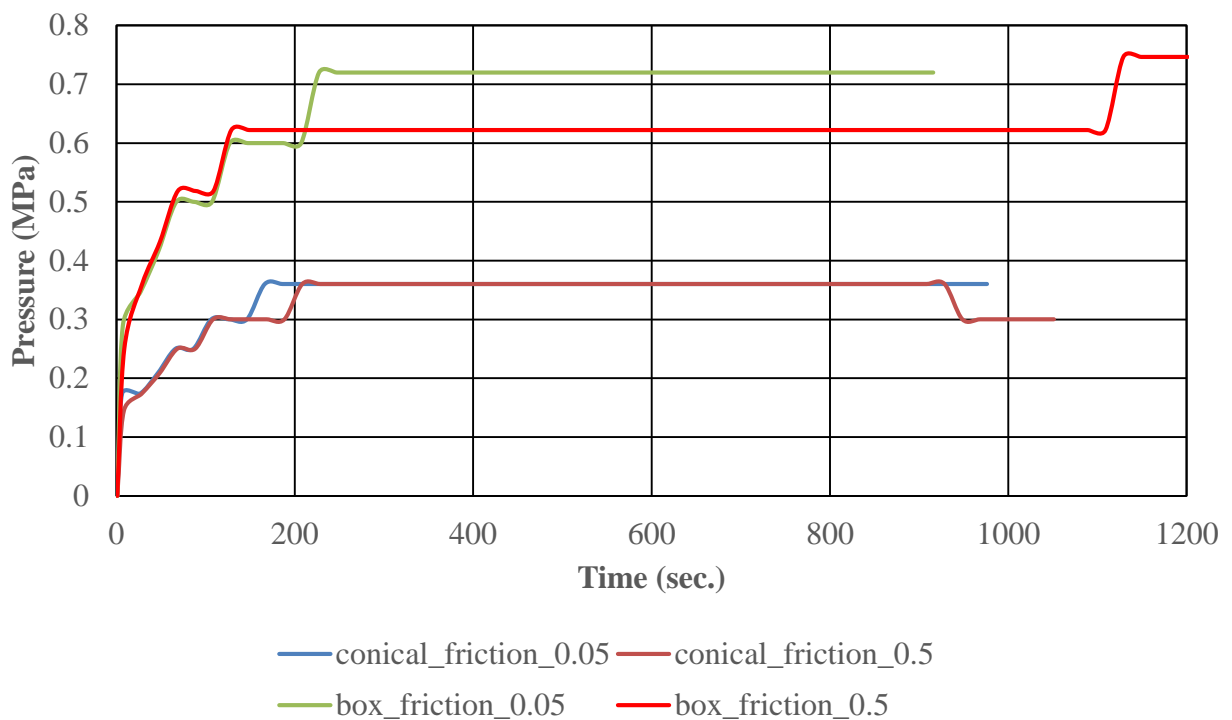


Figure 4.34: Comparison of pressure changes for conical and box forming for different friction coefficients

Figure 4.34 illustrates comparison of pressure changes for rectangular and conical parts for 0.05 and 0.5 friction coefficients. In the final stage of the forming of the conical part, pressure decreases because the area to be formed decreases compared to a rectangular box, and required pressure gets smaller.

4.4 Comparison of Forming Behaviour of Rectangular and Conical Box Forming

In previous sections, effects of process parameters on SPF process for the forming of rectangular and conical dies were investigated. In this chapter, rectangular and conical boxes are compared for application of SPF process.

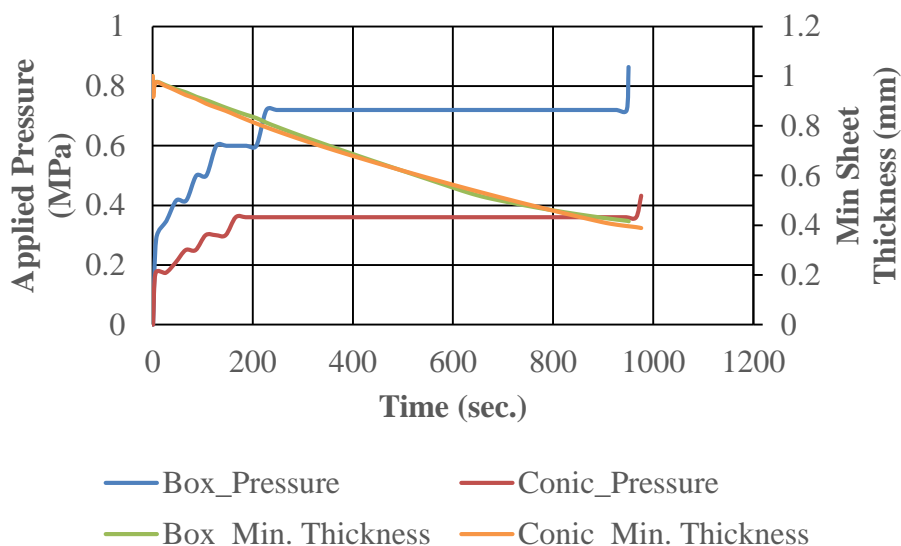


Figure 4.35: Comparison of applied pressure and minimum sheet thicknesses for conical and rectangular box forming

Figure 4.35 illustrates comparison of applied pressure and minimum sheet thicknesses for conical and rectangular box forming with respect to forming time for constant strain rate of 10^{-3} 1/sec. Although their geometric properties are different, it could be observed that required pressure curve behaviours are similar, there is a gradual increase in applied pressure for 20% of the total forming process time, later pressure seems to be constant, and finally, there is a gradual increase in applied pressure to the sheet similarly. Minimum sheet thickness curves have same behaviour while forming process. It could be observed that, required pressure, obtained final thickness and forming time values change with geometric properties, but behaviour of required pressure and change of sheet thickness with time is independent from that.

For both rectangular and conical die forming, an instant increase at the early stages of forming process is because of the increase in stresses, isotropic hardening and grain growth of sheet material, after that thinning effect and hardening can balance each other

and pressure becomes steady. At the final stages of process, sheet has contact with bottom part of the die, deformation is obstructed and effective area on which pressure is applied becomes smaller, hence to maintain the target strain rate, more pressure is required. (Deshmukh, 2003)

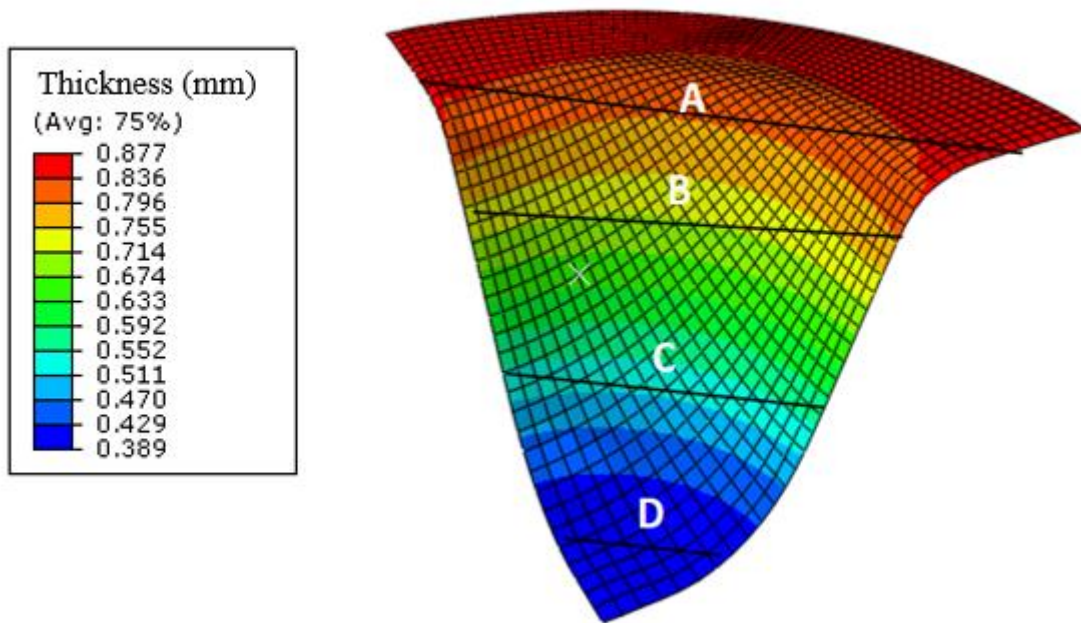
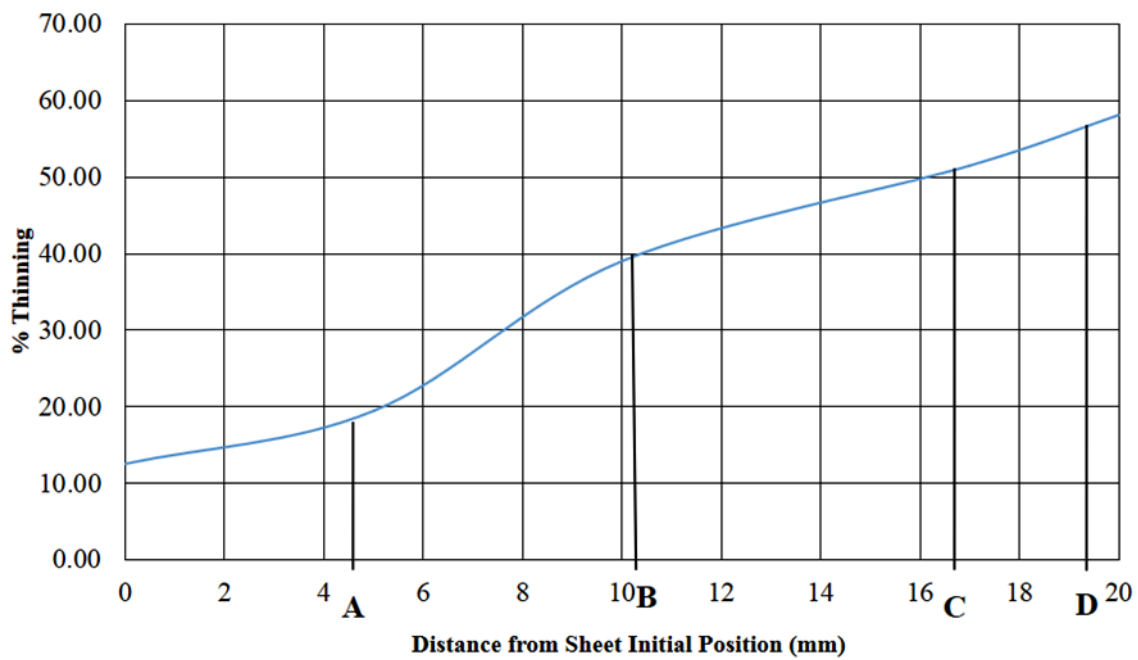
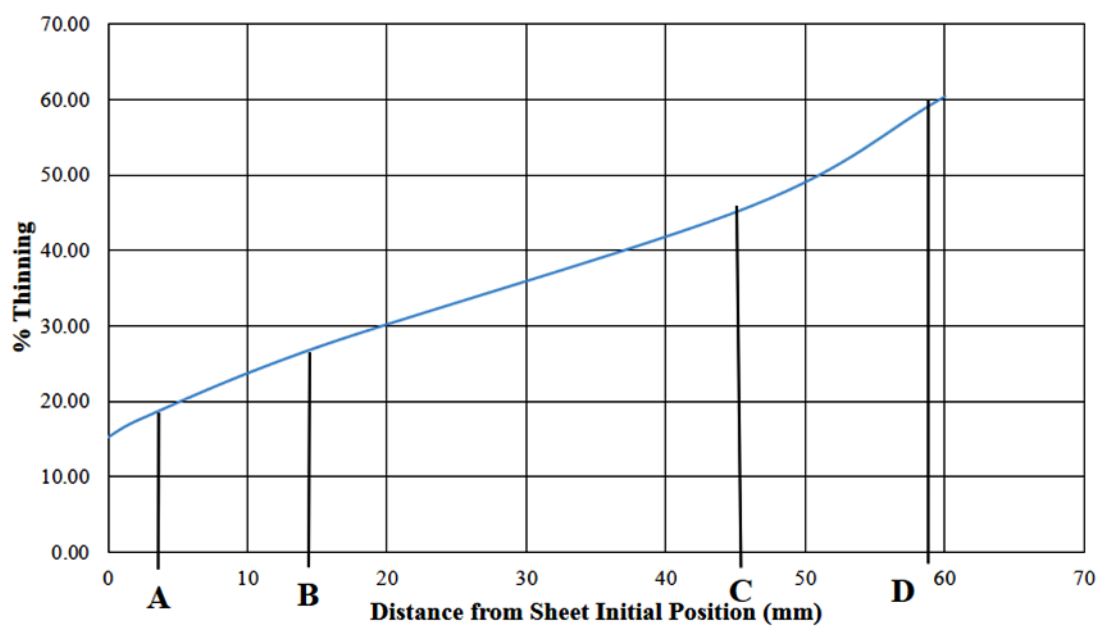


Figure 4.36 Dividing formed part to four different zones according to sheet thickness distribution

In order to compare the thinning behaviour of rectangular and conical parts conical formed part is also divided into four zones in **Figure 4.36** like rectangular box in Figure 4.24, and thinning percent is calculated for each zone by taking average of nodes around each region. **Figure 4.37** illustrates comparison of thinning percent for rectangular and conical parts, independent from geometry, thinning percent is maximum for both condition at bottom part of the parts, because maximum displacement, so maximum strains occur at bottom region of the die. Regions close to initial position of the sheet have already been formed at previous time steps, while bottom region have already been in contact with bottom region of the die.



a) rectangular box



b) conical box

Figure 4.37: Comparison of thinning percent for a) rectangular box and b) conical box

5 Development of an Equation for Estimation of Process Time for SPF Process by Machine Learning for a Rectangular Box

While investigating the process parameters of SPF process for rectangular and conical shape samples various finite element examples have taken into consideration in ABAQUS. Although most of the process parameters are in form of user inputs into the program, estimating the required forming time to complete the process is a handicap. Since, user needs to define the required time in the software, and the forming process continues until the end of this user defined duration. User cannot estimate process time at the beginning of the analysis. As a result of which, user has to conduct various analysis with different time inputs until finding an adequate time for process. This has been a challenge while investigating process parameters. This handicap can be prevented by developing an equation which can solve this problem. This equation could estimate the required forming time by entering the process inputs and required final dome height. Doing an iterative finite element analysis with various time inputs until finding the required formed part is time consuming, since each individual process takes a relatively long time, and user evaluates the final product, later conducts another analysis with the new time input. The equation developed in this study does not aim to give user an exact process time, but it aims to give an estimated time that user can start with and this can decrease the number of iteration steps and the consumed time by the user especially for a rectangular part particularly. It is possible to apply machine learning techniques so that the tool can self-train itself with subsequent iterations and as more input are gathered from analysis. In this way, the estimation of the tool will converge to a very close value to the necessary process time.

In order to develop an equation which can estimate the required time input machine learning and data mining is used. Theory of machine learning and used algorithms are explained in detail in Chapter 2.5.

In order to use machine learning and data mining for development of an equation for estimating the process time, first 527 different analyses are conducted with different process parameters and different time values by writing data collecting shell script for different parameters. (See Appendix, page 115). At the end of each analysis movement

of a specified node is measured to define the dome height. Different process parameters are listed in Appendix. Analysis is conducted from 10 to 3000 seconds in order to simulate effect of process parameters to the forming time. First a coarse analysis is conducted with less number of tests, later the number of tests are increased. Investigated process parameters are creep stress exponent and power law multiplier which can change according to process temperature, strain rate, sheet initial thickness, sheet length, die entry radius, friction coefficient, sheet width, die height and applied initial pressure values.

Shell scripting is used to run SPF process in ABAQUS simultaneously for different process parameters. Obtained data can be used for data mining in order to create an equation to estimate process time as functions of process parameters. For this purpose, an open source machine learning and data mining software called as WEKA (Waikato Environment for Knowledge Analysis) which is developed at University of Waikato, New Zealand is used.

WEKA is an open source tool which includes various machine learning algorithms in order to accomplish data mining tasks. Available algorithms in WEKA could be applied to available data sets which are collected by the user. (Waikato, 2016)

In order to find the best algorithm that fits to the SPF process, existing algorithms are tested with available data. In this study, Least Median of square regression method is used to predict required forming time, since it can detect anomalous data and is not affected from it. Furthermore, it takes effects of all variables into account (not only dominant ones). This helps to consider all parameters when calculating required forming time. In order to decrease the error of estimated time, number of analysis with different parameters for different time values are started with 160 samples and increased to 527.

$$\begin{aligned}
 T = & 126.9512 * n + 6228490.5316 * C - 675362.7565 * \varepsilon^{\circ} + 28.6226 * t \\
 & - 19.3798 * P_i - 30.427 * r_e + 0.22316 * L - 4.7336 * H - 8.1552 * w \\
 & - 81.6711 * \mu + 85.0899 h_f + 341.5586
 \end{aligned} \tag{5.1}$$

Obtained equation which predicts required process time for SPF process is given in **Equation (5.1)**. Here, T : predicted process time, n : creep stress exponent, C : power law multiplier, ε° : strain rate, t : sheet thickness, P_i : initial pressure, r_e : die entry radius, L :

sheet length, h : die height, w : sheet width, μ : friction coefficient, h_f : final dome height. Predicted time includes effects of all process parameters, enabling user to enter process parameters and required formed height and user obtains a predicted time to enter ABAQUS to simulate forming process. Summary of comparison of analysis results with results obtained using the obtained equation are given in Appendix.

The equation has its own limitations. Firstly, it is limited to Ti6Al4V material for rectangular box and this equation covers time values well from 350 to 1300 seconds, but for earlier or later times error % can increase to 60, which is based on the strain rate effect. For example, for strain rate 10^{-3} 1/sec. forming process behaves in a way that obeys the obtained equation. But, when sheet has the shape of the die, dome height cannot change as in the earlier times, which makes this equation inadequate. If a more accurate estimated time value is aimed, different equations are required for different strain rates. However, in the scope of this study most of the process parameters were investigated with 10^{-3} 1/sec. strain rate, which is covered by the obtained equation.

This equation is also converted to a tool to be used by the factory in order to calculate the necessary forming time with given process parameters, it is illustrated in **Figure 5.1**.

Parameter	Value
n	0.4
C	0.000012
ε°	0.001
t	1
P_i	1.0
re	4.0
L	60
h	20
w	40
μ	0.04
h_f	20
Process Time	970.2937658792

Figure 5.1: Process time calculator tool for SPF process of a rectangular box

6 Application of SPF Process for an Aircraft Blowout Door

SPF process has a history of more than 30 years, airplane engine company Rolls-Royce started manufacturing of fan blades using SPF with Ti material, due to excellent fatigue resistance, low weight and corrosion resistance of Ti. (Sieniawski and Motyka, 2007)

Furthermore, SPF process decreases number of components, because it enables to produce complex shapes in a single step as one component with less weight and enables to eliminate the need for welding or riveting parts together. (Slideshare,2016)

Ti6Al4V is an excellent material for superplastic forming and it has the capability of GBS when it is stretched under 10^{-3} 1/sec strain rate. Compared to Al or nickel based alloys, Ti can exhibit cavitation and can elongate until 1000%. (Moffat and Romilly, 2014)

SPF process has an important role in aerospace industry, and TEI aims to include this process to its capabilities in order to compete with other suppliers, since this process reduces metal consumption by decreasing machining. It eliminates the need for joining of metals, requires less powerful equipment and results in high quality and low weight products with longer service lives since low flow stresses occur while large elongations. (Ermachenko et al., 2011)

Advantages of this process are mentioned in detail in Chapter 2.2 and effects of process parameters to SPF process are investigated in detail in Chapters 4 and 5. In this section, application of SPF process for the production of an industrial part is realized. After process parameters are investigated for rectangular and conical parts, an industrial part called as aircraft blowout door of an aircraft which is formed with SPF process in order to simulate obtained information in previous sections.

Blowout doors are designed for aircrafts in order to diminish an over pressure in a specified area, they are opened when exposed to small amount of pressure difference to relieve pressure and prevent collapsing of larger panels in aircraft. They are designed because of early DC-10 crash in 1974 when the cargo door was opened in flight because of pressure difference and collapsed the main deck floor. (Patent,2017)

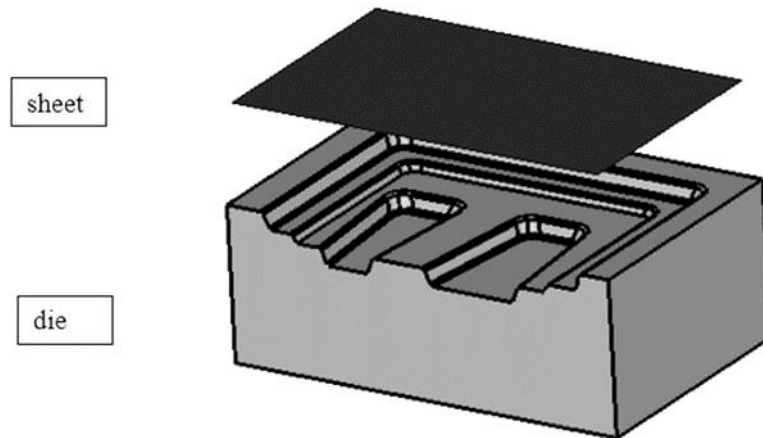


Figure 6.1: Representation of half die-sheet geometry to simulate SPF process for aircraft blowout door

Cold forming methods with welding were used to produce aircraft blow out doors, but SPF has been a popular method to produce these part, since it removes number of joining steps of large parts. So, SPF enables to create a blowout door which has lower weight, utilizes less steps to get the final product and lower stresses which enables to have higher service lives according to conventional methods. Also, SPF does not require surface finish operations which are required for conventional methods. Aircraft blowout door is made of Ti6Al4V material which is relatively expensive, so having higher lives and less weight by producing this part with SPF method enables cost reduction.

In aviation industry compliance is a very important issue for companies, because the components generally have high technology and excellent engineering design concepts, so companies do not want to share this information. Aircraft blowout doors are one of those components that companies do not want to share every design details and production methods. Because of lack of data and compliance reasons the geometry investigated here represents a simplified version of blowout door used in real life. Die shown in **Figure 6.1** has 1000 mm length, 640 mm width and maximum 100 mm height. (Nazzal et al, 2004)

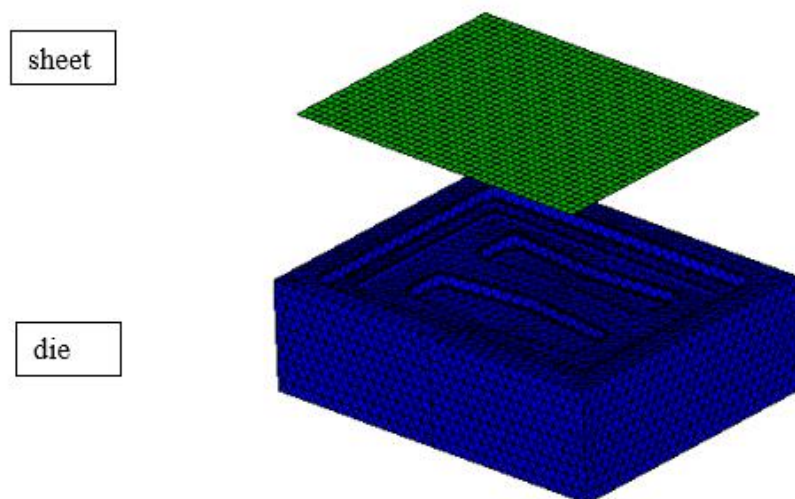


Figure 6.2: Representation of die-sheet meshes to simulate SPF process for aircraft blowout door

Sheet metal material used for this process is Ti6Al4V, sheet has 1 mm thickness and die is made from stainless steel. In this study, different process parameters are given in order to obtain an optimum design from both manufacturing and product perspectives. Cost intended here depends on the forming time, because less forming time enables to produce more parts. Here, supplier aims to produce blowout door with a good quality and minimum cost. Process parameter alternatives are listed in **Table 6.1**, If no lubrication is applied friction coefficient between stainless steel and die are expected to be 0.36 and with a good lubrication it could decrease to 0.1. (Eng, 2017) Strain rate is another process parameter which is very important for process time and product quality, and it is changed from 10^{-3} to 10^{-4} . Process temperature is kept at 900°C for all alternatives.

Sheet and die meshes are illustrated in **Figure 6.2**, and as in the previous sections, female die is modelled with R3D3 rigid elements and sheet is meshed with M3D4 membrane elements. Sheet is clamped on all its edges. In Chapters 5 and 6, it was observed that, process times and applied pressures are increasing with decreasing strain rates but most uniform thicknesses were obtained with lower strain rates. Regarding the effect of friction coefficient obtained with good lubrication conditions, more uniform thickness distribution is observed. According to those information, it is aimed to obtain a process which has optimum process time, optimum thickness distribution and optimum stress

distribution, so that final product could be produced in a reasonable time with a uniform thickness distribution and minimum stress distribution.

Table 6.1: Process parameter alternatives for production of blowout door

Test number	Friction coefficient (-)	Strain rate (1/sec)	Sheet thickness (mm)	Process time (sec.)
1	0.36	10^{-3}	1	260.000
2	0.36	5×10^{-4}	1	580
3	0.36	10^{-4}	1	3000
4	0.1	10^{-3}	1	260.000
5	0.1	5×10^{-4}	1	580
6	0.1	10^{-4}	1	3100

Different analyses are conducted for 6 different tests listed in **Table 6.1**, analyses are continued until sheet has the shape of the die. Obtained results are compared for different aspects such as process time, occurring stresses, sheet thickness distributions. **Table 6.2** summarizes results for all tests. When searching for the optimum process choice for aircraft blowout door, uniform sheet thickness distribution and minimum process time need to be considered. In order to check thickness distribution thinning factor is used which is defined as the ratio of minimum sheet thickness to the average sheet thickness at the end of the process. A high thinning factor signifies a more uniform thickness distribution.

Table 6.2: Summary of obtained results for different process parameters

Test number	Friction coeff. (-)	Strain rate (1/sec)	Sheet thick. (mm)	Process time (sec.)	Min sheet thick. (mm)	Average sheet thick. (mm)	Max. eqv. stress (MPa)	Thinning factor (-)
1	0.36	10^{-3}	1	260.00	0.769	0.853837	12.200	0.900641
2	0.36	5×10^{-4}	1	595.00	0.77	0.853363	8.522	0.902312
3	0.36	10^{-4}	1	3100.00	0.773	0.853779	3.25	0.905387
4	0.1	10^{-3}	1	250.00	0.780	0.851997	11.640	0.915496
5	0.1	5×10^{-4}	1	580.00	0.792	0.852104	7.78	0.927117
6	0.1	10^{-4}	1	3000	0.794	0.852433	3.318	0.929106

According to the obtained results in Table 6.2, most uniform sheet thickness distribution is obtained for test number 6, which has minimum strain rate and friction coefficient. These are in good agreement with those obtained for rectangular and conical parts. Test number 6 has a process time of 3100 seconds, which is relatively high compared to 260 seconds for test number 1 and 4 for 10^{-3} 1/sec. strain rate. Process time is also a very important criterion for producing a part, because in the same time 10^{-3} 1/sec. strain rates enable to obtain 10 parts while 10^{-4} 1/sec. strain rate produces only one part. In aviation industry, not only cost but also quality is a very important criterion. Therefore, test number 5, which can produce part in 580 seconds, it enables to produce nearly 5 parts while 10^{-4} 1/sec. strain rate produces one part, and it also it enables to get more uniform thickness distribution regarding to 10^{-3} 1/sec. strain rate and less stress on the blowout door. This increases the life span of the part in the aircraft. Table 6.2 results are also in a good agreement with the fact that good lubrication enables to obtain more uniform thickness distribution in the final product.

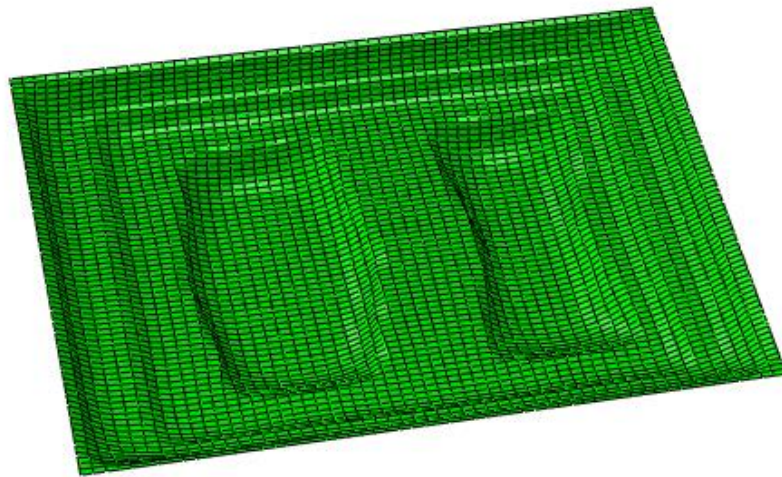


Figure 6.3: Deformed shape of sheet for test number 5

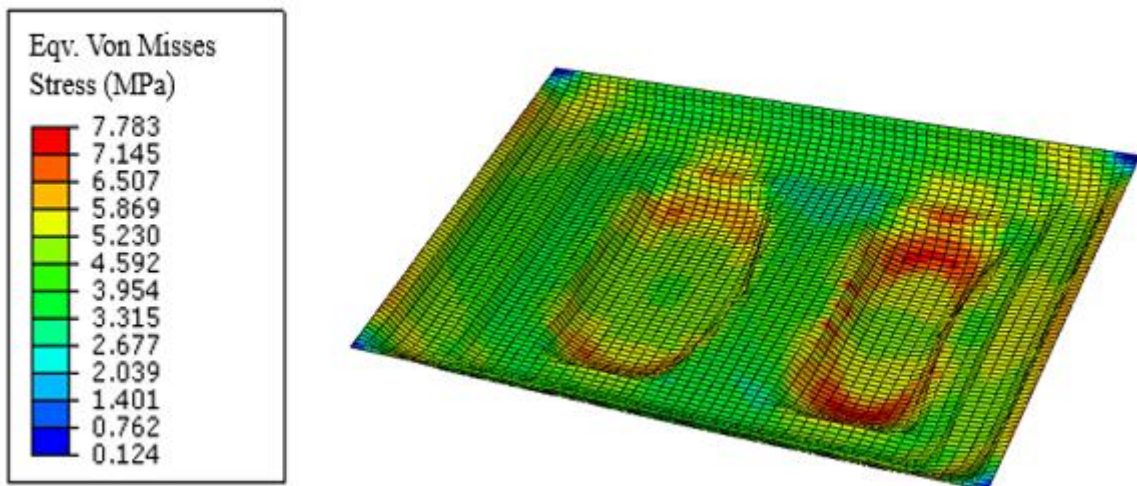


Figure 6.4: Equivalent stress plot of sheet for test number 5

Stress and thickness distribution on aircraft blowout door is shown in **Figure 6.4** and **Figure 6.5**, and maximum stress and maximum thinning occur at location which is formed finally, as expected from forming of rectangular and conical boxes. Because, those regions have maximum displacement at the end of the forming process, so have maximum plastic strains.

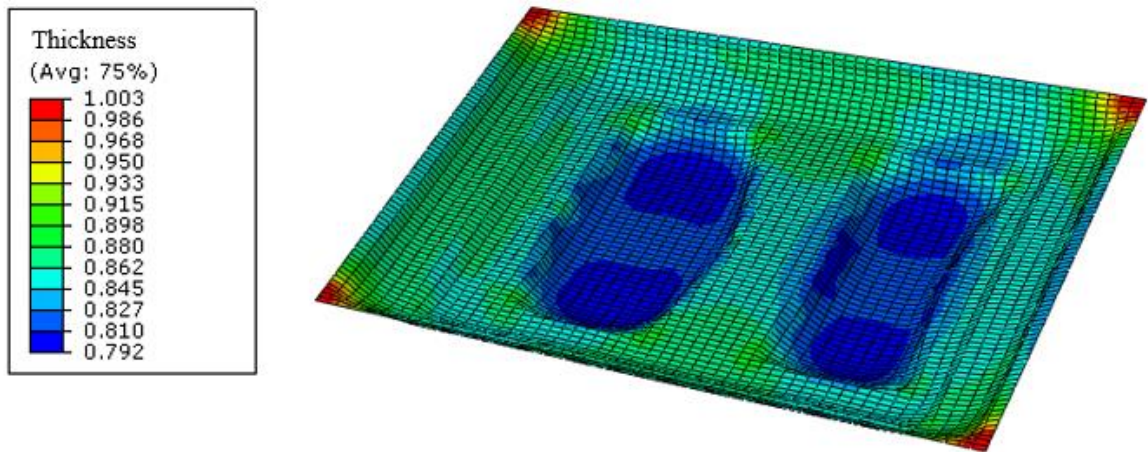


Figure 6.5: Thickness distribution plot of sheet for test number 5

7 Cost Analysis of SPF Process for the Factory

Process parameters are investigated for rectangular and conical parts and later an optimum process is chosen for an aircraft blowout door using FEM as mentioned in previous chapters. Investigation of process parameters was done with FEM instead of conducting experiments due to financial concerns. The FE study of this thesis is completed in approximately 170 days and effort for this is compared with an estimated cost for a possible experimental effort.

Total cost calculation for FEA portion of this study is shown in **Table 7.1**. Total cost consists of an engineer and FEA software. **Table 7.2** illustrates estimated time for a possible experimental study in order to investigate process parameters. Total cost is calculated by considering an engineer, an operator to produce parts, press, lubrication and die costs. Finally, total cost for FEA and experiment costs are compared, as seen from Table 7.2, investigating process parameters with FEA study enables to save 861,580 \$. The large amount of cost saving supports the idea of investigating process parameters for SPF process with FEA study.

Table 7.1: Total cost calculation for FEA study (TEI, 2017)

Test part	Number of analysis	Days of simulations	Engineer cost (\$)	ABAQUS program cost (\$)	Total cost (\$)
Rectangular box	35	70	4,666.67	-	-
Conical box	8	40	2,666.67	-	-
Aircraft blowout door	6	30	2,000.00	-	-
for equation development	527	30	2,000.00	-	-
Total cost	576	170	11,333.33	80,000.00	91,333.33

Table 7.2: Estimated cost calculation for experiments and comparison with FEA study
(TEI, 2017)

Test part	Number of tests	Days of tests	Engineer Cost (\$)	Operator cost (\$)	Mat. cost (\$)	Press cost (\$)	Lub. cost (\$)	Die cost (\$)	Total cost (\$)	Saved cost (\$)
Rectangular box	35	7	467	101	560	9×10^5	700	5×10^5	-	
Conical box	8	2	133	29	160	9×10^5	160	5×10^5	-	
Aircraft blowout door	6	3	200	43	240	9×10^5	120	5×10^5	-	
Total cost	-	-	800	173	960	9×10^5	980	5×10^5	952,913	861,580

8 Conclusion

The company, TEI, is looking forward to include SPF process to its capabilities for its various advantageous features in order to compete with other aerospace part suppliers. Because of considerably high cost of experiments, FEA study is preferred to investigate effect of process parameters of the SPF process. ABAQUS creep module was preferred for FEA, and in order to determine the accuracy of the FE method the results of the conducted study were compared with experimental results of Moscow State University for Ti6Al4V material. Later, various process parameters were investigated for rectangular and conical parts. Because process time is an input to the software, and it is difficult to estimate the process time before the analysis, it causes a handicap while investigating effect of process parameters. A tool is developed for rectangular box, in order to estimate process time by considering effect of different process parameters by using machine learning and data mining techniques. Later, for application of SPF process, an aircraft blowout door is analysed for different process choices in order to find an optimum process for production. Finally, a cost analysis was conducted to compare total cost of FEA study and estimated total cost for experimental study. Following transferrable knowledge is obtained throughout this thesis:

- ABAQUS creep module can be used in order to simulate SPF process, since FEA analysis results are in good agreement with experimental results of Moscow State University.
- While selecting process parameters for industrial applications to produce a part with SPF method both economical and quality aspects need to be considered.
- Instead of application of constant pressure, constant strain rate method should be preferred not to exceed allowable maximum strain rate and to avoid premature failures. Furthermore, constant strain rate method enables shorter process times.
- Increasing process temperature could be an option in order to decrease process time, stress and applied pressure and also to obtain more uniform thickness distribution.
- In order to decrease process time of SPF, constant target strain rate value of process can be increased, but decreasing process time results in problems

associated with the product quality, since increasing strain rate causes more nonuniform thickness distribution, higher stresses on the specimen and increase of required pressure.

- Decreasing initial sheet thickness of the specimen enables to obtain final products with more uniform thickness distribution with less applied pressures in a shorter time compared to higher sheet thicknesses.
- Utilizing lubricants in order to decrease friction coefficient between die and sheet metal enables to obtain products with more uniform thickness distribution with less required pressures in shorter time compared to higher friction coefficients.
- Geometry of the die is another concern for SPF process, since increasing die entry radius enables to produce final products with more uniform thickness distribution in shorter time. Also, for a conical die aspect ratio of the die is an important design criterion for SPF process, since increasing aspect ratio enables to decrease process time and obtain products with more uniform thickness distribution.
- The tool developed in order to estimate process time for different process parameters for rectangular box successfully decreases the number of iterations necessary for final FEA, and enables the company to estimate required process time for different process parameters, such that they can try different design choices which are not investigated in this study.
- For production of aircraft blowout door with SPF process, test number 5 among 6 different process choices is chosen for production because it gives the optimum design choice based on cost and quality criteria.
- Economical study shows that investigating process parameters with FEA study instead of conducting experiments saved considerable amount of cost to the factory.

Throughout this study, it was found out that further investigations can be conducted to develop the current study:

- If the factory decides to add SPF process to its current production methods, analysis results in this study should be compared to experimental results.
- Developed equation in order to find estimated process time for SPF process of rectangular box can be improved for various strain rates and for different die

geometries. When various analyses are conducted for different process parameters and different parts by adding different process parameters which were not investigated in this thesis, a perfectly suitable equation can be obtained. As a result of that, process time can be estimated more accurately such that production could be realized according to this without doing further analysis.

Bibliography

- Shojaeefard, M.H., Khalkhali, A., Miandoabchi, E., 2014. Effects of Process Parameters on Superplastic Forming of a License Plate Pocket Panel. *Int J Advanced Design and Manufacturing Technology* 7(2), pp. 25-33.
- Sieniawski, J., Motyka, M., 2007. Superplasticity in Titanium Alloys. *Journal of Achievements in Materials and Manufacturing Engineering* 24 (1), pp. 123-130.
- Ermachenko, A. G., Lutfullin, R.Y., Mulyukov, R.R., 2011. Advanced Technologies of Processing Titanium Alloys and Their Applications in Industry. *Rev.Adv.Mater. Sci.* 29, pp. 68-82.
- Marinho, E.P., Ribeiro, F.C., 2012. Set Up Control of Superplastic Forming of Aluminum Alloys and Strategy for Rheological Characterization of Materials by Bulge Test. *ABCM Symposium Series in Mechatronics* 5, pp. 380-389.
- Chandramouli, R., 2016. Fundamental Concepts of Metal Forming Technology <http://www.nptel.ac.in>. Retrieved on 02.01.2016.
- N.N., 2016. Metal Forming Fundamentals and Applications <http://www.asminternational.org>. Retrieved on 05.01.2016.
- Altan, T., Oh, S.I., Gegel, H.L., 1983. *Metal Forming: Fundamentals and Applications*. American Society for Metals.
- Altan, T., Ngaile, G., Shen, G., 2004. *Cold and Hot Forging: Fundamentals and Applications*. ASM International.
- Groover, Mikell P., 2012. *Springer Handbook of Experimental Solid Mechanics*, Wiley.
- Tyne, C.J.V., 2016. *Design of Forming Processes: Bulk Forming* <https://www.forging.org>. Retrieved on 12.01.2016.
- Barnes, A.J., 2007. Superplastic Forming 40 Years and Still Grooving. *ASM International* 16, pp. 440-454.
- Grabski, M., 1973. *Fine-structure Superplasticity in Metals*. Silesian Press.
- Mukherjee, A.K., 2002. An Examination of the Constitutive Equation for Elevated Temperature Plasticity. *Materials Science Engineering A* 322, pp. 1-22.

-
- Deshmukh, P.V., 2003. Study of Superplastic Forming Process Using Finite Element Analysis. University of Kentucky Master's Thesis.
- N.N., 2008. Superplastic Forming. ASM Handbooks Online 14, pp. 61.
- Cappetti, N., Garofalo, L., Naddeo, A., Nastasia, M., Pellegrino, A., 2010. A Method for Setting Variables in Super Plastic Forming Process. Journal of Achievements in Materials and Manufacturing Engineering 38 (2), pp. 187-194.
- Naka, T., Torikai, G. Hino, R., Yoshido, F., 2001. The Effects of Temperature and Forming Speed On the Forming Limit Diagram for Type 5083 Aluminium, Magnesium Alloy Sheet. Journal of Materials Technology 113, pp. 648-653.
- Luckey, J., Friedmana, P., Weinmannb, K., 2009. Design and Experimental Validation of a Two-Stage Superplastic Forming Die. Journal of Materials Processing Technology 209, pp. 2152-2160.
- Ceschini, L., Afrikantov, A., 1992. SPF of Materials and SPF Combined With Diffusion Bonding: Technological and Design Aspects.
- Ghosh, A.K., Hamilton, C.H., 1986. Superplastic Forming and Diffusion Bonding of Titanium Alloys. Def Sci J 36 (2), pp. 153-177.
- Miller, D.A., Mohamed, F.A., Langdon, T.G., 1979. An Analysis of Cavitation Failure Incorporating Cavity Nucleation with Strain. Materials Science and Engineering 40, pp. 159-166.
- Nazzal, M. A., Khraisheh, M. K., 2005. Finite Element Simulation of Superplastic Forming Using a Microstructure Based Constitutive Model. ABAQUS User's Conference, pp. 1-14.
- Chen, Y., Kibble, K., Hall, R., Huang, X., 2001. Numerical Analysis Of Superplastic Blow Forming of Ti-5Al-4V Alloys. Materials and Design 22, pp. 679-685.
- Hibbitt, K., Hibbit, S., 2001. ABAQUS/Standard User's Manual.
- Nazzal, M. A., Khraisheh, M. K., Darras, B. M., 2004. Finite Element Modelling and Optimization of Superplastic Forming Using Variable Strain Rate Approach. ASM International 13, pp. 691-699.
- N.N., 2016. Data Mining for Scientific and Engineering Applications
<http://twin-cities.umn.edu>. Retrieved on 20.12.2016.

-
- N.N., 2016. Data Mining with Weka
<http://www.waikato.ac.nz/>. Retrieved on 24.12.2016.
- Simon, P., 2013. Too Big to Ignore: The Business Case for Big Data. Wiley pp. 89.
- Hosch, W. L., 2009. Machine Learning
<https://global.britannica.com>. Retrieved on 24.12.2016.
- Ray, S., 2015. 7 Types of Regression Techniques
<https://www.analyticsvidhya.com/>. Retrieved on 25.12.2016.
- Dallal, G. E., 1992. LMSMVE: A Program for Least Median of Squares Regression and Robust Distances. *Computers and Biomedical Research* 25, pp. 394-391.
- Vasin, R.A., Enikeev, F.U., Tokuda, M., Safiullin, R.V., 2003. Mathematical Modelling of Superplastic Forming of a Long Rectangular Sheet. *International Journal of Non-Linear Mechanics* 38, pp. 799-807.
- Warren, J., Wadley, H.N.G., (n.d.). The Superplastic Deformation Behaviour of Mechanical Vapour Deposited Ti-6Al-4V. Department of Materials Science Engineering, University of Virginia.
- Panicker, S. S., Panda, S. K., 2017. Improvement in Material Flow During Nonisothermal Warm Deep Drawing of Nonheat Treatable Aluminium Alloy Sheets. *Journal of Manufacturing Science and Engineering* 139.
- Hwang, Y. M., Yang, J. S., Chen, T. R. Huang, J. H., Wu, W. U., 1997. Analysis of Superplastic Forming in a Conical Closed Die. *Int. J. Mech. Sci.* 40 (9), pp. 867-885.
- Zamani, N., Katarya, N., Reza, H., Maniyar, G., 2013. Superplastic Forming and Diffusion Bonding in Aerospace Industries
<http://www.slideshare.net>. Retrieved on 31.01.2016.
- Moffat, M., Romilly, P., 2014. Breakthrough Technologies in Aerospace Industry For Titanium Processing. Titanium Europe.
- N.N., 1956. Blow-Out Safe Aircraft Doors
<https://www.google.com/patents/US2748855>. Retrieved on 01.02.2017.

N.N., 2017. Coefficient of Friction

http://www-eng.lbl.gov/~ajdemell/coefficients_of_friction.html. Retrieved on 4.02.2017.

N.N.,2017. TEI Purchasing Department. Retrieved on 15.03.2017.

Appendix

Summary of Obtained Predicted Time for Different Process Parameters:

n	C	strain rate	sheet thickness	initial press. (MPa)	die entry rad.	sheet length	die height	sheet width	friction	dome height	Real forming time	predicted Forming Time	% error
1.70	1.20E-05	1.00E-03	1.00	1.00	4.00	60.00	20.00	40.00	0.00	10.52	350.00	332.51	-5.00
1.58	1.20E-05	1.00E-03	1.00	1.00	4.00	60.00	20.00	40.00	0.00	12.78	500.00	509.22	1.84
1.70	1.50E-05	1.00E-03	1.00	1.00	4.00	60.00	20.00	40.00	0.00	10.48	350.00	347.93	-0.59
1.70	1.20E-05	8.00E-04	1.00	1.00	4.00	60.00	20.00	40.00	0.00	18.64	1500.00	1157.93	-22.80
1.70	1.20E-05	1.00E-03	1.60	1.00	4.00	60.00	20.00	40.00	0.00	16.37	900.00	846.94	-5.90
1.70	1.20E-05	1.00E-03	1.00	0.60	4.00	6.00	20.00	40.00	0.00	18.05	950.00	967.98	1.89
1.70	1.20E-05	1.00E-03	1.00	0.60	4.00	6.00	20.00	40.00	0.00	18.42	990.00	999.85	0.99
1.70	1.20E-05	1.00E-03	1.00	1.00	4.00	45.00	20.00	40.00	0.00	17.87	950.00	954.38	0.46
1.70	1.20E-05	1.00E-03	1.00	1.00	4.00	60.00	18.00	40.00	0.00	17.40	950.00	927.59	-2.36
1.70	1.20E-05	1.00E-03	1.00	1.00	4.00	60.00	20.00	45.00	0.00	17.61	900.00	894.72	-0.59
1.70	1.20E-05	1.00E-03	1.00	1.00	4.00	60.00	20.00	40.00	0.04	13.92	600.00	618.52	3.09
1.70	1.20E-05	2.00E-04	1.00	1.00	4.00	60.00	20.00	40.00	0.00	13.04	3000.00	1086.62	-63.78

Shell Script Code Example for Simultaneous Analysis for Change of Friction

Parameter:

```
#!/bin/bash

timefile='time.txt'

fr=( 0.05 )

#sed -i '/^$/d' $timefile

cat $timefile | while read line
do

echo $line

time=$(echo ${line} | awk ' { print $1; } ')

echo $time

for f in "${fr[@]}"
do

model="friction"

case="$time"

prefix=${model}_${f}_${case}

echo " ** loop

" >> ${prefix}.inp

echo "

*NODE

**node and element information for sheet is deleted

*membrane section,elset=sheet,material=Ti6Al-4V

1,

*material,name=Ti6Al-4V

*ELASTIC

1e3, .3
```

```
*CREEP, LAW=TIME
1.2e-5,1.7, 0.
*node,nset=DIE
10000, 0.0, 0.0, 0.0
*RIGID BODY, ELSET=ERIGID, REFNODE=10000
*NODE
**node and element information for sheet is deleted
*SURFACE,NAME=DIE
ERIGID,SPOS
*SURFACE,TYPE=NODE,NAME=SLAVES
NCONT,
*CONTACT PAIR, INTERACTION=DIE_NODE, smooth=0.2
SLAVES,DIE
*SURFACE INTERACTION,NAME=DIE_NODE
*Friction, slip tolerance=0.005
${f},
**
** BOUNDARY AND INITIAL CONDITIONS
**
*BOUNDARY
EDGE1,3
EDGE7,2,3
EDGE3,1
EDGE5,1,2
10000,1,6
*INITIAL CONDITIONS, TYPE=STRESS, UNBALANCED STRESS=STEP
```

sheet, 0.01, 0.01

*AMPLITUDE,DEFINITION=SOLUTION DEPENDENT,NAME=AUTO

1.,0.1,100

**

** STEP 1

**

*STEP, NLGEOM, unsymm=yes

*STATIC

3.E-3,1,

*DLOAD

sheet,P,-1

*CONTACT PRINT, FREQUENCY=100

*CONTACT FILE, FREQUENCY=100, NSET=NSELECT

*EL FILE, ELSET=sheet , FREQUENCY=100

S, E,

CE,

SINV,

*PRINT, CONTACT=YES

*NODE PRINT, NSET=EDGE3, FREQUENCY=100

U,

*NODE FILE, NSET=EDGE3, FREQUENCY=100

U,

*OUTPUT,FIELD, Frequency=100

*NODE OUTPUT,NSET=sheet

U,

*ELEMENT OUTPUT,ELSET=sheet

S, E,

CE,

SINV,

*Element Output, directions=YES

ALPHA, ALPHAN, CE, CEEQ, CEMAG, CEP, CESW, CS11, CTSHR, E, EE, ER, IE, LE,
MISES, MISESMAX

MISESONLY, NE, PE, PEEQ, PEEQMAX, PEEQT, PEMAG, PEQC, PRESSONLY, PS, S,
SALPHA, SE, SEE, SEP, SEPE

SPE, SSAVG, THE, TRIAX, TSHR, VE, VEEQ, VS, STH

*END STEP

** STEP 2

*STEP, INC=500000, NLGEOM, unsymm=yes

*VISCO, CETOL=0.05

0.0001, \${time}, 1e-20, 1

*DLOAD,AMPLITUDE=AUTO

sheet,P,-1

*CREEP STRAIN RATE CONTROL, ELSET=sheet,

AMPLITUDE=AUTO

0.001 ,

** TO WRITE THE AUTOMATIC SOLUTION CONTROL

** VARIABLES AMPCU AND RATIO TO THE RESULTS

** FILE EVERY INCREMENT SUCH FILE HAS TO BE

** ACTIVATED

*NODE FILE, NSET=CENTER, FREQUENCY=1

U,

*OUTPUT,FIELD, Frequency=20

*NODE OUTPUT

```
U,
*ELEMENT OUTPUT,ELSET=sheet
S, E,
CE,
SINV,
STH,
*Element Output, directions=YES
ALPHA, ALPHAN, CE, CEEQ, CEMAG, CEP, CESW, CS11, CTSHR, E, EE, ER, IE, LE,
MISES, MISESMAX
MISESONLY, NE, PE, PEEQ, PEEQMAX, PEEQT, PEMAG, P, STH
*END STEP
" >> ${prefix}.inp
done
done
time=( 600 700 800 900 950 1050 )
fr=(0.05 )
for tm in "${time[@]}"
do
for f in "${fr[@]}"
do
#cd /C/Users/elif/Desktop/createtool/m/m_${m}_${tm}
abq6131.bat j=friction_${f}_${tm} interactive input=friction_${f}_${tm}.inp
mkdir friction_${f}_${tm}
mv friction_${f}_${tm}.* friction_${f}_${tm}
done
done
done
```